BUREAU OF RECLAMATION

Technical Report No. ENV-2023-045

A Three-Tiered Approach to Assess Erosion and Deposition on and Downstream from New Melones Dam's Auxiliary Spillway

New Melones Dam, California
California Great Basin Region

U.S. Department of the Interior **March 2023**

Mission Statements

The U.S. Department of the Interior protects and manages the Nation's natural resources and cultural heritage; provides scientific and other information about those resources; honors its trust responsibilities or special commitments to American Indians, Alaska Natives, and affiliated Island Communities.

The mission of the Bureau of Reclamation is to manage, develop, and protect water and related resources in an environmentally and economically sound manner in the interest of the American public.

Cover Photo – View from the hillslope adjacent to the New Melones Spillway, looking upstream toward New Melones Reservoir. (Photo by M. Foster, Bureau of Reclamation).

Technical Report No. ENV-2023-045

A Three-Tiered Approach to Assess Erosion and Deposition on and Downstream from New Melones Dam's Auxiliary Spillway

New Melones Dam, California
California Great Basin Region

Prepared by: Aaron Hurst, PhD and Melissa Foster, PhD, PG

Bureau of Reclamation
Technical Service Center
Denver, Colorado

U.S. Department of the Interior **March 2023**

A Three-Tiered Approach to Assess Erosion and Deposition on and Downstream from New Melones Dam's Auxiliary Spillway

New Melones Dam, California
California Great Basin Region

AARON HURST

Digitally signed by AARON HURST
Date: 2023.03.16 14:32:52 -06'00'

Prepared by: Aaron A. Hurst, Fluvial Geomorphologist, PhD

MELISSA FOSTER

Digitally signed by MELISSA FOSTER
Date: 2023.03.16 14:01:55 -06'00'

Prepared by: Melissa A. Foster, Fluvial Geomorphologist, PhD, PG

Peer Review Certification

This section has been reviewed and is believed to be in accordance with the service agreement and standards of the profession.

DANIEL DOMBROSKI

Digitally signed by DANIEL DOMBROSKI
Date: 2023.03.16 18:59:19 -06'00'

Peer reviewed by: Dan Dombroski, Hydraulic Engineer, PhD, PE

Citation: Hurst. A.A., Foster, M.A., 2023. A Three-Tiered Approach to Assess Erosion and Deposition on and Downstream from New Melones Dam's Auxiliary Spillway. US Bureau of Reclamation, Technical Service Center, Sedimentation and River Hydraulics Group, Report ENV-2023-045.

Acronyms and Abbreviations

ac-ft	acre foot
1D	one-dimensional model
2D	two-dimensional model
cfs	cubic feet per second
CGB	California-Great Basin Region 10
DEM	digital elevation model
FDEM	frequency domain electromagnetic mapping
ft	foot (feet)
ft^3	cubic feet
g	gram(s)
GPS	global positioning system
H1DE	Hurst 1D erosion model
kyr	thousand years
lb/sq-ft	pound per square foot
m	meter(s)
mi	mile(s)
mm	millimeter(s)
MP	monitoring point
Myr	million years
NAVD 1988	North American Vertical Datum 1988
NM	New Melones
NM1049	New Melones starting reservoir elevation 1049 ft
NM1088	New Melones starting reservoir elevation 1088 ft
Reclamation	Bureau of Reclamation
RI	recurrence interval
RTK	real-time kinetic
s	seconds
SMS	Surface-water Modeling Solution
SRH	Sedimentation and River Hydraulics
SRH-2D	Sedimentation and River Hydraulics two-dimensional model
TSC	Technical Services Center
USACE	U.S. Army Corps of Engineers
WSE	Water Surface Elevation
yd^3	cubic yards
yr	year(s)

Contents

Page

Tables

Figures

Appendices

Appendix

Abstract

We developed a novel three-tiered approach to quantify and spatially represent zones of sediment erosion, bedrock erosion, and subsequent sediment deposition associated with a range of flow events on an unlined spillway at New Melones Dam, located approximately 45 miles northeast of Modesto, California. Our three-tiered approach includes the application of: (1) the Sedimentation and River Hydraulics two-dimensional (SRH-2D) sediment transport model to inform sediment removal and deposition; (2) a two-dimensional (2D) probabilistic erosion model using the Annandale Erodibility Index Method (Annandale, 1995) to inform the potential for bedrock erosion across the full spatial extent of the spillway; and (3) the Hurst one-dimensional (1D) Erosion model (H1DE), a 1D bedrock incision model (Hurst et al., 2021), to inform the timing and magnitude of vertical incision into bedrock and the potential for knickpoint (headcut) propagation.

We routed a range of flood events up to a 1 million-year (Myr) recurrence interval (RI) event to the New Melones Lake reservoir at two different initial reservoir water surface elevations for New Melones Lake of 1,049 and 1,088 ft (North American Vertical Datum 1988 (NAVD88)). The spillway is activated at the 100-year (yr) RI event with a reservoir elevation of 1,088 ft and at the 20 thousand-year (kyr) RI event with the lower 1,049 ft reservoir elevation. SRH-2D model results indicate the New Melones Spillway and Bean Gulch, a small channel located between the spillway and the Stanislaus River, are dominated by sediment erosion for all the modeled flows. Using a starting sediment volume of 210,000 yd^3 on the spillway, the minimum volume of modeled spillway sediment erosion for the 20 kyr RI flow with a starting elevation of 1,049 ft in New Melones Lake is 77,490 yd^3 and the maximum amount of modeled sediment erosion on the spillway for the 1 Myr RI flow with a starting elevation of 1,088 ft in New Melones Lake is 207,703 yd^3. The removal of sediment from the spillway exposes the underlying rock to potential bedrock-erosion by rock plucking and knickpoint propagation. The 2D Annandale Erodibility Index Method indicated that for low-recurrence interval floods, only the gully connecting the spillway to Bean Gulch is likely to erode bedrock. At higher flows, bedrock erosion is also probable downstream along the serpentinite contact within Bean Gulch, but this model did not indicate erosion within the spillway. The H1DE model results also show that erosion is limited to the gully downstream of the spillway in almost all cases. However, the H1DE model did indicate significant bedrock erosion on the lower portion of the spillway for the 1 Myr RI flow, using a starting elevation of 1,088 ft in New Melones Lake. For the H1DE model, we ran two 1D transects along the left and right edges of the spillway with a random initial bed constrained by field observations of rock properties. We run the model for 50 different randomized initial beds and use the average incisional profile (depth of erosion) for the 50 runs. The rock was more fractured along the right spillway and thus experienced more incision. If we applied the incisional profile from each transect across the width of the spillway to infer a total volume of erosion, the HIDE results from the left-modeled transect indicate 11,111 yd^3 (~300,000 ft^3) of bedrock erosion and results from the right-modeled transect indicate 23,889 yd^3 (645,000 ft^3) of bedrock erosion for the maximum modeled event (1 Myr RI with 1,088 ft elevation in New Melones Lake). The volume of eroded bedrock material is 5 to 10% of the maximum volume of eroded sediment for the same 1 Myr event. Eroded sediment and rock are

transported to the Stanislaus River, which is heavily impacted by sediment deposition. Sediment deposition is greatest near Bean Gulch and decreases with distance downstream due to the tailwater effect from Tulloch Reservoir. For the range of modeled flows, sediment deposition (>0.5 ft depth) extends from the confluence with Bean Gulch to between 2,120 ft and 8,750 ft downstream on the Stanislaus River. The upstream extent of Tulloch Reservoir, marked at the O'Byrnes Ferry Road crossing, is located approximately 18,500 ft downstream from the confluence between Bean Gulch and the Stanislaus River, outside of the depositional zone. Simulated bed change at the upstream extent of Tulloch Reservoir is negligible at a maximum of 0.13 ft of bed change, indicating that the reservoir is not impacted by the flood event. These results use a downstream boundary condition (base level) of 500 ft to 515 ft water surface elevation (WSE) at Tulloch Reservoir based on normal operations, which creates a backwatered condition in the Stanislaus River channel. However, if Tulloch Reservoir were heavily drawn down during a large flood event, sediment transport would extend farther downstream and would potentially reach the reservoir.

1.0 Introduction

The Sedimentation & River Hydraulics Group at the Technical Service Center (TSC) of the Bureau of Reclamation (Reclamation) was funded by the Reclamation Dam Safety Office (DSO) to investigate erosional risk to an unlined spillway as part of the Public Protection Guidelines framework to support risk-informed decisions for Dam Safety. New Melones Spillway, which exits New Melones Lake in Calaveras County, California (Figure 1), was identified by Dam Safety as a pilot location to explore the incident risk associated with unlined spillways. This project is not a dam failure investigation but an attempt to gain understanding of the potential transportation of sediment cover in the spillway, potential erosion of underlying bedrock, and subsequent deposition of eroded material downstream. An incident is an adverse occurrence that is visible and unusual enough to result in public concern or disruption (DSO, 2022). The importance of understanding incidents associated with spillways was highlighted by the recent spillway erosion event at Oroville Dam in California (Koskinas et al., 2019).

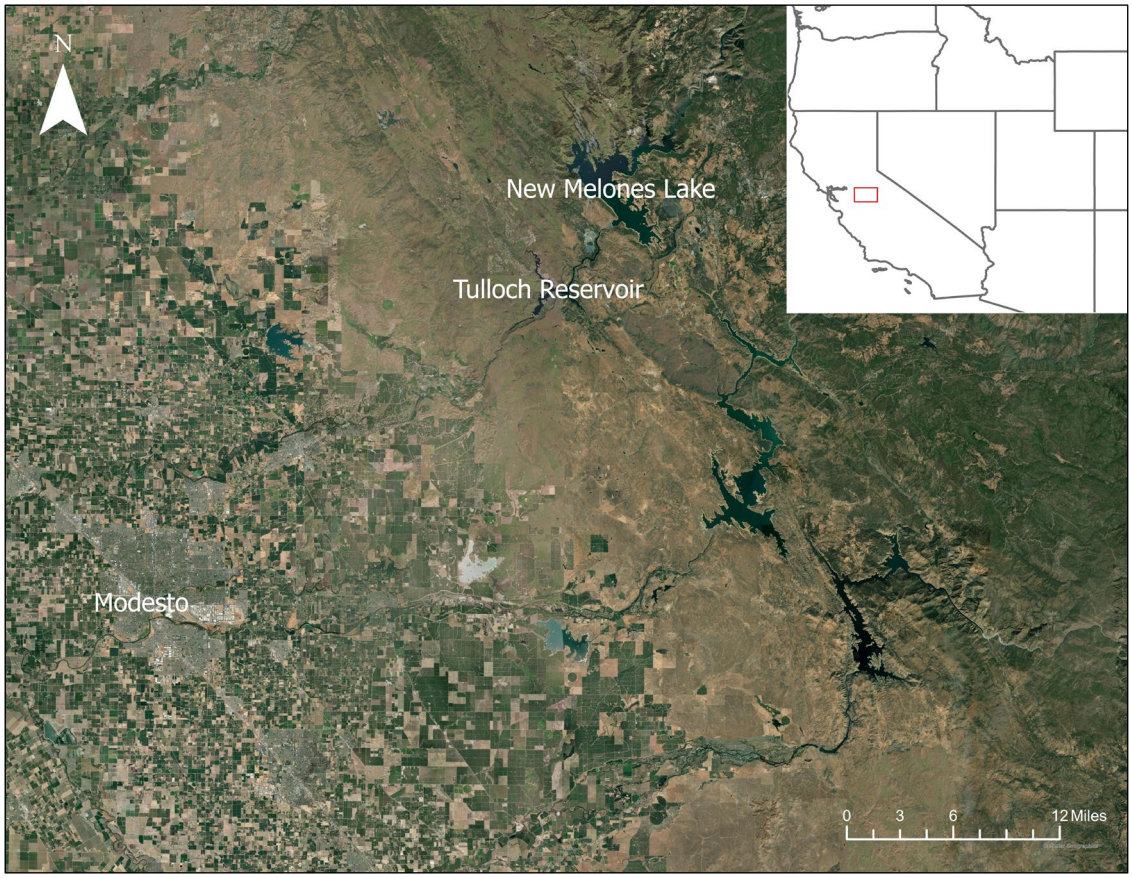

Figure 1.—New Melones Lake is located on the Stanislaus River about 45 miles northeast of Modesto, California. Tulloch Reservoir is downstream of New Melones Lake and is the downstream boundary condition for our model.

1.1 Study Site

The New Melones Reservoir is a 2,400,000 acre-foot (ac-ft) reservoir located on the Stanislaus River approximately 45 miles (mi) northeast of Modesto, California (Figure 1). The embankment dam was designed by the U.S. Army Corps of Engineers (USACE) and operated by Reclamation following completion in 1979. The reservoir stores water for irrigation, flood control, power generation, and recreation.

The main dam is a zoned earthfill and rockfill embankment with a structural height of 637 feet (ft) and a hydraulic height of 578 ft. It is the sixth tallest dam in the United States and the second tallest earthfill embankment dam. The emergency spillway is located approximately 1.5 mi north of the right abutment of the dam (Figure 2). The spillway consists of an unlined 5,945 ft long open channel blasted into rock. The channel bottom is approximately 200 ft wide with stepped, variable-sloped side walls and is covered with a thin layer of excavated debris and sediment (Figure 2). A reinforced concrete sill structure was constructed 2,170 ft downstream from the channel entrance. Discharge from the spillway exits onto a soil-covered hillslope on the left valley wall of a small stream, Bean Gulch, approximately one mile upstream from its confluence with the Stanislaus River. The confluence between Bean Gulch and the Stanislaus River is 2,900 ft below the New Melones Dam outlet (Figure 2). The discharge capacity of the spillway is 112,600 cubic feet per second (cfs) at water surface elevation 1,123.4 ft (Feinberg, 2009**)**.

The spillway area is generally covered by tan gravelly clay sand from two to six ft deep. Boreholes indicate that the bedrock is highly weathered to 10 to 25 ft depth (Department of the Army, 1979). The geology of the spillway channel is mostly meta-sandstone with lesser amounts of meta-basite, diorite, slate and meta-volcanics. The rock at the concrete sill invert is meta-tuff. The meta-sandstone is moderately hard and occurs in scattered lenses and layers from one to 20 ft thick. The downstream end of the spillway transitions to serpentinite, which is very soft and weathers into chips. Where the spillway joins Bean Gulch, the geology is also serpentinite (Holmes, 2021). The majority of the gulch channel follows the contact between serpentinite and diorite along the mile from the spillway outlet to the confluence with the Stanislaus River. From observation, most of the channel bottom in Bean Gulch is exposed bedrock, with limited sediment cover. To date, this spillway has not been utilized.

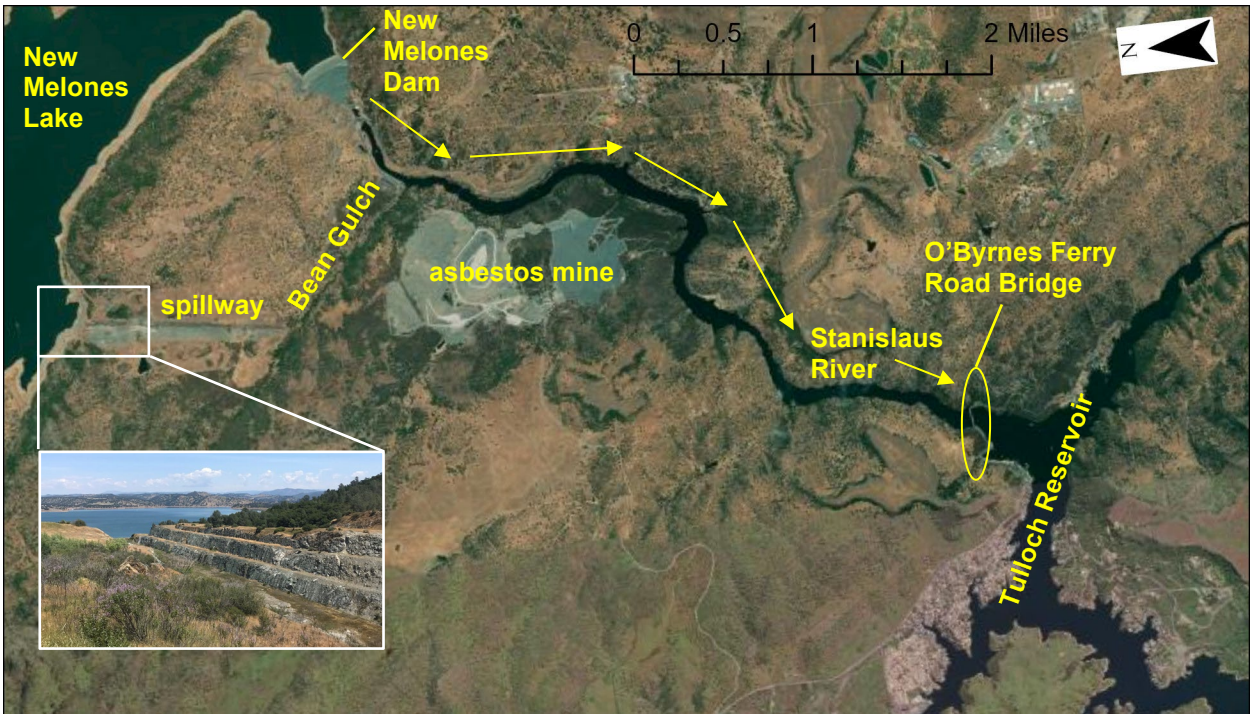

Figure 2.—Detailed site map of the study area using satellite imagery from ESRI Arc GIS. The inset figure is a photo taken from the hillside adjacent to the spillway, looking upstream (photo by M. Foster).

1.2 Study Purpose

This study aims to answer five key questions:

(1) Will a flow event on the New Melones Spillway erode the colluvial sediment overlying the spillway bedrock?

(2) Is bedrock on the spillway susceptible to erosion?

(3) Where will eroded sediment and rock transported by these flows be deposited?

(4) Will Tulloch Reservoir, located below the O'Byrnes Ferry Road Bridge (Figure 2), be impacted by deposition?

(5) Does a flow event on the New Melones Spillway likely result in a Dam Safety incident?

This study requires a model for an unlined spillway with variable lithology and the ability to model headward knick propagation. After extensive literature review, we identified several models that address spillway erosion. The most widely used are the SITES model, WinDAM, and the Comprehensive Scour Model (Bollaert, 2004; Wahl, 2016). However, these models typically apply a general erosivity parameter rather than explicitly dealing with erosion by

plucking or are only applicable within plunge pools and do not allow for knickpoint propagation. The New Melones Spillway erosion model requires a sediment transport model coupled with the physics-based model for bedrock erosion that was simple enough to constrain with geologic mapping and field observations.

Deposition associated with erosion of sediment and rock could impact the Stanislaus River and Tulloch Reservoir, located approximately 3.5 mi downstream. There is an environmental risk associated with rock erosion sourced from highly erodible serpentinite rock, located near the downstream end of the spillway. Even though New Melones Dam has never utilized the spillway, overland flow from precipitation and groundwater infiltration has eroded gullies into the serpentinite at the downstream end of the spillway, demonstrating the high susceptibility to erosion in a spillway flow event.

To meet the project needs, we developed a new three-tiered approach to spillway erosion that incorporated:

(1) **SRH-2D (Lai, 2010)**: a two-dimensional (2D) hydraulic and sediment transport model to calculate sediment transport of colluvium and alluvium by fluvial processes. We applied this model to the spillway, Bean Gulch (a small stream located immediately downstream from the spillway), and the Stanislaus River between the New Melones Dam outlet works and the upstream extent of Tulloch Reservoir, which we defined at the O'Byrnes Ferry Road bridge crossing the Stanislaus River.

(2) **Annandale 2D Erodibility Index model (Annandale, 1995)**: a 2D probabilistic model that identifies spatial zones at-risk for bedrock erosion. We applied this model to the spillway and Bean Gulch.

(3) **Hurst one-dimensional (1D) Erosion model (H1DE; Hurst et al., 2021):** a 1D bedrock incision model which calculates the timing and amount of bedrock eroded, incorporating upstream propagation of knickpoints (headcuts). We applied this model to the spillway and gully connecting the spillway to Bean Gulch (see reference locations in Figure 2).

We use this three-tiered approach to test the hypotheses that (1) most of the sediment cover will be eroded from the spillway, (2) bedrock erosion on the spillway will be minimal and concentrated at the downstream end of the spillway, and (3) sediment and rock eroded from New Melones Spillway and Bean Gulch will not result in significant deposition at Tulloch Reservoir. The results of our study will allow Dam Safety to make an informed decision as to whether this type of spillway erosional event constitutes an incident.

2.0 Data Collection

2.1 Topobathymetric Data

The topobathymetric surface used in this study combines bathymetric survey data collected by Reclamation's TSC and lidar data collected by the U.S. Geological Survey for Calaveras and Tuolumne counties in California (Figure 3). We conducted the bathymetric survey in October of 2020 and included the Stanislaus River from New Melones Dam to Tulloch Reservoir and the upstream portion of Tulloch Reservoir. The USGS collected lidar point cloud data between November 2011 and December 2011 and created a 1 meter (m) digital elevation model (DEM) (USGS, 2011). We combined the DEM and bathymetry data into a single surface using ArcMap v. 10.6. We interpolated across data gaps on the banks of the river and reservoir using the natural neighbor interpolation method. At the downstream end of Bean Gulch, we incorporated datapoints from a topographic foot survey using real-time kinematic (RTK) global positioning system (GPS) to track our horizontal and vertical position. All bathymetric and GPS points were collected in North American Datum 1983 (NAD 1983) and State Plane coordinates California III FIPS 0403 (US Feet) in the horizontal and North American Vertical Datum 1988 (NAVD 1988), Geoid 12A for the vertical. The details of the bathymetric survey are included in Appendix A.

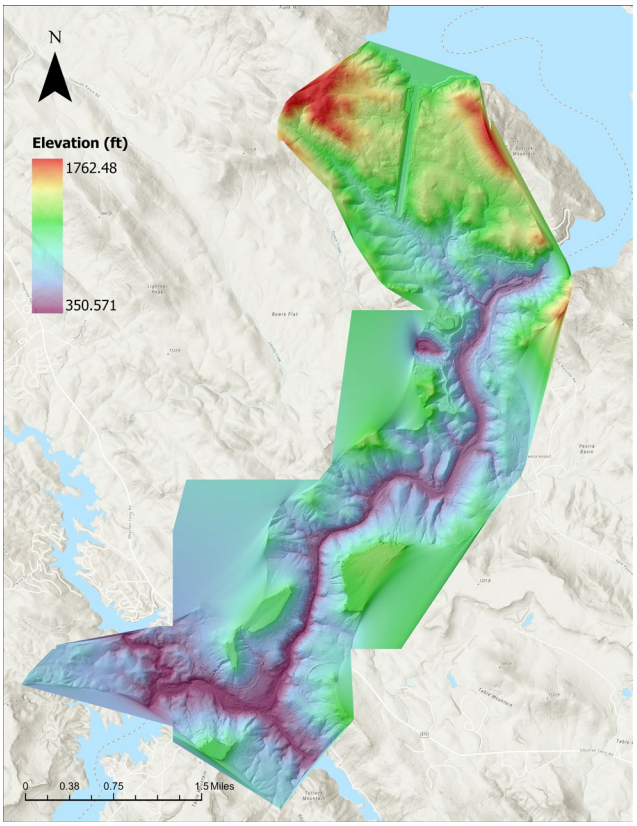

Figure 3.—Topobathymetric data extents. The raster surface covers the spillway, New Melones Dam, Bean Gulch, the Stanislaus River between New Melones and Tulloch Reservoir, and the upstream end of Tulloch Reservoir. The background image is a USGS Topographic map from ESRI. Flow direction in the Stanislaus River is from northeast to southwest.

2.2 Geologic and Sediment Data

2.2.1 Geologic Data, Holmes 2021

The Reclamation, California-Great Basin Region 10 (CGB) geologists performed geologic mapping at the New Melones Dam spillway in late March and early April 2021. The goal of the field geologic mapping was to provide engineering geology parameters to inform the current study of potential for rock erosion within the spillway and Bean Gulch. Four CGB geologists spent five days mapping the excavated portion of the spillway from Station 92+00 (a little upstream of the spillway invert) to 137+74.96 (end of spillway), and the gully that connects the end of the spillway with the upstream end of Bean Gulch. The geologists focused their mapping efforts on the first spillway bench, approximately 40 ft above the invert. CGB geologists extended prominent features above the first bench based on observations within the first 40 ft, but they did not actually access elevations above the first bench. Much of the rock invert was unable to be mapped due to vegetation, seepage ponding, and residual rock from excavation. We made educated interpolations across the invert for the final map used in this report. The geologists mapped and evaluated geologic contacts, lithology, major joints and joint sets, shear zones, foliation, weathering, alteration, and other engineering rock properties. Several hand samples were collected and shipped to TSC in Denver for further testing. They performed limited mapping within Bean Gulch.

The deliverables from this effort were the geologic report (Holmes, 2021), a geologic map, stereonets for joint orientations within the spillway and gully, and tables describing the jointing characteristics, rock quality, and lithology along the spillway. We modified the geologic map from Holmes (2021) to extend into Bean Gulch and to the confluence with the Stanislaus River (Figure 4). These modifications were based on a 1979 map generated by USACE during spillway development plans (Department of the Army, 1979).

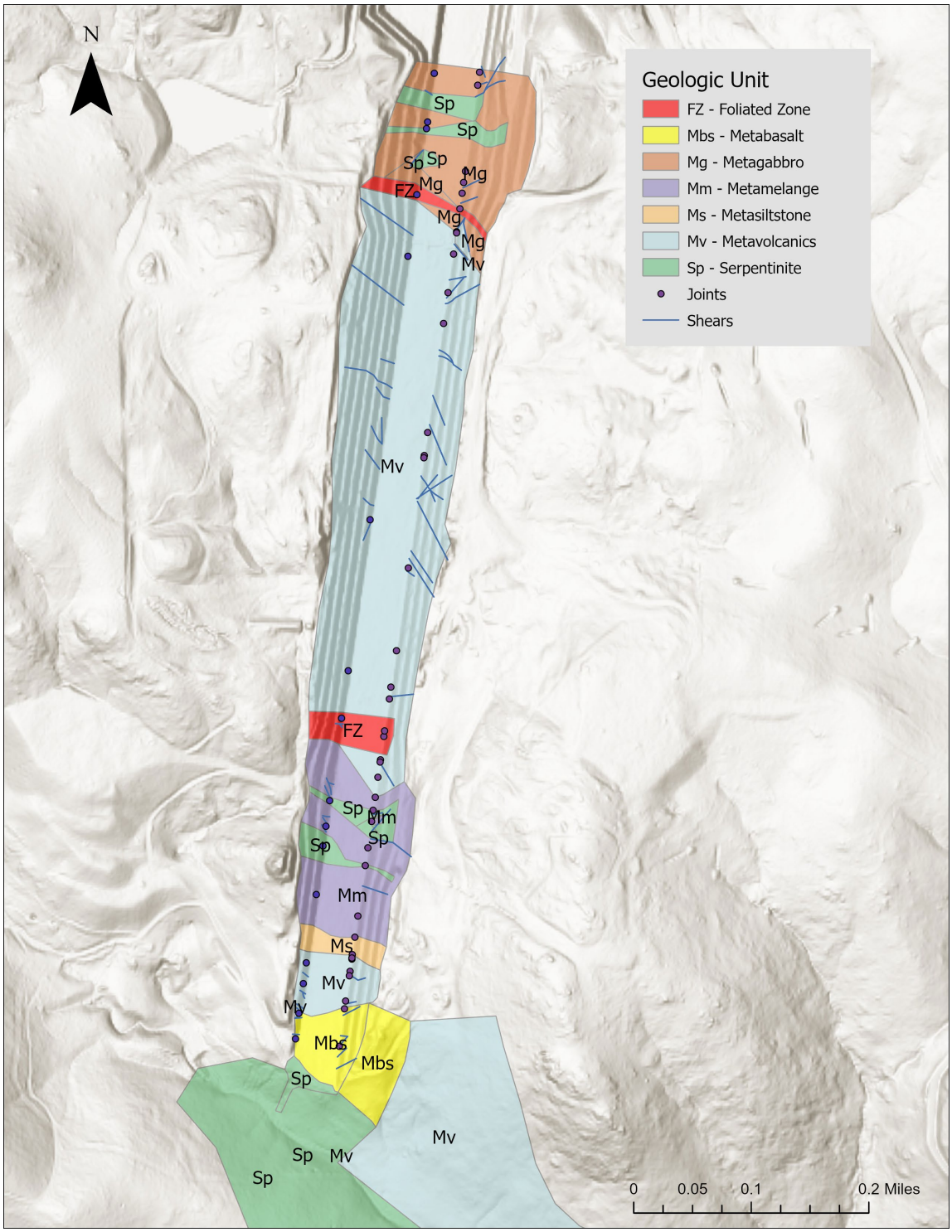

Figure 4.—Geologic map of the New Melones Spillway (modified from Holmes, 2021). We extended the map downstream into Bean Gulch using the 1979 USACE map (Department of the Army, 1979). The black dots are locations where the MP Geology team collected joint data, and the blue lines are mapped shears. Flow in the spillway travels from north to south.

2.2.2 Geophysical Data, Rittgers et al., 2020

Reclamation's TSC Geology & Geophysics Group collected seismic p-wave and s-wave velocity distributions to infer the depth to weathered bedrock (Figure 5). They also mapped the locations of electrical conductively zones and interfaces which indicate changes in rock properties and structural features (Rittgers, 2020). The depth to weathered bedrock likely overestimates the thickness of sediment cover, as highly fractured but in-place bedrock may be grouped into loose material overlying rock. However, the geophysical data were the only available source for sediment thickness for the majority of the model domain and these data were key to our estimates of sediment zone thicknesses in the sediment transport model.

We also utilized the 2D frequency-domain electromagnetic (FDEM) mapping to aid in geologic contact interpolation across the spillway. We overlaid the FDEM data on the geologic map and proprietary aerial imagery from Google Earth Pro. Changes in the electromagnetic resistivity aligned with visible lithology changes in the aerial imagery. We then extended geologic contacts across the spillway for later use in the 2D Annandale Erodibility Index Method by following the breaks in resistivity.

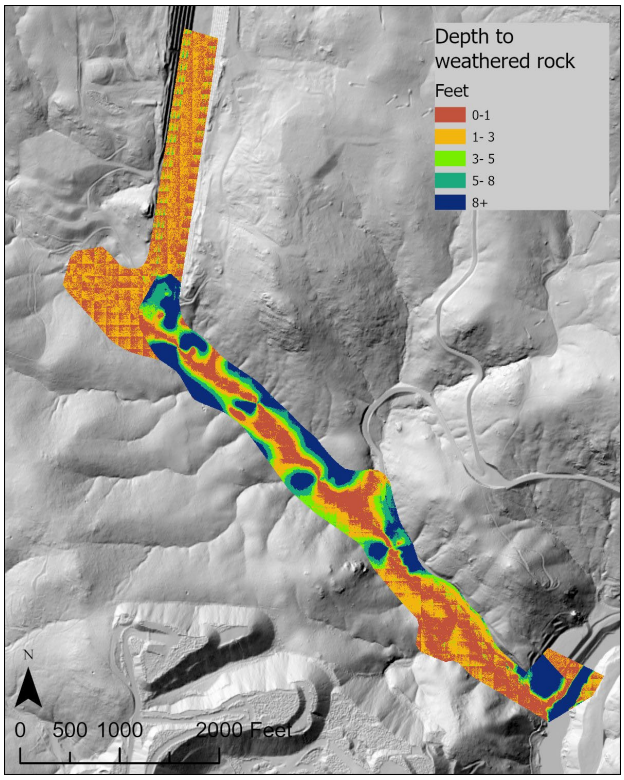

Figure 5.—Depth to bedrock, inferred from geophysical measurements. Data from J. Rittgers, Reclamation. The spillway and Bean Gulch are pictured, the confluence with the Stanislaus River is in the southeast portion of the figure.

2.2.3 Rock Density Measurements

We measured rock density for 23 hand samples from the spillway using the siphon can method. We first took the dry mass of each specimen. Each specimen was then placed in a siphon can filled with water. We used a beaker of known mass to collect the displaced water from the can and then weighed the water. Because 1 cubic centimeter (cm^3) of water weighs 1 gram (g), we were able to divide the mass of the sample by the mass of the displaced water to calculate the density. We averaged all the densities for each rock type in the spillway to get a mean density for that unit (Table 1).

Table 1.—Densities for each of the mapped rock units. Sample locations are shown in Figure 7. R indicates that the sample was taken from the right side of the spillway, and L indicates the left side of the spillway.

Rock Type (number of samples)	Density (g/cm^3)	Stations (ft)
Metavolcanic (5)	2.96	108+13 (R), 119+48 (R), 119+64 (R), 119+64 (R), 133+70 (R)
Metagabbro (2)	2.85	92+45 (R), 92+45 (R)
Metabasalt (2)	2.87	136+15 (R), 136+15 (R)
Serpentinite (5)	2.61	95+15 (L), 127+28 (R), 127+28 (R), 94+93 (R), BG2
Metamelange (2)	2.97	130+30 (L), 129+62 (R)
Foliated Zone (4)	2.68	97+95 (R), 98+30 (L), 121+64 (R), 122+50 (L)
Metasiltstone (3)	2.62	131+50 (L), 131+50 (L), 131+85 (R)

2.2.4 Additional Fracture Data, 2022

In August 2022, we collected additional fracture data in the spillway at locations marked in. For this collection effort, we measured the spacing between parallel joint sets in all visible orientations (Table 2). We took as many measurements as were available in each location and captured a photograph of the entire wall with a tape measure for scale so that we could map larger scale joint spacings using Adobe Illustrator (i.e., Figure 6). The measurements were assigned a label (dx, dw, or dz) corresponding to how their orientations aligned with the orientation of a block in our model. dx is the downstream length, dw is the cross-stream width, and dz is the height of a block.

Table 2.—Fracture spacing data collected at New Melones Dam's spillway. dx, dw, and dz are shown as a mean value +/- a standard deviation. Hyphens indicate areas where we couldn't measure that fracture orientation. IDs have the form FS for fracture spacing, the measurement location number, and then R or L for right or left spillway.

ID	dx (m)	dw (m)	dz (m)
FS1-L	-	-	6.22 +/ -1.37
FS1-R	cohesive	cohesive	cohesive
FS2-L	0.22 +/ -0.07	-	1.47 +/ -1.11
FS3-L	-	-	6.48 +/ -5.91
FS3-R	5.05 +/ -14.1	-	0.49 +/ -0.52
FS4-L	4.54 +/ -4.49	-	2.58 +/ -3.51
FS5-R	0.26 +/ -0.36	0.33 +/ -0.56	0.33 +/ -0.46
FS6-L	-	-	0.75 +/ -0.75
FS6-R	-	-	0.26 +/ -0.26

Table 2.—Fracture spacing data collected at New Melones Dam's spillway. dx, dw, and dz are shown as a mean value +/- a standard deviation. Hyphens indicate areas where we couldn't measure that fracture orientation. IDs have the form FS for fracture spacing, the measurement location number, and then R or L for right or left spillway.

ID	dx (m)	dw (m)	dz (m)
FS7-L	-	0.98 +/ -0.56	1.64 +/ -3.87
FS8-L	3.99 +/ -1.39	-	4.64 +/ -3.99
FS8-R	0.75 +/ -0.13	-	0.39 +/ -0.13
FS9-L	-	-	0.82 +/ -1.28
FS10-R	0.13 +/ -0.07	-	1.87 +/ -0.43

Figure 6.—An example of fracture spacing in the spillway. Dx is in the red dashed line, dz is in the yellow dashed line, and dw would project into the page.

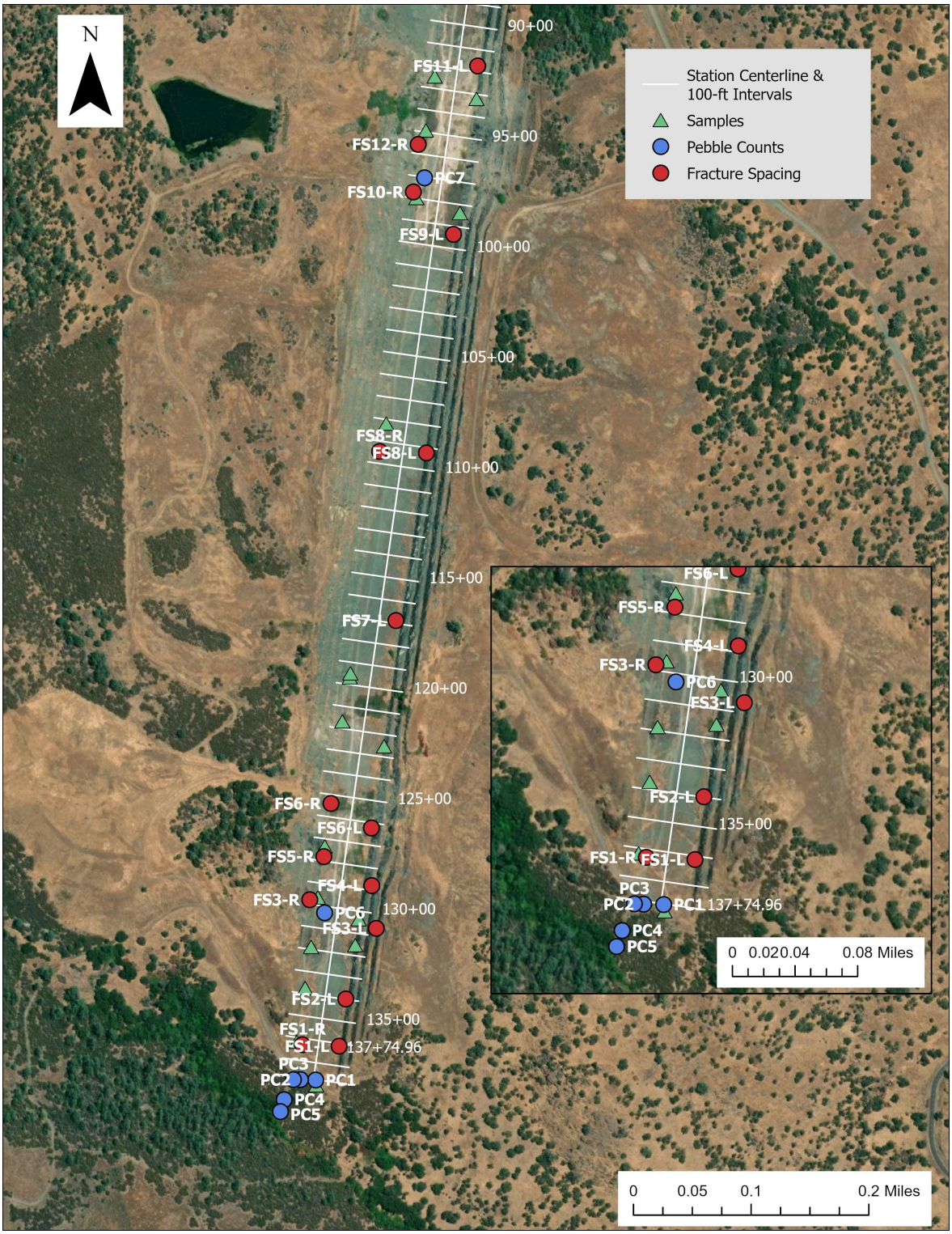

Figure 7.—Pebble count data (blue circles), fracture spacing data (red circles), and samples for rock density measurements (green triangles) were collected along the entirety of the spillway. FS11-L and FS12-R were not included in the fracture spacing analysis because the 1D model only extends from the invert to the base of the gully. The inset shows more detail at the downstream end of the spillway and within the gully. The basemap is from ESRI World Imagery data.

2.2.5 Pebble Count Data, 2022

We collected modified Wolman pebble count data in August of 2022 (Wolman, 1954; locations in Figure 7). We measured the B-axis of thirty random samples at 4 locations in the gully between the spillway and Bean Gulch and three locations in the spillway (Appendix B). These data were used to generate grain size distributions on the spillway and in the gully (Figure 8).

Pebble counts are collected on the ground surface and can represent the sediment size distribution throughout the sediment layer if the deposit or alluvial cover is uniform with depth. This assumption is dubious for the spillway sediment, where deeper layers may consist of fractured rock generated during spillway blasting. Therefore, we suspect that the sediment cover consists of a higher fraction of coarse sediment than the Wolman pebble counts represent. To adjust the data to account for coarser sediment with depth, we adjusted the percentage of grains coarser than 250 millimeters (mm) to 15% and percentage of grains coarser than 600 mm to 5% (Figure 8b). We ran our sediment transport models using this assumed coarse fraction on the spillway but conducted a sensitivity test using the original grain size distribution (Figure 8a). We note that we originally planned to include a test pit as part of the geological investigation. This would confirm or refute the presence of coarser grains with depth, but only localized to the location of the test pit. Ultimately, due to scheduling difficulties resulting from the COVID-19 pandemic, we opted to omit the test pit unless our study indicated that further investigations should be conducted on the spillway.

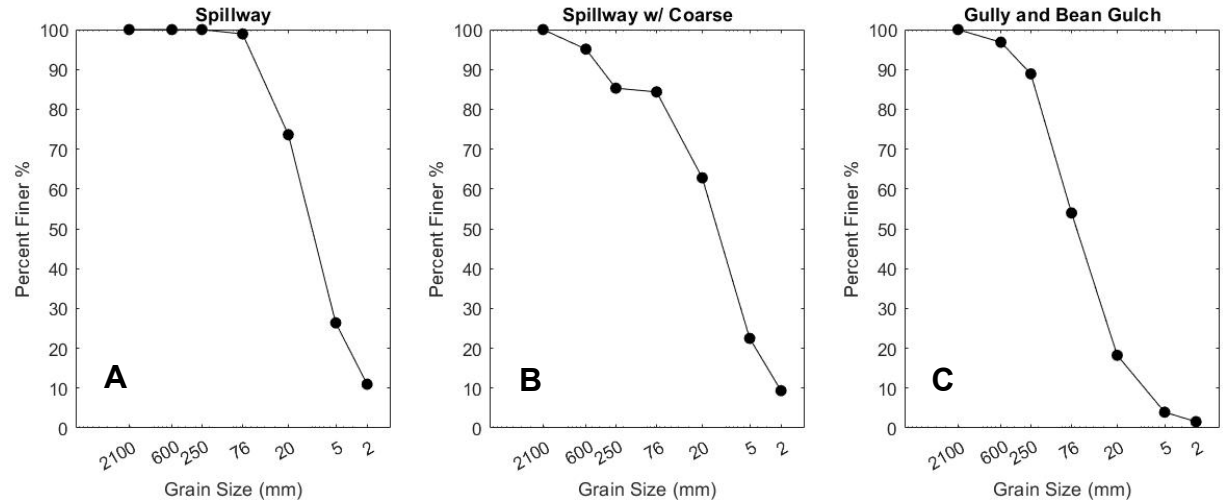

Figure 8.—Pebble count data, show at major grain size breaks. (A) Amalgamated data for 3 pebble count locations on the New Melones Spillway. (B) Adjusted data (from A) on the New Melones Spillway to account for coarser grain size beneath the surface. (C) Amalgamated data for 4 pebble count locations on the hillslope gully downstream from the spillway and at the confluence between the gully and Bean Gulch.

2.3 Hydrology Data

We acquired hydrology data from Jason Schneider in the Reclamation TSC Civil Engineering Services group. They provided spillway and outlet works discharges for a range of flood recurrence intervals (RI). The flood routing results came from the 2007 flood routing effort. New Melones Reservoir flood control goals include maintaining flows less than 8,000 cfs in the Stanislaus River. Therefore, this flood routing assumed that the outlet works would operate at 8,000 cfs or less until the spillway starts operating. Once flow breaches the spillway, the outlet works release is decreased to avoid exceeding the 8,000 cfs maximum. When spillway flows meet or exceed 8,000 cfs, the outlet works cease operation until the spillway discharge drops below 8,000 cfs again (J. Schneider, 3/20/2020).

The flood routings have initial New Melones Reservoir water surface elevations (NM WSE) at New Melones Lake of 1,049 ft and 1,088 ft (NM1049 and NM1088). The lower initial NM WSE results in lower peak flows for the same RI (Figure 9). The 1 million year (Myr) flow for a NM1049 has a slightly lower peak than the 5 thousand year (kyr) flow for NM1088, for example. The maximum peak flow discharge on the spillway for the modeled flow events is 124,404 cfs for the 1 Myr RI event (NM1088) (Table 3). The lowest peak flow discharge on the spillway is 3,523 cfs for the 20 kyr RI event (NM1049), with a concurrent release of 4,477 cfs at the outlet works (Table 3); thus, the cumulative flow is 8,000 cfs.

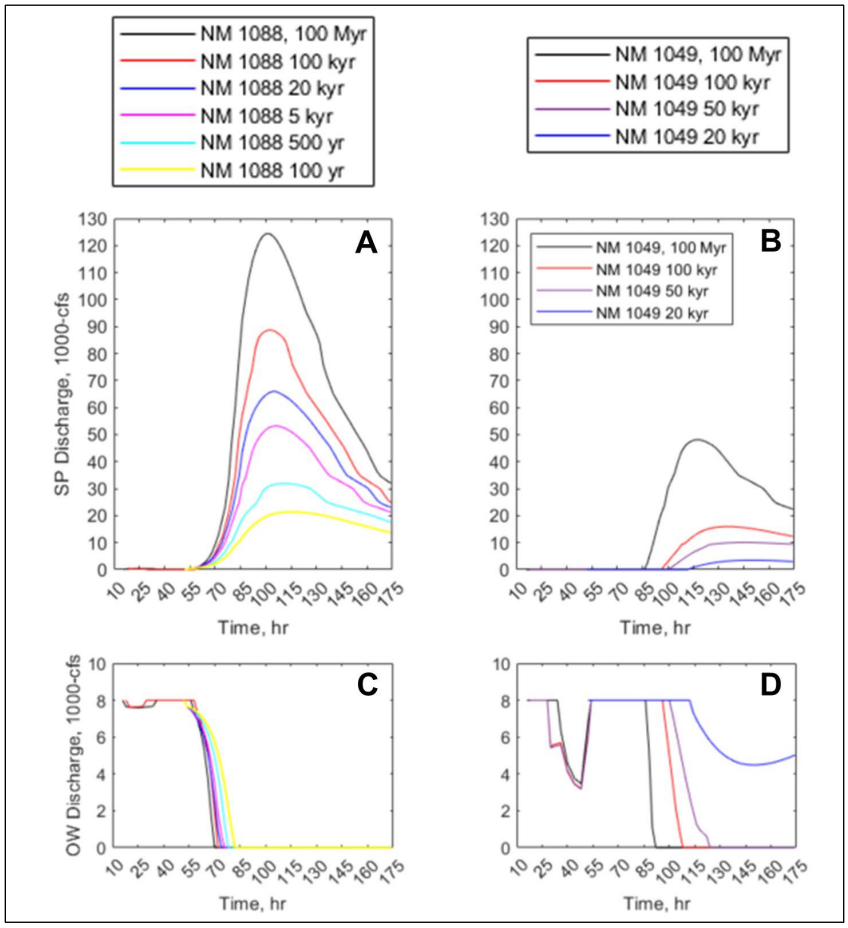

Figure 9.—Spillway flow hydrographs (A,B) and outlet works hydrographs (C,D) for modeled flood events. Floods are labeled by recurrence intervals (RI) and starting water surface elevations (WSE) in New Melones (NM) Reservoir of 1088 ft (left plots A and C) and 1049 ft (right plots B and D).
Note that the lower water surface elevation results in lower peak flows; the 1 Myr flow with a starting NM WSE of 1049 ft has a slightly lower peak flow than the 5 kyr flow with a starting NM WSE of 1088 ft.
Myr= million year; kyr = thousand year; yr= year; SP= spillway; OW= outlet works.

Table 3.—Peak flows on the New Melones Spillway for each hydrograph and concurrent flow from the New Melones Dam outlet works

RI (years)	NM WSE (ft)	Spillway Discharge (cfs)	Outlet Works Discharge (cfs)	RI (years)	NM WSE (ft)	Spillway Discharge (cfs)	Outlet Works Discharge (cfs)
20 kyr	1,049	3,523	4,477	100 yr	1,088	21,342	0
50 kyr	1,049	10,102	0	500 yr	1,088	31,911	0
100 kyr	1,049	15,962	0	5 kyr	1,088	53,220	0
1 Myr	1,049	48,121	0	20 kyr	1,088	65,977	0
				100 kyr	1,088	88,706	0
				1 Myr	1,088	124,404	0

RI = Recurrence Interval
NM WSE = New Melones Water Surface Elevation

2.4 Tulloch Water Surface Elevation

Water surface elevations (WSE) at the downstream boundary of Tulloch Reservoir fluctuate between 485 ft and 512 ft, with typical operations between 500 and 512 ft (USGS gage 11299995; Figure 10). Tulloch WSE operations are independent of discharge coming out of New Melones Dam, as measured on the Stanislaus River (USGS gage 11299200; Figure 11). We therefore chose to hold the downstream boundary condition at Tulloch Reservoir constant at four different WSEs (base level): 500 ft, 505 ft, 510 ft, and 515 ft. We assume that during high flow events where New Melones Reservoir is full, Tulloch Reservoir is also likely relatively full. Therefore, 505 ft was chosen as our primary comparative WSE in our model runs and represents a worst-case scenario for potential sediment deposition within the Stanislaus River and Tulloch Reservoir.

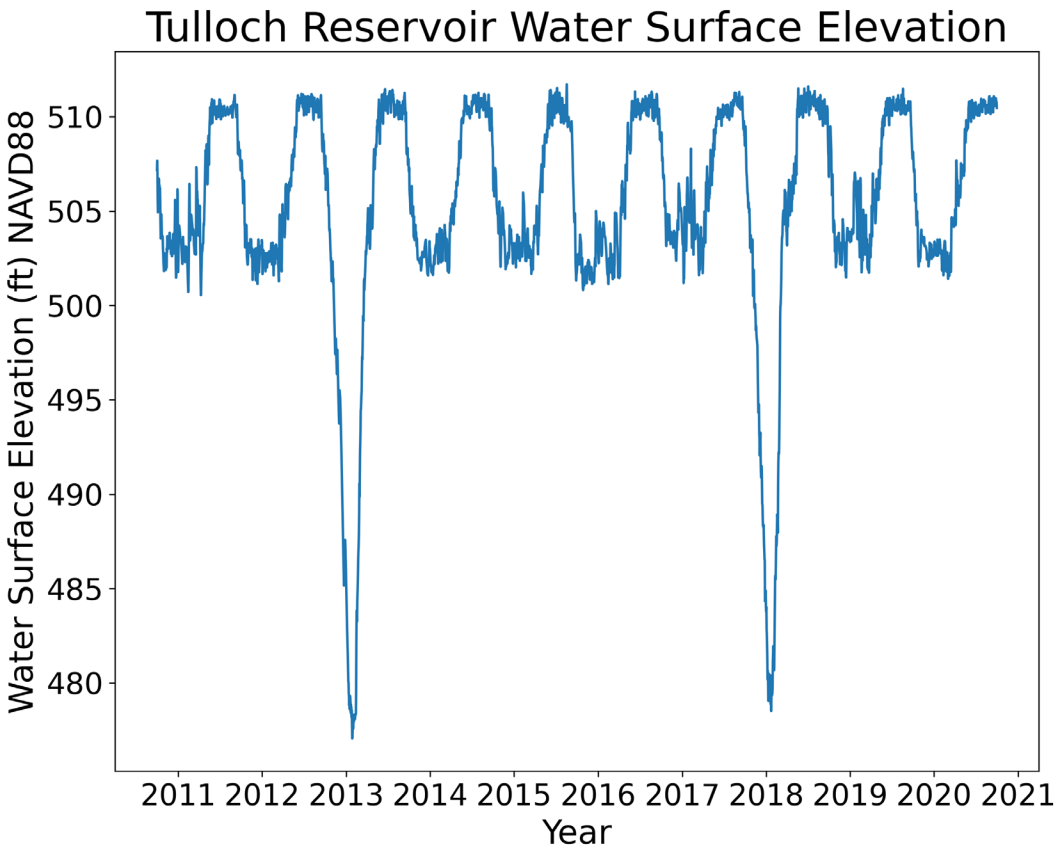

Figure 10.—Historical water surface elevations (WSE) for Tulloch Reservoir (USGS gage 11299995) typically fluctuate between approximately 500 and 512 ft. Extreme drawdowns can drop the WSE to around 480 ft.

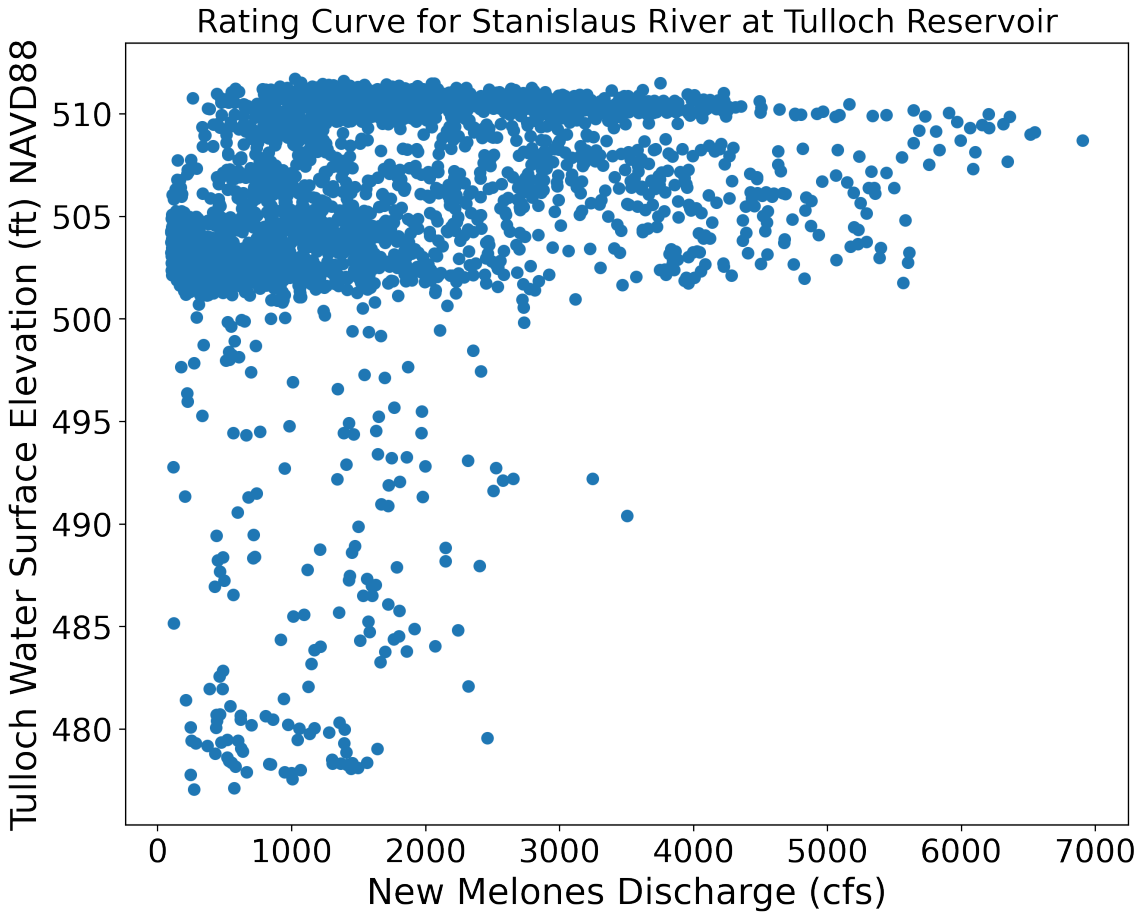

Figure 11.—The rating curve for Tulloch Reservoir water surface elevation is independent of the discharge released from New Melones Dam (USGS gage 11299200).

3.0 Modeling Methods

We applied a three-tiered approach to model the risk of erosion and the volumes and locations of potential deposition for the New Melones Spillway, Bean Gulch, and the Stanislaus River. The first step applied the SRH-2D flow and sediment transport models to calculate locations of sediment erosion and subsequent deposition. Once the sediment cover has been removed, the second tier of the approach then applies a 2D version of the Annandale Erodibility Index Method to look at where the spillway is likely to erode and generate new sediment. We finally apply the H1DE model to calculate the timing, location, and volume of eroded bedrock material in the spillway. We used the combination of the Annandale Erodibility Index Method and H1DE model because the H1DE model is time-intensive to run and only accounts for 1D hydraulics. The Annandale Erodibility Index Method can be used to locate at-risk areas that can then be analyzed in more detail with the H1DE model. We outline all three of these models in the following sections.

3.1 SRH-2D Flow and Sediment Transport Model

3.1.1 SRH-2D Model Background

SRH-2D uses an unstructured hybrid mesh to model open channel flow. The hybrid mesh consists of quadrilateral and triangular cells (elements) that the user constructs using a zonal approach. Quadrilateral cells are computationally efficient and commonly used to fill stream channels whereas triangular cells best fill irregular geometries. The user may also increase the mesh density, or total number of cells, in zones of interest. The model solves 2D depth-averaged St. Venant equations at the center of a mesh element. The model is robust, handling the wetting and drying of cells without stability issues, simulating flows from subcritical to supercritical, and handling both steady and unsteady flow scenarios (Lai, 2010).

SRH-2D simulates flow with either a static or mobile bed scenario. A static bed does not simulate sediment transport and the bed does not change throughout the model. The mobile bed scenario does allow sediment transport and the bed elevation will decrease due to erosion or increase due to deposition. The sediment model simulates fractional transport for different particle size classes using a variable-load sediment transport equation (Greimann, 2008), where a transport mode parameter is introduced to simultaneously model suspended load, bed load, and mixed load (Lai, 2020). Sediment transport is calculated at element nodes (corner points of an element) offset from the modeled flow solution at cell centers. In the model, the active layer of the streambed can exchange sediment with the stream channel's substrate alluvium; underlying bedrock is not eroded. The user can adjust the sediment thickness from no cover (bedrock river) to a thin alluvial cover (more like a mixed-bedrock alluvial river), or to a thick alluvial cover (alluvial river). The model allows the user to apply one of several equilibrium sediment transport equations to obtain the total load transport capacity, although Lai (2019) suggests specific transport models for various sediment layer characteristics. For mixed-gravel and sand bed rivers, Lai (2019) recommends implementing the Parker sediment transport equation (Parker, 1990; Andrews, 2000).

3.1.2 SRH-2D Model Application to New Melones Spillway

The SRH-2D model applied the topobathymetric elevation data for the New Melones Spillway, Bean Gulch, and the Stanislaus River to the model mesh (Figure 3; Figure 12). The model contained two inlet boundary conditions: the spillway and the New Melones Dam outlet works. There was a single downstream boundary flow exit near Tulloch Reservoir on the Stanislaus River (Figure 12). The inlet boundary conditions input a constant discharge to test for the initiation of sediment transport (Table 4) or flow hydrograph to mimic a storm event (Figure 9). Since Tulloch Reservoir water surface elevations are not dependent upon the incoming flow, we used a constant water surface elevation between 500 ft and 515 ft at the downstream boundary, based on typical reservoir data (Figure 10).

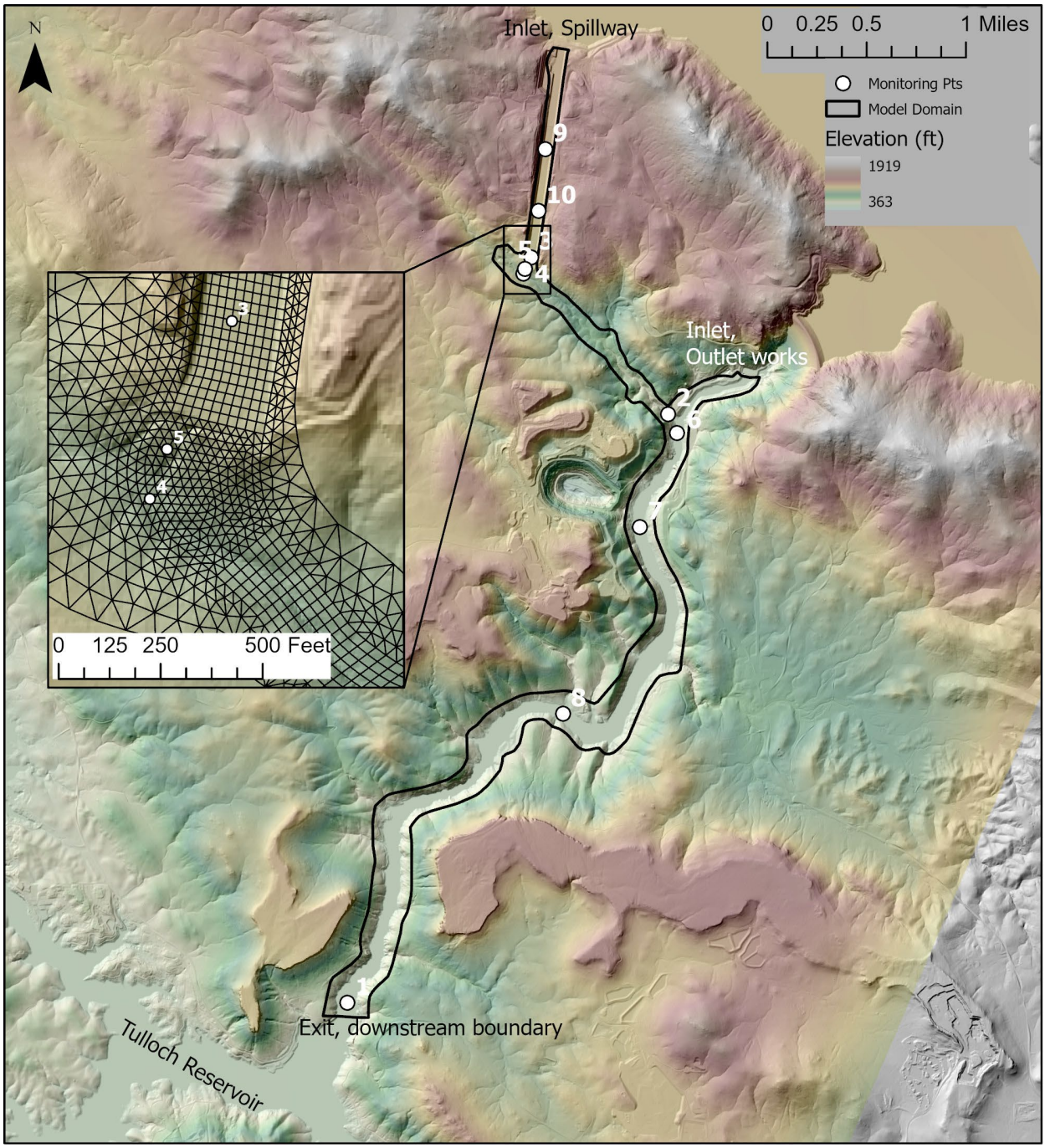

Figure 12.—SRH-2D model domain, showing model inlets (upstream boundaries) and model exit (downstream boundary). The inset figure shows the model mesh detail at the junction between the spillway and Bean Gulch. Monitoring points (MPs), which contain detailed model output, are also shown. Flow is from inlet to exit, generally north to south. The figure backdrop is elevation values draped upon a hillshade image.

SRH-2D calculates bed friction using the Manning's roughness coefficient *n*, applied to the mesh elements. SRH-2D treats the Manning's coefficient as a constant that does not change with flow, unless the user selects different meshes for different flow ranges. The model is most often run with constant Manning's *n* values that vary spatially and remain constant through time. We mapped various stream and land cover characteristics to constrain the Manning's *n* roughness values for the model based on observations, professional judgement, and literature (Table 5; Chow, 1959; Phillips and Tadayon, 2006; Figure 13). When calibration data exist, Manning's *n* is the recommended parameter to adjust. There are no calibration data for the flood events we tested, and the water surface elevations in this model are controlled by the downstream Tulloch Reservoir. Uncertainty in the roughness will lead to uncertainty in the final water surface elevations and modeled hydraulics. However, we did not test the model sensitivity to roughness as the model uncertainty associated with potential flow hydrographs and sediment cover characteristics likely exceed the uncertainty due to roughness.

Table 4.—Steady flows to test initiation of motion on the spillway

Spillway, cfs	Outlet works, cfs
50	7950
100	7900
250	7750
500	7500
1000	7000
2000	6000
3000	5000
4000	4000
5000	3000

Table 5.—Roughness values assigned to mapped land use type

Land use ID	Land use type	Manning's Roughness (*n*)
1	smooth grass (not dense)	0.030
2	predominantly coarse stream bed	0.032
3	spillway/ smooth rock	0.040
4	cobbles with large boulders	0.050
5	light to medium vegetation	0.060
6	dense vegetation	0.070

The mobile bed model simulation requires information about the sediment stratigraphy or sub-surface layering, sediment thickness, and grain size distribution for each defined sediment zone (Figure 13). Lai states at least two layers are necessary to model sediment erosion, even if the sediment properties are the same (Lai, 2020). We used two layers with the same properties since we did not have subsurface data to support further precision. For Sediment Zone 2 (Figure 13), where bare bedrock is exposed, we used a value of 0 for sub-surface layers, which allows for deposition on a non-erodible bed.

On the spillway and in Bean Gulch, we inferred sediment thickness based on geophysical data (Figure 5), geologic data (Holmes, 2021), and field observations. The depth to weathered rock can in some cases overestimate the thickness of alluvium or soil, as highly fractured but in-place immobile saprolite may be excluded from bedrock based on geophysical properties. In the spillway, we wanted to ensure that we didn't underestimate the sediment thickness, and thus underpredict the impact of sediment deposition downstream. The geophysical data indicate a thickness of 1-3 ft, but the data do not cover the entirety of the spillway. Holmes (2021) states that the volume of residual debris and rock fragments on the spillway invert may be as much as 210,000 yd^3; this volume of sediment equates to approximately 5.4 ft of uniform sediment thickness across the spillway. We used the 5.4 ft thickness (Sed Zone 1 in Figure 13; Table 6), but also tested the model sensitivity to thicker and thinner spillway cover. In reality, there are bedrock outcrops visible on the spillway surface and likely pockets of deep sediment cover. However, we do not have the available data to map sediment cover with this level of precision and decided a uniform sediment cover was best. We used a grain size distribution in the spillway based on pebble counts and assumed that coarser grains exist under the surface (Figure 8b). In areas surrounding the spillway, where bare bedrock is visible, we used a sediment thickness of 0 ft (Sed Zone 2, Figure 13; Table 6).

At the end of the spillway, a narrow, erosional gully formed from surface runoff down the hillslope to Bean Gulch. Descriptions within the gully indicate that 2 ft of saprolite and soil overlie intensely weathered serpentinite. CGB geologists used a crude method of advancing a steel rod into the ground to estimate thickness of overburden soils on top of bedrock. They noted thinner cover than the geophysical estimates, at 0 to 6 inches with abundant bedrock outcrops of metavolcanic (Mv) rock (Holmes, 2021). Based on these data, we used a 1 ft thickness of sediment in the Bean Gulch channel and adjacent hillslopes (Sed Zone 4) and a grain size distribution based on pebble count data (Figure 8c). We used thicker sediment cover (Sed Zones 3 and 5) on the surrounding hillslopes where the geophysical data indicated very thick cover (Figure 5; Table 6). For Sediment Zone 3, we used the same grain size distribution as Bean Gulch. For Sediment Zone 5, we used the same grain size distribution as the upstream end of the Stanislaus River (also mapped as Sediment Zone 5 because we estimated the same approximate 8 ft sediment cover thickness, described below).

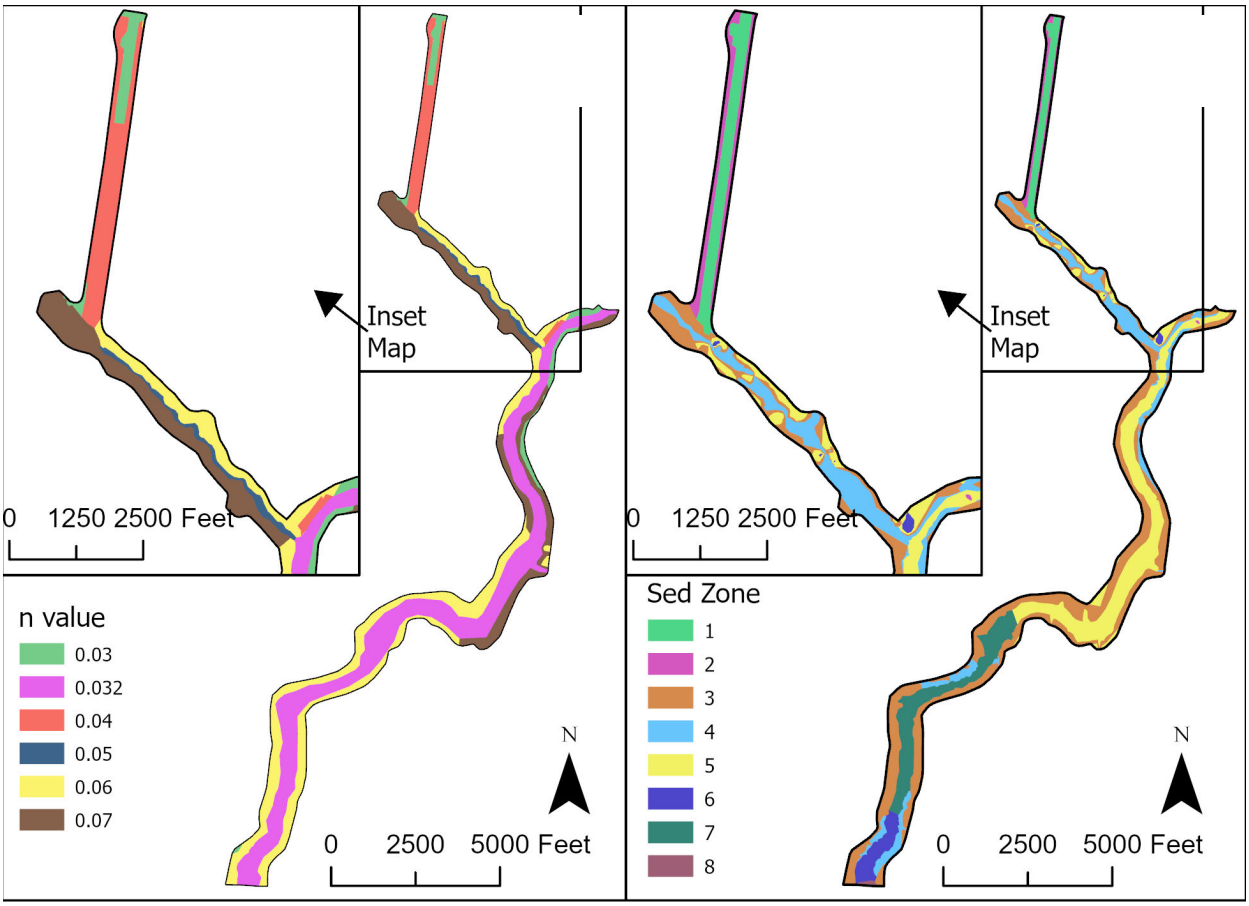

Figure 13.—A. Spatial mapping for Manning's *n* values, which represent resistance to flow. B. Spatial mapping for sediment zones, which have unique characteristics for sediment size distribution and depth to bedrock. Flow is from north to south.

Table 6.—Sediment Zone thickness and gradation

Sed Zone	Thickness (ft)	Cumulative % finer						
		2 mm	5 mm	20 mm	76 mm	250 mm	600 mm	2100 mm
1	5.4	9	22	63	84	85	95	100
2	0	-	-	-	-	-	-	-
3	4	2	4	18	54	89	97	100
4	1	2	4	18	54	89	97	100
5	8	5	8	20	60	89	97	100
6	15	8	11	27	70	97	100	100
7	11	7	10	25	65	95	99	100
8	20	8	11	27	70	97	100	100

Outside of Bean Gulch and the spillway, we did not have pebble count data or sediment thickness data for the Stanislaus River. The entire reach of the Stanislaus River is backwatered, and we suspected that very little erosion was likely to occur within this reach. Most likely, we hypothesized that sediment transported from the spillway and Bean Gulch would deposit in the Stanislaus River and distribute some distance downstream. Therefore, the grain size assumptions for Sediment Zones 5-8 mapped in the Stanislaus River are less important than in zones likely to erode. Our field observations indicated a mix of grain sizes. To approximate sediment characteristics, we adjusted data from Bean Gulch to increase sediment thickness and decrease grain size with distance downstream, as the river approached the Tulloch Reservoir delta (Figure 13; Table 6).

SRH-2D treats cohesive sediment differently than non-cohesive sediment. However, pebble count data did not indicate a large fraction of fine-grained Sediment (Appendix B; Figure 8). We used a minimum grain size of 0.04 mm, but less than 2% of the sediment had a grain size less than 2 mm in the spillway and Bean Gulch. Pedogenic clay likely exists on hillslope soils. However, most of the flow from the spillway will likely flow predominately through an incised gully where soil cover has been removed or is thin. The spatial extent of hillslope erosion is small compared to the overall model. Therefore, we did not account for any cohesive sediment.

For the SRH-2D sediment transport equation, we followed Lai's (2019) recommendation for the Parker equation (Parker, 1990). We also conducted a subset of simulations using the Wilcock and Wu transport equations to test the model's sensitivity to the transport equation (Wilcock and Crowe, 2003; Wu et al., 2000). These transport equations are also appropriate for mixed sand and gravel bed rivers; however, the Wu and Wilcock transport equations more commonly exhibit numerical instability when implemented in SRH-2D (Y. Lai, oral comm. 1/29/2023). For all scenarios, we used the default parameters for each capacity formulation. This includes a constant adaptation length for bedload transport of gravels, which is the distance traveled by sediment in a constant flow environment. The recommended length is 1 to 5 times the channel width. The channel width throughout our model changes greatly and we selected a length of 155 meters (~500 ft) to fall within the appropriate range throughout the model domain. For the active layer, which helps constrain how sediment is exchanged between bedload and the stream bed, we used the default of $T_{PARA} \cdot D_{90}$, where the active layer is defined as a multiple of D_{90} based on empirical data (Lai, 2019). Because T_{PARA} is between 1 and 3 for gravel bed rivers, we used T_{PARA} equals 2. The D_{90} represents the diameter at which 90% of the grains are finer and varies depending on the Sediment Zone (see input gradations in Table 6). These selections are shown on the Script Input File (SIF), a text file read by the model preprocessor containing user-specified parameters and data inputs. An example SIF file illustrating these parameters is included for the 100 kyr recurrence interval flow for a starting New Melones Reservoir elevation of 1088 ft and Tulloch Reservoir elevation of 505 ft (Appendix C; Table A-2).

3.2 2D Annandale Erodibility Index Method

We applied the Annandale Erodibility Index Method in two-dimensional space to generate a 2D map of erodibility within the spillway and Bean Gulch. The primary inputs for this methodology were the geologic data collected within the spillway and Bean Gulch (Holmes, 2021). The Annandale Erodibility Index Method (Annandale, 1995) parameterizes the erosive power of water such that parameters that can be easily measured in the field can then be related to the likelihood that rock or soil will erode due to the shear stress exerted by the flow. The energy exerted by the water is represented using stream power, and the erodibility index, K_h, is used to represent an earth material's resistance to erosion, where:

$$\boldsymbol{K_h = M_s K_b K_d J_s} \quad \textbf{[1]}$$

M_s is the mass strength number, K_b is the particle or block size number, K_d is the discontinuity or inter-particle bond shear strength number, and J_s is the relative ground structure number. All of these parameters can be readily assessed in the field and are based on standard tables from Kirsten (1982).

At Reclamation, standardized methods are used to collect geologic data, which we describe in Section 2.2.1. We translated the Reclamation standards to the inputs for K_h in Equation 1 (Table 7-Table 9). We then used the geologic data to generate individual maps for each of these parameters (Figure 14 and Figure 15).

We calculated M_s by converting the Reclamation Field definitions of Hardness (Reclamation, 1998) to the International Society for Rock Mechanics (ISRM) Standard Rock Strength Field Determination (Barton, 1978). The ISRM value utilizes an unconfined compressive strength (UCS), which is directly related to M_s. In cases where there was potential overlap between two categories, we chose the more conservative estimate of M_s that would make the rock more susceptible to erosion. We also prioritized descriptions over UCS in categories that were up to interpretation. The conversions are outlined in Table 7, and the resulting M_s map boundaries in Figure 14a were drawn along the geologic boundaries from Figure 4.

Table 7.—Mass strength number (M_s) conversion

Reclamation Field Definitions of Hardness			ISRM Rock Strength Field Determination				Annandale Mass Strength Number for Rock (M_s)			
Label	Hardness	Identification in Profile	Label	Hardness	Identification in Profile	UCS (MPa)	UCS (MPa)	Hardness	Identification in Profile	Mass Strength Number (M_s)
H1	Extremely hard	Core, fragment, or exposure cannot be scratched with knife or sharp pick; can only be chipped with repeated hammer blows	R6	Extremely strong	Specimen can only be chipped with geological hammer.	>250	>212	Extremely hard rock	Specimen requires many blows with geological pick to break through intact material.	280
H2	Very hard	Cannot be scratched with knife or sharp pick. Core or fragment breaks with repeated heavy hammer blows.	R5	Very strong	Specimen requires many blows of a geologic hammer to break intact sample.	100-250	53-106	Very hard rock	Hand-held specimen breaks with hammer end of pick under more than one blow.	70
H3	Hard	Can be scratched with knife or sharp pick with heavy difficulty (heavy pressure). Heavy hammer blow required to break specimen.	R4	Strong	Specimen requires more than one blow of geological hammer to fracture it.	50-100	26.4-53	Very hard rock	Hand-held specimen breaks with hammer end of pick under more than one blow	35
H4	Moderately Hard	Can be scratched with knife or sharp pick with light or moderate pressure. Core or fragment breaks with moderate hammer blow.	R3	Medium strong	Specimen cannot be scraped or cut with a pocket knife. Specimen can be fractured with single firm blow of geologic hammer.	25-50	13.2-26.4	Hard rock	Cannot be scraped or peeled with a knife; hand-held specimen can be broken with hammer end of geological pick with a single firm (moderate) blow.	17.7

Table 7.—Mass strength number (M_s) conversion

Reclamation Field Definitions of Hardness			ISRM Rock Strength Field Determination				Annandale Mass Strength Number for Rock (M_s)			
Label	**Hardness**	**Identification in Profile**	**Label**	**Hardness**	**Identification in Profile**	**UCS (MPa)**	**UCS (MPa)**	**Hardness**	**Identification in Profile**	**Mass Strength Number (M_s)**
H5	Moderately Soft	Can be grooved 1/16 inch (2mm) deep by knife or sharp pick with moderate or heavy pressure. Core or fragment breaks with light hammer blow or heavy manual pressure.	R2	Medium weak	Shallow cuts or scrapes can be made in a specimen with a pocket knife. Geological hammer point indents deeply with firm blow.	5.0-25	3.3-6.6	Soft rock	Can just be scraped and peeled with a knife; indentations 1mm to 3mm show in the specimen with firm (moderate) blows of the pick point.	3.95
H6	Soft	Can be grooved or gauged easily by knife or sharp pick with light pressure. Can be scratched with fingernail. Breaks with light to moderate manual pressure.	R1	Very weak	Specimen crumbles under sharp blow with point of geological hammer, and can be cut with a pocket knife.	1.0-5.0	1.7-3.3	Very soft rock	Material crumbles under firm (moderate) blows with sharp end of geological pick and can be peeled off with a knife; is too hard to cut tri-axial sample by hand.	1.86
H7	Very soft	Can be readily indented, grooved, or gauged with fingernail, or carved with a knife. Breaks with light manual pressure.	R0	Extremely weak	Indented by thumbnail	0.25-1.0	<1.7	Very soft rock	Material crumbles under firm (moderate) blows with sharp end of geological pick and can be peeled off with a knife; is too hard to cut tri-axial sample by hand.	0.87

We calculated K_b using a combination of parameter conversions and professional judgement. For rock materials, Annandale calculates K_b as:

$$K_b = \frac{RQD}{J_n} \quad [2]$$

where RQD is the Rock Quality Designation, a standard parameter in drill core logging (Deere, 1988) and J_n is the joint set number, which is a function of the number of joint sets. K_b should range between 1 and 100 for rock materials. Because Reclamation geologists did not drill core logs or measure RQD by other means, we had to calculate it based on converting fracture spacing and weathering parameters from chapters 4 and 5 of the Engineering Geology Field Manual (Reclamation, 1998), which are indicators of rock quality, to RQD ranges based on rock quality from Deere (1988). We summarize our comparisons in Table 8. We then assigned a RQD value to the entries in the Holmes (2021) geologic report's Table 3A and Table 3B for the left and right spillway. We again chose conservative values that would make the rock more susceptible to erosion. We used professional judgement based on photos and the geology report to then map the RQD values onto the spillway. We separated any mapped shears and assigned them an RQD value that was lower than the surrounding rock. For J_n, we assigned a value from Annandale's (1995) Table 6 for each geologic unit from Figure 4, sub-divided based on the number of joint sets present in the Holmes (2021) geologic report's Tables 2A and 2B. We used these results to generate a separate map for J_n. The RQD and J_n maps were intersected in ArcGIS Pro to generate unique polygon combinations for the two values and a new column was created where K_b was calculated following Equation 2. Figure 14b shows the resulting map of K_b.

Table 8.—RQD conversion

RQD classification index (Deere, 1989)		USBR Weathering		USBR Fracture Density	
RQD	Rock mass quality	Alpha-numeric descriptor	Descriptor	Alpha-numeric descriptor	Descriptor
<25%	Very poor	W9	Decomposed	FD9	Very intensely fractured
		W8	Very intensely weathered	FD8	Very intensely to intensely fractured
		W7	Intensely weathered	FD7	Intensely fractured
25-50%	Poor	W6	Intensely to moderately weathered	FD6	Intensely to moderately fractured
50-75%	Fair	W5	Moderately weathered	FD5	Moderately fractured
		W4	Moderately to slightly weathered	FD4	Moderately to slightly fractured
75-90%	Good	W3	Slightly weathered	FD3	Slightly fractured
		W2	Slightly weathered to fresh	FD2	Slightly to very slightly fractured
				FD1	Very slightly fractured
90-100%	Excellent	W1	Fresh	FD0	Unfractured

K_d is determined by the proportion of the joint roughness number (J_r) to the joint alteration number (J_a):

$$K_d = \frac{J_r}{J_a} \quad [3]$$

These parameters were directly related to Reclamation field measurements. We again used Holmes' (2021) Tables 2A and 2B for information on joint parameters. Reclamation roughness correlated to J_r (Annandale, 1995 his Table 5) and openness correlated to J_a (Annandale, 1995 his Table 6). For J_a, the field geologists recommended that we use 0.75-1.0 for joint sets and 4.0-10.0 for shear zones. We assigned values within this range based on the descriptors within the geology report and descriptors for joint openness and filling thickness from chapter 5 in the Engineering Geology Field Manual (Reclamation, 1998). For J_r, we assigned values based on converting Reclamation joint roughness to an Annandale value (Table 9). We interpolated where we felt that Reclamation assignments fell between Annandale joint roughness values. We mapped the values in ArcGIS and again interpolated in areas where we had no data. We intersected the polygons for the two maps in a similar manner as for K_b and calculated a new map for K_d, which is shown in Figure 14c.

Table 9.— Joint Roughness Number (J_r) conversion

Annandale			Reclamation		
Joint Separation	**Condition of Joint**	**Joint Roughness Number (Annandale)**	**Alpha-numeric descriptor**	**Descriptor**	**Joint Roughness Number (Assigned)**
Joints/fissures tight or closing during excavation	Stepped joints/fissures	4.0	R1	Stepped (planar)	4.0
	Rough or irregular, undulating	3.0	R2u	Rough (undulating)	3.0
			R3u	Moderately rough (undulating)	2.5
	Smooth undulating	2.0	R5u	Smooth (undulating)	2.0
	Slickensides undulating	1.5			
	Rough or irregular, planar	1.5	R2p	Rough (planar)	1.5
			R3p	Moderately rough (planar)	1.25
			R4	Slightly rough (planar and undulating)	1.25
	Smooth planar	1.0	R5p	Smooth (planar)	1.0
	Slickensides planar	0.5	R6	Smooth and shiny	0.5

The final parameter required for calculating K_h is J_s, or the relative ground structure number. This parameter represents the least favorable discontinuity in terms of rock erosion and incorporates the joint orientation relative to the stream flow and joint spacing. This incorporates the effective dip, which is the dip of a discontinuity adjusted for the slope of the stream channel relative to the direction of flow, and the ratio of joint spacing, which is the ratio of vertical joint spacing to downstream joint spacing. We first plotted all of the measured joint orientations from the Holmes (2021) geologic report's Tables 2A and 2B on the map and grouped them by similar orientations (Holmes, 2021). We assigned that grouping the average strike and dip from all of the inputs and assigned a downstream joint spacing that was the average of the inputs for a region. We obtained the vertical joint spacing from drill core logs from 1979 (Department of the Army, 1979). We calculated the ratio of joint spacing, *r*, from these values. We then measured the dip and dip direction of the flow in the spillway and used that to calculate an effective dip for each region. These were then cross-referenced to Annandale's (1995) Table 7 to assign J_s to each region. We interpolated between values where gaps existed in Annandale's (1995) Table 7. Figure 14d shows the final map for J_s.

The final product of these parameterizations are four different maps for the four different inputs needed to calculate K_h. We intersected these maps in ArcGIS Pro to generate a final map of K_h, which is the unique intersection of all of the polygons used in every input and with their parameters multiplied by each other following Equation 1. Figure 15 shows the final erodibility map.

In the area downstream of the spillway through Bean Gulch, we used the United States Army Corps of Engineers (USACE) 1979 geologic map (Department of the Army, 1979) to extend the mapping of the serpentinite and meta-volcanics. Bean Gulch follows the contact between these two geologic units. We assigned the serpentinite the weighted average of K_h values for the downstream section of serpentinite in the spillway, and we assigned the meta-volcanics a weighted average value for the most downstream mapped meta-volcanic unit. For any areas where there were discrepancies in the lithology, we checked the geophysical data (Rittgers, 2020) and moved the contact as needed to correspond to the field mapper data.

To calculate the likelihood that the bed would erode for a given flow, we then had to convert the SRH-2D results to streampower. We calculated streampower (kW/m) as

$$\boldsymbol{\omega = \tau * u/100} \quad \textbf{[4]}$$

where ω is streampower, τ is the basal shear stress, and u is the velocity in the x-direction. This results in a value for streampower at every mesh grid. We then calculate the critical streampower (ω_c) needed to erode a given section of the channel in Figure 15 using the relationship derived by Annandale (1995) that utilized 150 field observations and published data for erosion of rock:

$$\boldsymbol{\omega_c = K_h^{0.75}} \quad \textbf{[5]}$$

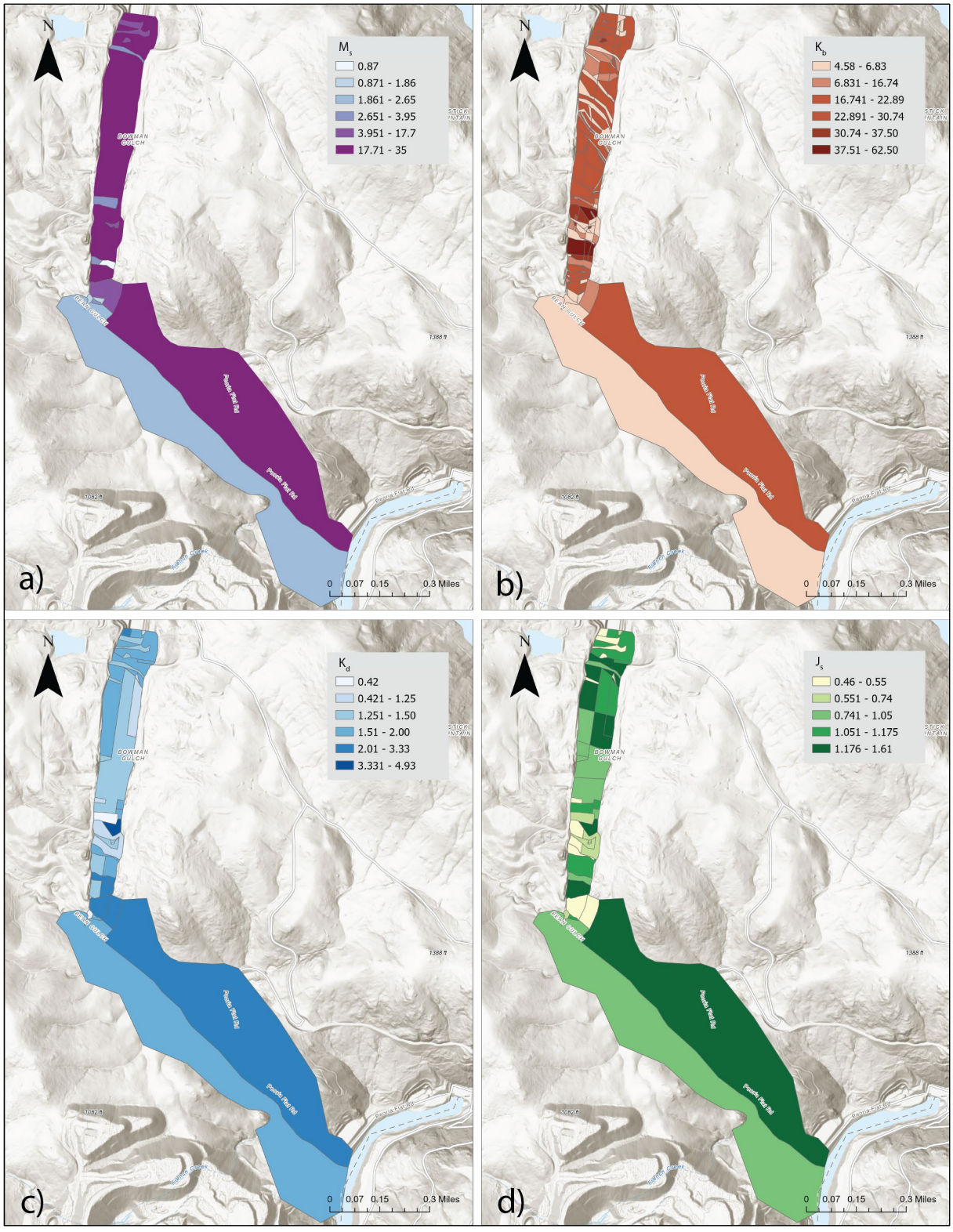

Figure 14.—Maps of inputs used to calculate the erodibility of the spillway, K_h. (a) shows the mass strength number, M_s. (b) shows the particle or block size number, K_b. (c) shows the discontinuity or inter-particle bond shear strength number, K_d. (d) shows the relative ground structure number, J_s.

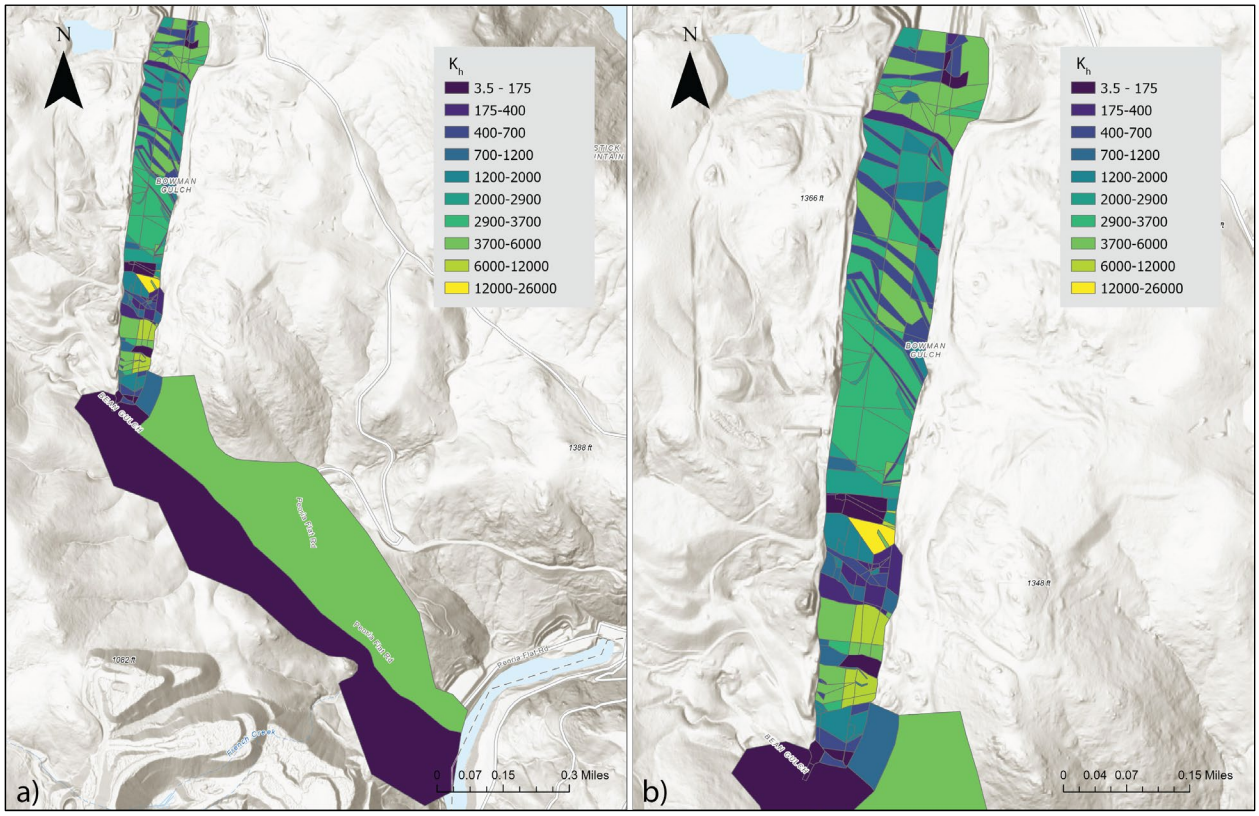

Figure 15.—Erodibility (K_h) map for the entire 2D Annandale model domain (a) and zoomed into just the spillway (b).

3.3 1D Bedrock Erosion Model

We apply the Hurst one-dimensional (1D) erosion (H1DE) model to calculate the timing and magnitude of bedrock erosion on the spillway and in the gully between the spillway and Bean Gulch. The H1DE model is a 1D bedrock erosion model that models erosion of fractured bed material by plucking along a 1D transect (Hurst, 2021). A flow hydrograph is routed through the model using either Gradually Varied Flow Equation, which requires a subcritical inlet and outlet condition. The use of Gradually Varied Flow Equation requires the assumption that changes in velocity and depth are slow enough in the downstream direction that pressure remains hydrostatic. The model explicitly tracks the erosional susceptibility of all fractured blocks that are exposed to flow to plucking. Block plucking is represented as a Poisson process in which a critical pressure on the downstream side of a block and shear stress on the top surface of the block govern its susceptibility to plucking. A waiting time for each block is cataloged according to an assumed distribution of low pressures on the downstream side and shear stresses on the top side of the block, both of which are informed by characteristics of the flow. The physics integrated in the model are derived from the work of Hurst and others (2021), which utilized 2D flow hydraulics to develop relationships that can be applied based on the average characteristics

of a 1D flow. This model was tested on a spillway erosion event at Canyon Lake Gorge, Texas, and was shown to reasonably capture the magnitude of total volume and depth of bedrock erosion in the spillway (Hurst, 2021).

The H1DE model inputs are all measured from DEMs or in the field. Because the CGB geologists only conducted detailed mapping along the left and right walls of the spillway, we were limited to only two lines of data. The fracture characteristics of the rock were quite different along these transects, so we generated two different transects: one along the right side of the spillway and one along the left side of the spillway. Both transects overlap once they reach the end of the spillway and extend into the downstream gully (Figure 16). We end the transects at the base of the gully and the upstream end of Bean Gulch. The two transect approach allows us to test what the outcome would be if the rest of the spillway has characteristics more similar to the left spillway or the right spillway. We generate initial elevation profiles from transects drawn in ArcGIS Pro along these two lines using the elevation profile tool to extract elevations from the raster shown in Figure 3.

Figure 16.—This map shows the two transects used to run the H1DE model. The transects overlap in the gully at the downstream end of the spillway. The basemap is from ESRI World Imagery data.

We assign densities at geologic breaks along the transects based on the measurements from Table 1. The fracture spacing data (Table 2) is used to generate blocks with dimensions dx (in the flow direction), dz (vertical), and dw (cross-channel) (Figure 6). This dataset was an additional dataset that was not used in the 2D Annandale assessment. We interpolated these measurements within a lithology based on field observations. In places that we did not have data in one or more dimension, we assumed the missing dimension was cohesive (un-fractured) unless within a foliated zone or within the serpentinite on the downstream end of the spillway due to the highly fractured nature of these lithologies. In those cases, we assigned the missing dimensions the value of the measured dimension, which resulted in a smaller block size in these locations than if we had assumed un-fractured rock. The missing dimension was most often dw, which is difficult to observe in a 2D plane. Proper measurements of dw would require digging pits at various locations along the spillway. In the absence of this, we assigned dw as the spillway width. We did not have data for the foliated zone or the metasiltstone, so we assigned them the same value as the serpentinite because that lithology was most consistent with those two units in terms of fracture characteristics. These measurements differed for the left and right spillway, and we chose to keep them separate to represent two endmembers of possible fracture networks across the spillway invert (Table 10). These dimensions vary with distance along the transect depending on the localized measurements in the field.

Because it is unrealistic with current methodologies to perfectly map every fracture in the spillway, we generate a bed with randomized fracture spacing using the longitudinal variation in mean and standard deviation of the fracture spacing to generate blocks with different sizes within each lithology. We assume flat-lying beds because the rock is highly metamorphosed and therefore had no bed dip data. Without any pits, we also assume that the joint spacing is consistent with depth and that blocks intersect as rectangular prisms. Due to the metamorphosed nature of the rock, we allow the block boundaries to overlap rather than lying along a constant bedding plane. We can generate any number of random beds to iterate through and obtain a mean and standard deviation of potential bedrock erosion scenarios. For our results, we chose to run 50 random bed iterations for each flow.

At the downstream boundary of the model, we assign a water surface elevation downstream boundary condition from the SRH-2D unsteady model outputs at monitoring point (MP) 4. We assume no erosion at the base of the gully based on the outputs from the SRH-2D mobile bed model results that show no erosion at MP 4. Because all of the sediment was removed from the spillway in almost all of the SRH-2D mobile bed runs, we are assuming no sediment cover in the initial condition of the model. At the upstream boundary, we input the hydrographs for various flood scenarios using a New Melones starting reservoir elevations of 1,049 ft and 1,088 ft (Figure 9).

We calculate the eroded volume as the total height of removed blocks (dz) times the length (dx) times the channel width. This means that we are assuming any bedrock erosion along the 1D transect occurs across the entire width of the channel. The result is separate calculations for total volume of spillway erosion for the left and right transects that represent the range of possible erosion scenarios based on the available field data. We believe that any calculated volume of bedrock erosion is likely to be an over-estimate because the fracture spacing across the spillway is most likely not consistent.

Table 10.—H1DE model inputs for the left and right spillway

Spillway side	Station From (ft)	Station To (ft)	Rock Type	Density (g/cm^3)	dz (ft)	dx (ft)	dw (ft)
Right	0	2112.68	Mv	2.96	0.4 +/ -0.13	0.74 +/ -0.14	-
Right	2112.68	2262.25	FZ	2.68	0.33 +/ -0.46	0.26 +/ -0.36	0.33 +/ -0.56
Right	2262.25	2295.38	Mv	2.96	0.4 +/ -0.13	0.74 +/ -0.14	-
Right	2295.38	2508.02	Mm	2.97	0.49 +/ -0.52	5.05 +/ -14.1	-
Right	2508.02	2557.09	Sp	2.61	0.26 +/ -0.26	-	-
Right	2557.09	2687.53	Mm	2.97	0.49 +/ -0.52	5.05 +/ -14.1	-
Right	2687.53	2800.82	Sp	2.61	0.33 +/ -0.46	0.26 +/ -0.36	0.33 +/ -0.56
Right	2800.82	3097.63	Mm	2.97	0.49 +/ -0.52	5.05 +/ -14.1	-
Right	3097.63	3199.31	Ms	2.62	0.33 +/ -0.46	0.26 +/ -0.36	0.33 +/ -0.56
Right	3199.31	3487.92	Mv	2.96	1.48 +/ -1.12	0.23 +/ -0.07	-
Right	3487.92	3709.29	Mbs	2.87	cohesive	-	-
Right	3709.29	3945.71	Sp	2.61	0.33 +/ -0.46	0.26 +/ -0.36	0.33 +/ -0.56
Left	0	2116.19	Mv	2.96	4.59 +/ -3.94	3.94 +/ -1.31	-
Left	2116.19	2282.36	FZ	2.68	0.82 +/ -0.75	-	-
Left	2282.36	2471.58	Mv	2.96	4.59 +/ -3.94	3.94 +/ -1.31	-
Left	2471.58	2537.21	Mm	2.97	2.59 +/ -3.51	4.53 +/ -4.49	-
Left	2537.21	2658.44	Sp	2.61	0.82 +/ -0.75	-	-
Left	2658.44	2781.83	Mm	2.97	2.59 +/ -3.51	4.53 +/ -4.49	-
Left	2781.83	2792.89	Sp	2.61	0.82 +/ -0.75	-	-

Table 10.—H1DE model inputs for the left and right spillway

Spillway side	Station From (ft)	Station To (ft)	Rock Type	Density (g/cm^3)	dz (ft)	dx (ft)	dw (ft)
Left	2792.89	3112.85	Mm	2.97	6.49 +/ -5.9	-	-
Left	3112.85	3192.62	Ms	2.62	0.82 +/ -0.75	-	-
Left	3192.62	3432.52	Mv	2.96	1.48 +/ -1.12	0.23 +/ -0.07	-
Left	3432.52	3813.2	Mbs	2.87	6.23 +/ -1.34	-	-
Left	3813.2	4067.36	Sp	2.61	0.82 +/ -0.75	-	-

4.0 Results and Discussion

4.1 SRH-2D Flow and Sediment Transport Model

4.1.1 Flow-Only Models

We ran several steady flow-only models to determine model stability before adding the mobile bed component. The steady flows also allowed us to determine flow inundation to limit the model mesh size. We ran the peak flows from each hydrograph and observed the model results, iterating on mesh boundaries and element size and placement. Our initial mesh had over 500,000 cells and a much larger footprint than necessary. Following preliminary runs, we limited the model domain to extend only 1-2 elements outside of the maximum flow inundation. We also increased the cell size away from our area of interest. Our final mesh has fewer than 15,000 cells yet retains the granularity needed to represent important zonal characteristics and an accurate representation of hydraulic processes.

After finalizing the mesh and ensuring model stability, we ran steady flows with an immobile bed to use as restart files for unsteady flow runs and mobile bed runs. SRH-2D recommends starting the mobile bed with a restart file from a previous run so that the model cells are wet rather than dry, similar to conditions at the beginning of a model run hydrograph. We used the maximum 8,000 cfs outlet works release to create a restart file for our unsteady flow and mobile bed models (Figure 17), as this is where our hydrographs start for flood events (Figure 9). The spillway was not wet in the restart file, which was consistent with conditions at the beginning of our modeled flood events.

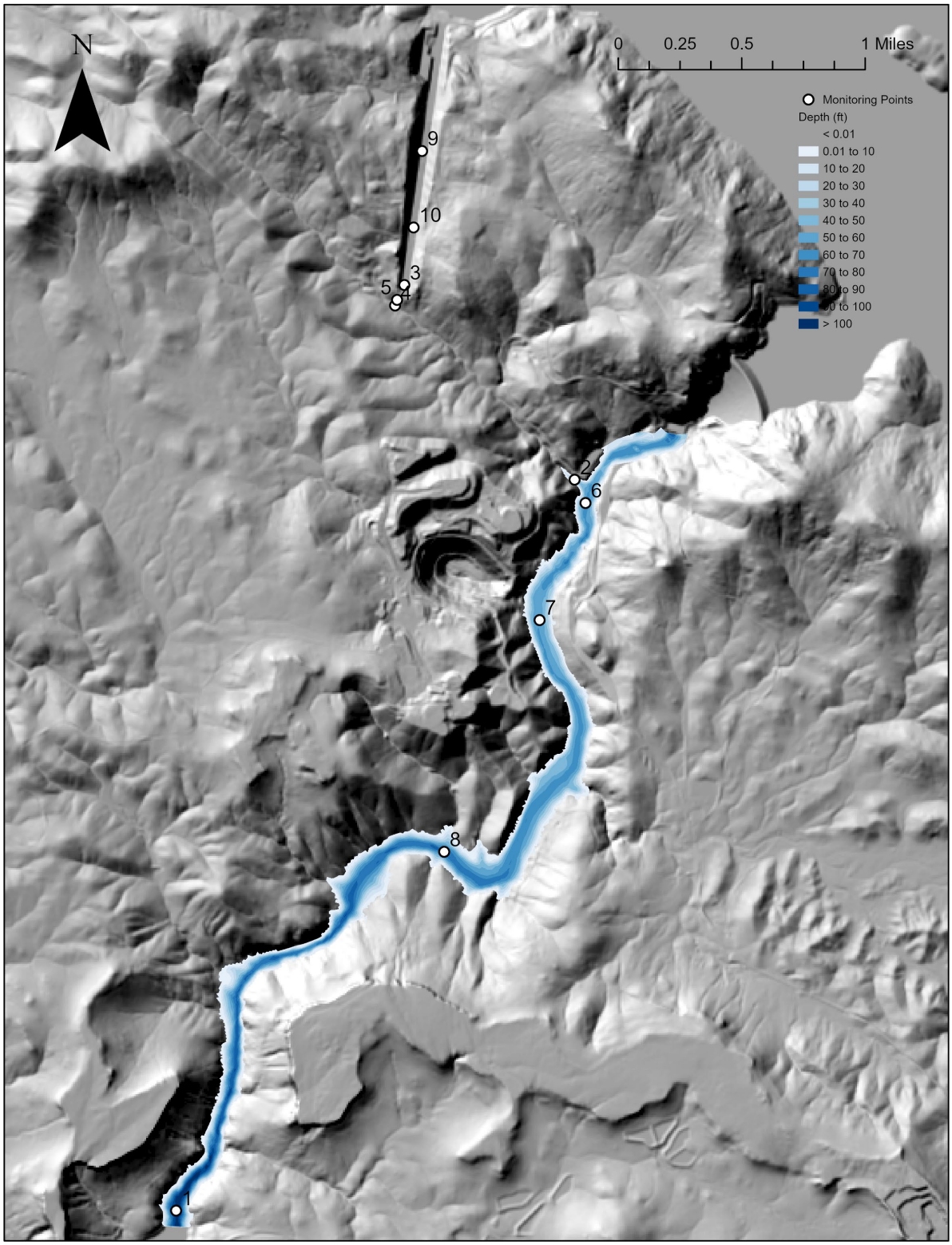

Figure 17.—Flow depths associated with the maximum 8,000 cfs discharge from the outlet works. This flow represents the starting condition for unsteady flow hydrographs and mobile bed model simulations.

Next, we ran unsteady flow-only models with an immobile bed to slowly increase the model complexity prior to progressing to a mobile bed simulation. To discern erosion and deposition trends, we extracted model results from monitoring points located at key areas of concern (See MP locations in Figure 12). Also, we needed to generate a rating curve at MP 4 (Figure 18). This rating curve was used to set the downstream boundary condition for the H1DE model, which utilizes flow depth. The rating curve is the same for all recurrence interval floods and all downstream boundary conditions at Tulloch. The slight mismatch between depths plotted between 60,000 cfs and 100,000 cfs is the result of slightly different depths on the rising and falling limbs of the hydrograph, largely due to interpolation onto a smaller timescale. We used the depth associated with each limb of the hydrograph through time.

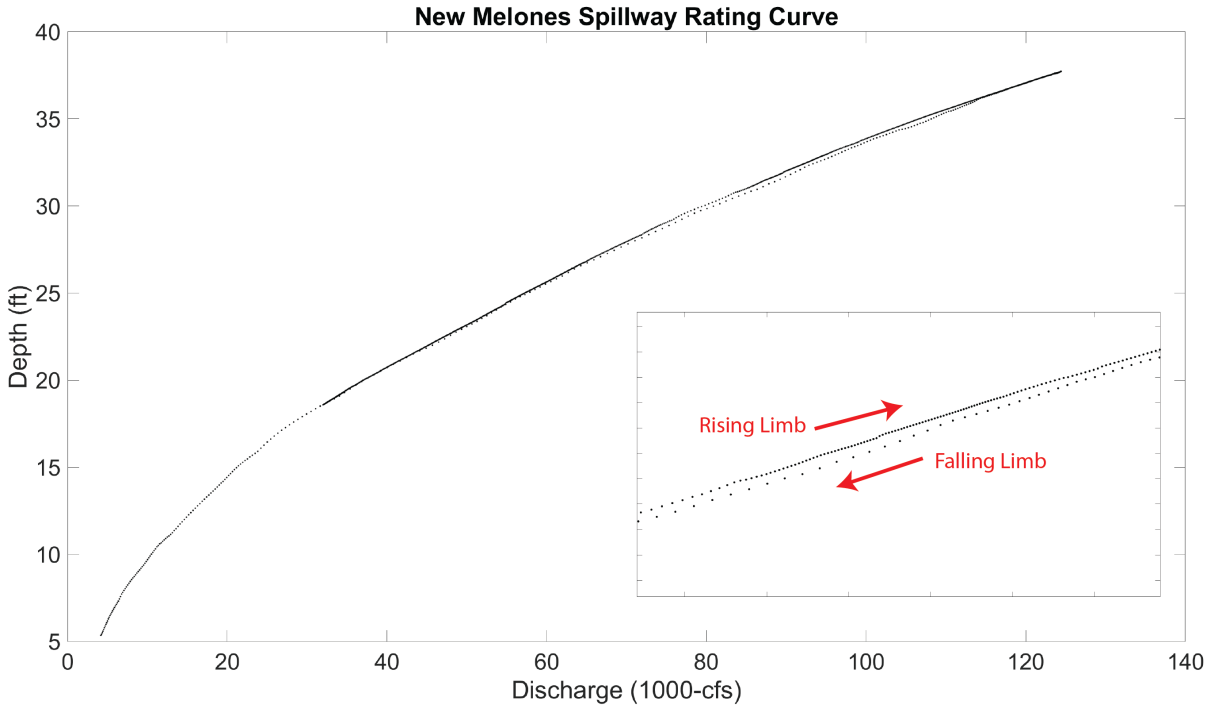

Figure 18.—Rating curve at MP 4 used to assign a downstream boundary condition in the H1DE model. This rating curve is the same for all recurrence interval flows and all Tulloch Reservoir water surface elevations.

4.1.2 Steady Runs with a Mobile Bed, Initiation of Motion

We performed several steady flow simulations with a mobile bed using low magnitude discharges (<5,000 cfs) to assess the sediment movement within various grain size fractions. The unsteady flow events we modeled can have spillway discharges between 3,000 and 125,000 cfs. As the spillway has never been breached and experienced a flood event, we also wanted to explore how sediment on the spillway would erode during a lower magnitude event. We ran the steady flow for 30 hours of model time. The 20 kyr RI flow (NM1049) was able to wet the

spillway for at least 60 hours, and only 38 hours exhibited flows above 3,000 cfs on the spillway. Our reasoning for choosing 30 hours was that lower flows breaching the spillway would likely wet the surface for a shorter period of time but that 30 hours would still allow enough time to observe significant sediment transport trends. The observations at the end of the model are meant to inform what would happen during a shorter event with lower magnitude flows and the model time is not meant to be representative of a specific flood routing event.

Three monitoring points are located on the spillway: MP 9 (most upstream), MP 10, and MP 3 (most downstream). All three points fall within Sediment Zone 1 and have the same starting sediment gradation data (Table 6). Silts and sands are the first fraction to mobilize, as expected. Silts and sands mobilize at MP 9 at the 50 cfs flow and net erosion occurs at this point as well. A relative increase is observed in fine pea gravel and pebbles as they become more concentrated in the sediment package due to removal of sands at the 50 cfs flow (Table 11). The removal of silts and sands is apparent in time series data for the 100 cfs flow (Figure 19); this flow is also able to transport pea gravel away from MP 9 to maintain a constant fraction of 13% pea gravel in an eroding bed with decreasing thickness (Table 11).

MP 10 experiences net deposition and MP 3 experiences no net change in sediment thickness for modeled flows between 50 cfs and 250 cfs (Table 11). However, even though MP 10 is experiencing deposition for the 100 cfs flow, the time series data show an increase in the fraction of silt and sand followed by a decrease as transport of silts and sand away from MP 10 exceeds the supply of silt and sand from upstream toward the end of the model run (Figure 19).

Coarser fractions show similar trends from upstream to downstream. As fine fractions are preferentially transported, the coarse fraction at a site initially increases, unless there is a supply of fine sediment sourced from upstream. The increase in coarse fractions and decrease in finer fractions is visible in the time series data (Figure 19). There is a wave of deposition that moves toward the downstream monitoring points, first to MP 10 then MP 3. If we ran the model for a longer period of time, there would likely be a net removal of finer grain sizes at all three monitoring points on the spillway for low discharges.

By 3,000 cfs, sands, fine pea gravel, and pebbles are depleted at all sites at the end of the modeling run. All sites experience net erosion during this simulation. This indicates that a 3,000 cfs flow for this duration would likely impact downstream areas with deposition. At 4,000 cfs, the remaining sediment cover is thin, and the fraction data can greatly change within a timestep because so little sediment remains (see lower right plot in Figure 19). However, it appears that the persistence of boulders at MP 9 and MP 10 dominate the remaining sediment fraction, whereas boulders have been transported from MP 3 and only 0.2 ft of sediment remain there. With additional model time, results at MP 9 and MP 10 would likely mimic the results at MP 3.

Aside from upstream to downstream location of each monitoring point, the difference in the results is also influenced by topography. The spillway is not entirely smooth, allowing for localized hydraulics. However, we are most interested in the general trends we observe from the points, rather than the effects of site-specific hydraulics. These trends include: (1) silts and sand mobilize at flows as low as 50 cfs, (2) upstream zones within the spillway are likely to display

net erosion first, whereas downstream zones may experience a wave of deposition prior to a net erosion of sediment, (3) flows of 1,000 cfs or less for a short duration of time (<30 hours) will likely bury the lower spillway and cause minimal transport of sediment off of the spillway, (4) flows of 2,000 cfs or greater, for a duration of 30 hours, are likely to transport sediment off of the spillway and impact downstream areas.

Table 11.—Sediment size fractions at the start and end of steady flow simulations with a mobile bed

		Silt & Sand		Fine Pea Gravel		Pebbles		Cobbles & Stones		Boulders		Sediment Thickness (ft)	
		0.04-2 mm		2 – 5 mm		5 – 76 mm		76 – 600 mm		600 – 2100 mm			
Flow	MP	Start	End	Start	End	Start	End	Start	End	Start	End	Start	End
50	9	9	4	13	15	62	65	11	11	5	5	5.4	5.2
	10	9	17	13	12	62	56	11	10	5	5	5.4	5.7
	3	9	9	13	13	62	62	11	11	5	5	5.4	5.4
100	9	9	1	13	13	62	70	11	11	5	5	5.4	5.0
	10	9	9	13	16	62	61	11	10	5	5	5.4	5.6
	3	9	9	13	13	62	62	11	11	5	5	5.4	5.4
250	9	9	0	13	9	62	73	11	12	5	5	5.4	4.5
	10	9	7	13	16	62	65	11	8	5	4	5.4	6.1
	3	9	10	13	13	62	62	11	11	5	5	5.4	5.4
500	9	9	0	13	5	62	74	11	14	5	6	5.4	4.2
	10	9	5	13	14	62	70	11	8	5	3	5.4	6.5
	3	9	7	13	14	62	63	11	11	5	5	5.4	5.5
1000	9	9	0	13	1	62	37	11	43	5	20	5.4	2.4
	10	9	4	13	12	62	71	11	9	5	4	5.4	6.2
	3	9	13	13	13	62	60	11	10	5	4	5.4	5.8
2000	9	9	0	13	1	62	10	11	61	5	29	5.4	1.9
	10	9	4	13	9	62	68	11	13	5	6	5.4	5.1
	3	9	1	13	2	62	36	11	27	5	34	5.4	1.5
3000	9	9	0	13	1	62	30	11	48	5	21	5.4	2.0
	10	9	0	13	1	62	14	11	56	5	29	5.4	1.5
	3	9	0	13	1	62	7	11	39	5	53	5.4	0.5
4000	9	9	0	13	0	62	13	11	61	5	26	5.4	0.9
	10	9	0	13	1	62	11	11	57	5	31	5.4	1.0
	3	9	97	13	0	62	0	11	3	5	0	5.4	0.2
5000	9	9	0	13	0	62	2	11	67	5	31	5.4	0.8
	10	9	0	13	0	62	2	11	61	5	36	5.4	1.1
	3	9	0	13	0	62	100	11	0	5	0	5.4	0.1

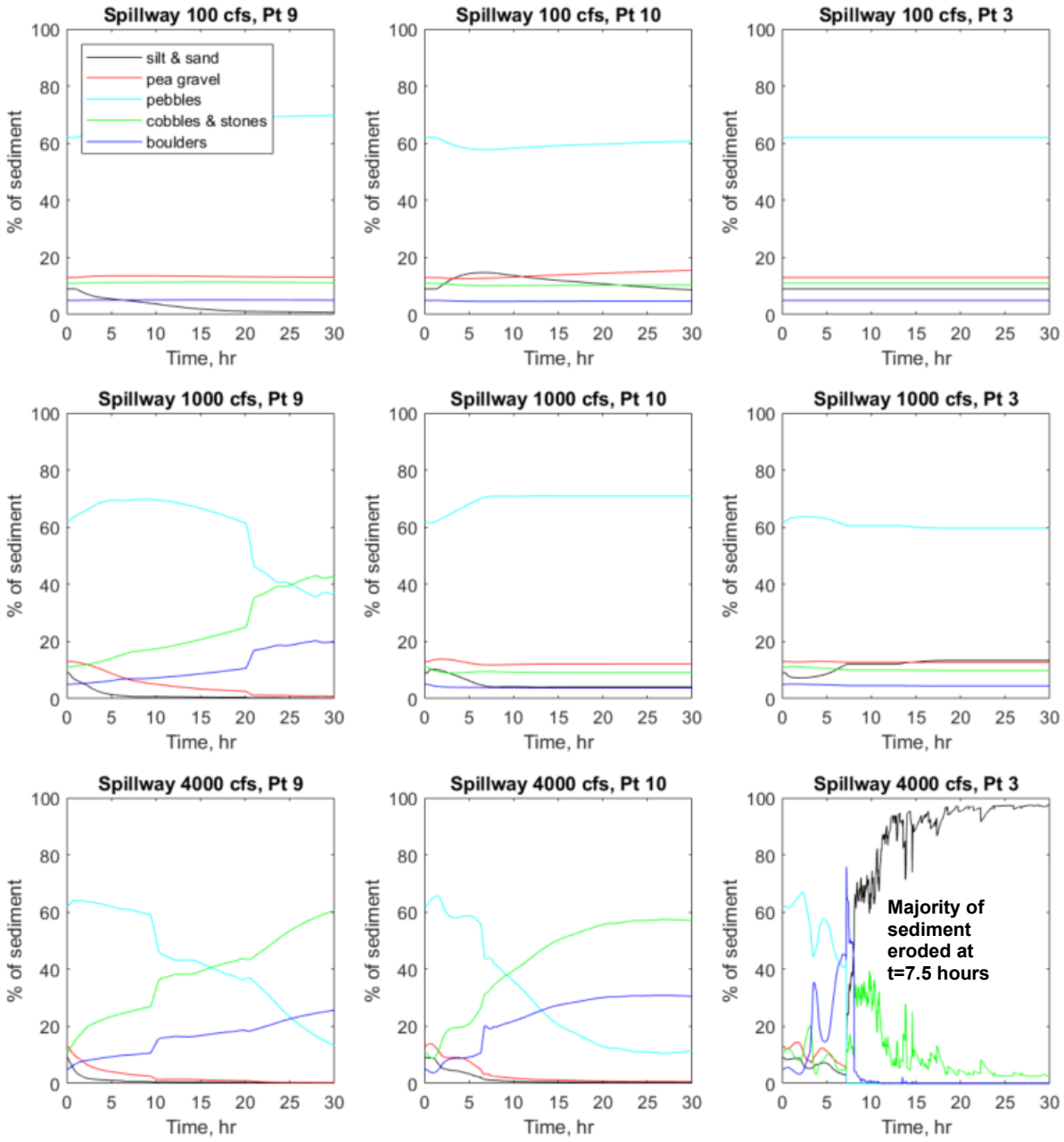

Figure 19.—Change in sediment composition throughout the modeling run at monitoring points on the spillway for three different flows.

4.1.3 Unsteady Flow Runs with a Mobile Bed

The unsteady flow runs use a series of flood hydrographs routed through New Melones Reservoir at two starting elevations, 1,049 ft (NM1049) and 1,088 ft (NM1088). Each hydrograph starts with 8,000 cfs flowing from the New Melones Dam outlet works and 0 cfs on

the spillway. As flow breaches the spillway, the outlet works reduce their flow to avoid exceeding 8,000 cfs in the Stanislaus River. If flow in the spillway reaches or exceeds 8,000 cfs, the outlet works cease operation. The 20 kyr RI flood event (NM1049) generated the lowest peak flow on the spillway, at 3,549 cfs, within the range of flows modeled for the steady flow runs above. All other modeled floods exhibit peak flows on the spillway in excess of 10,000 cfs (Table 3). The discussion of results moves from upstream to downstream, starting on the spillway and ending at Tulloch Reservoir. From upstream to downstream: MP 9, MP 10, and MP 3 are located on the spillway; MP 5 is located in the gully connecting the spillway way to Bean Gulch; MP 4 and MP 2 are located in Bean Gulch; MP 6, MP 7, and MP 8 are located in the Stanislaus River; and MP 1 is located at the upstream extent of Tulloch Reservoir, near O'Byrnes Ferry Road bridge crossing (Figure 12).

Key findings at the end of the model simulations, from upstream to downstream

- Erosion occurs on the spillway. MP 9, MP 10, and MP 3 experienced erosion in every modeled hydrograph. Less than 1 ft of the initial 5.4 ft sediment cover remains for all modeled flows at MP 9 and MP 10 (Table 12, Table 13). At MP 3, approximately 3 ft of sediment remain for the 20 kyr RI flood (NM1049), with the lowest spillway peak flow of 3,549 cfs. MP 3 is located on the downstream end of the spillway, and therefore receives a large influx of sediment from upstream; this likely influences the lower net erosion observed for the lowest modeled flood event. By the 50 kyr RI flood (NM1049), with the second lowest peak flow of 10,102 cfs, less than 1 ft of sediment remains at MP 3 as well (Table 13).

- The net volume of change on the spillway is between 77,490 yd^3 of erosion for the 20 kyr RI flood (NM1049, Tulloch WSE 515) and 207,703 yd^3 for the 1 Myr flood (NM1088, Tulloch WSE 500). We estimated this volume by summing individual element erosion by the element area on the spillway. For comparison, the original spillway sediment volume was approximately 210,000 yd^3.

- At the lowest modeled flood event (20 kyr RI, NM1049), both flow and erosion are concentrated against the left and right spillway walls (Figure 20A, Figure 21A, Figure 22A), but by higher flows the entirety of the spillway was inundated and experienced erosion (Figure 20- Figure 22).

- Flow exits the spillway onto a hillslope bounding the left valley wall of Bean Gulch. At lower flows, MP 5 experiences little to no erosion at the model conclusion (Table 12, Table 13), with peak flows on the spillway <18,000 cfs (i.e., Table 3). At higher flows, the majority or all of the 4 ft sediment cover is removed. This portion of the hillslope exhibits the highest velocities and bed shear stresses at high flows (Figure 21, Figure 22), due to the high gradient on the hillslope between the spillway and Bean Gulch.

- As flows exit the spillway, deposition occurs in Bean Gulch at MP 4 for all modeled flows. This is an isolated pocket of deposition that likely occurs as large volumes of sediment exit the above hillslope and enter the lower gradient Bean Gulch. The flow also

takes a 90-degree turn at this junction. Some of the flow and sediment are forced in the upstream direction, as evidenced by the plume of sediment that is deposited upstream from the confluence of Bean Gulch and the hillslope below the spillway (Figure 20). This is an extremely dynamic point and the results at this MP are very sensitive to model changes in base level or timestep (see further discussion in 4.1.4 SRH-2D Sensitivity testing). This pocket of deposition is surrounded by erosion in all the model simulations (e.g., Figure 20).

- Results from the model represent the potential for sediment transport and flow hydraulics associated with extreme flood events. Flow velocities exceed 50 ft/s and the model simulated bed shear stresses over 200 lb/sq-ft (e.g., Figure 21; Figure 22).

- The majority of Bean Gulch experiences erosion by the end of the model simulation, but there are small pockets of deposition throughout the channel (e.g., Figure 20). The areas of deposition are located at areas of lower bed shear stresses at the intermediate output, 80 hours after the hydrographs start time (Figure 21; Figure 22). We chose this time interval for model output because the hydrographs peak close to 80 hours after their start time (Figure 9).

- The net volume of erosion on Bean Gulch and the hillslope below the spillway is 7,279 yd^3 of erosion for the 20 kyr RI flood (NM1049, Tulloch WSE 515), which is an order of magnitude less than the erosion simulated on the spillway for the same flow. The net volume of erosion on Bean Gulch and the hillslope below the spillway is 88,880 yd^3 for the 1 Myr flood (NM1088, Tulloch WSE 500), which is approximately a factor of 2.3 times less than the erosion simulated on the spillway for the same flow. We estimated this volume by subtracting the volume of erosion on the spillway from the volume of deposition on the Stanislaus River.

- At the lowest flow hydrographs, MP 2 experiences several feet of deposition (Table 12, Table 13). In addition, at higher base levels (higher Tulloch WSE) and mid-range flows, the point is more likely to experience deposition, totaling 2.5 ft or less. In almost all modeled flows, except for the 20 kyr hydrograph flow (NM1049 ft) and higher base flow conditions, the small pocket of deposition at MP 2 is surrounded by erosion; the pocket of deposition in some flows is so spatially small it is obscured by the monitoring point label (in Figure 20). At the highest flow hydrographs, the amount of deposition decreases and then shows net erosion for the highest modeled flow event of 1Myr RI (NM1088) (Table 12). Aside from localized deposition, the general trend within Bean Gulch is erosion. Thus, most of the sediment eroded from the spillway passes through Bean Gulch to deposit in the Stanislaus River.

- Massive deposition (>10 ft) occurs at MP 6 in the Stanislaus River immediately downstream from the confluence with Bean Gulch for all model simulations (Table 12; Table 13). The depth of deposition at MP 6 at first increases with increasingly larger hydrographs. However, the largest hydrograph of 1 Myr RI (NM1088) has less deposition at MP 6 than the smaller 100 kyr RI hydrograph (NM1088) (Table 12); this is likely

because the increased flow duration at high discharge enables sediment transport farther downstream, outpacing the supply of incoming sediment. Higher water surface elevations in Tulloch Reservoir result in greater deposition at MP 6, likely because of additional backwatering in the Stanislaus and decreased sediment transport farther downstream (Table 12, Table 13).

- Deposition distributes downstream into the Stanislaus, but the thickest portion of the deposit is close to the confluence (Figure 20). The sediment plume extends farther downstream for larger flow hydrographs (Figure 23). The next monitoring point, MP 7, is located approximately 2,700 ft downstream from MP 6. This point experiences no change in sediment thickness (defined as <0.5 ft change) for the smallest hydrograph simulated (20 kyr, NM1049 ft) and deposition for all other simulations, depending on the base level. For higher base levels at Tulloch Reservoir, the Stanislaus River experiences more backwatering, and less sediment is transported downstream of MP 6. Thus, as deposition increases at MP 6 due to base level, MP 7 exhibits lower net deposition because of decreased sediment transport within the Stanislaus River (Table 12, Table 13).

- MP 8 is located 8,140 ft downstream of MP 2. This monitoring point experiences no change (<0.5 ft deposition) for all modeling simulations (Table 12, Table 13).

- Tulloch Reservoir is not impacted. MP 1, located near the downstream boundary, experiences a maximum deposition of 0.13 ft, a negligible amount (Table 12, Table 13). It is likely that this bed change is associated with transport of closer sediment, sourced from the reach of the Stanislaus River immediately upstream, rather than the spillway.

- The net volume of change in the Stanislaus River is 84,769 yd^3 of deposition for the 20 kyr RI flood (NM1049, Tulloch WSE 515) and the deposit extends approximately 2,120 ft downstream along the river centerline. The net volume of change in the Stanislaus River is 296,583 yd^3 for the 1 Myr flood (NM1088, Tulloch WSE 500), extending approximately 8,750 ft downstream along the river centerline (Figure 23). We calculated the net volume change by comparing the initial and final bed elevation along the entire Stanislaus River. The extent is defined as the continuous region of deposition exceeding 0.5 ft. The total amount of deposition in the Stanislaus River is greatly influenced by the amount of erosion that occurs on the spillway. Deposition in the Stanislaus River slightly exceeds the erosion on the spillway due to additional erosion of sediment in Bean Gulch.

Table 12.—Starting bed elevations, starting sediment thickness, and erosion or deposition results at model conclusion, NM Reservoir WSE of 1,088 ft

MP	RI	Bed start (ft)	Sed thick (ft)	Tulloch 500 ft	Tulloch 505 ft	Tulloch 510 ft	Tulloch 515 ft	
PAGE 47				Bed Change (ft)	Bed Change (ft)	Bed change (ft)	Bed end (ft)	Erosion or Deposition >0.5 ft
1	100	397.6	15	0.03	0.02	0.01	0.01	No
1	500	397.6	15	0.03	0.02	0.01	0.01	No
1	5000	397.6	15	0.06	0.03	0.01	0.01	No
1	20000	397.6	15	0.09	0.06	0.03	0.02	No
1	100000	397.6	15	0.11	0.08	0.06	0.04	No
1	1000000	397.6	15	0.13	0.10	0.08	0.06	No
2	100	514.5	1	-0.30	-0.33	0.12	2.40	No/Deposition
2	500	514.5	1	-0.07	-0.31	0.08	2.00	No/Deposition
2	5000	514.5	1	0.53	0.19	0.62	1.29	No/Deposition
2	20000	514.5	1	1.89	2.02	2.51	2.32	Deposition
2	100000	514.5	1	0.34	0.86	0.82	0.76	No/Deposition
2	1000000	514.5	1	-0.48	-0.43	-0.26	-0.58	No/Erosion
3	100	982.3	5.4	-5.17	-4.95	-5.17	-4.93	Erosion
3	500	982.3	5.4	-4.88	-5.37	-5.38	-5.37	Erosion
3	5000	982.3	5.4	-5.45	-5.45	-5.45	-5.45	Erosion
3	20000	982.3	5.4	-4.77	-4.77	-4.78	-4.77	Erosion
3	100000	982.3	5.4	-5.44	-5.44	-5.44	-5.44	Erosion
3	1000000	982.3	5.4	-5.47	-5.47	-5.47	-5.47	Erosion
4	100	888.7	1	8.51	6.31	8.64	10.11	Deposition
4	500	888.7	1	9.02	6.60	9.10	9.47	Deposition
4	5000	888.7	1	12.14	11.42	11.41	12.47	Deposition
4	20000	888.7	1	12.10	12.22	11.99	13.52	Deposition
4	100000	888.7	1	13.86	12.60	12.83	13.88	Deposition
4	1000000	888.7	1	11.14	13.28	14.44	14.19	Deposition
5	100	932.3	4	-1.74	-1.75	-1.70	-1.75	Erosion
5	500	932.3	4	-3.27	-3.27	-3.49	-3.48	Erosion
5	5000	932.3	4	-4.01	-3.97	-3.98	-4.01	Erosion
5	20000	932.3	4	-3.99	-3.99	-4.01	-3.97	Erosion
5	100000	932.3	4	-3.97	-3.97	-3.97	-3.97	Erosion
5	1000000	932.3	4	-3.96	-3.96	-3.97	-3.96	Erosion
6	100	489.8	8	14.82	16.04	17.93	20.80	Deposition
6	500	489.8	8	15.24	16.64	18.04	21.14	Deposition

Table 12.—Starting bed elevations, starting sediment thickness, and erosion or deposition results at model conclusion, NM Reservoir WSE of 1,088 ft

MP	RI	Bed start (ft)	Sed thick (ft)	Tulloch 500 ft	Tulloch 505 ft	Tulloch 510 ft	Tulloch 515 ft	
PAGE 47				Bed Change (ft)	Bed Change (ft)	Bed change (ft)	Bed end (ft)	Erosion or Deposition >0.5 ft
6	5000	489.8	8	17.04	16.73	17.77	19.97	Deposition
6	20000	489.8	8	18.28	17.81	18.00	20.67	Deposition
6	100000	489.8	8	18.09	17.93	17.75	21.57	Deposition
6	1000000	489.8	8	17.50	16.21	17.55	18.71	Deposition
7	100	485.9	8	1.74	1.10	0.75	0.43	Deposition
7	500	485.9	8	3.02	1.90	1.22	0.77	Deposition
7	5000	485.9	8	3.72	4.09	2.59	1.54	Deposition
7	20000	485.9	8	4.70	4.81	3.77	2.06	Deposition
7	100000	485.9	8	5.80	5.72	4.70	3.25	Deposition
7	1000000	485.9	8	5.66	7.10	6.60	5.02	Deposition
8	100	459.0	8	0.01	0.00	0.00	0.00	No
8	500	459.0	8	0.04	0.01	0.01	0.00	No
8	5000	459.0	8	0.08	0.06	0.04	0.03	No
8	20000	459.0	8	0.09	0.08	0.06	0.04	No
8	100000	459.0	8	0.11	0.08	0.07	0.06	No
8	1000000	459.0	8	0.13	0.10	0.08	0.07	No
9	100	1072.2	5.4	-4.88	-4.88	-4.88	-4.88	Erosion
9	500	1072.2	5.4	-4.96	-4.96	-4.96	-4.96	Erosion
9	5000	1072.2	5.4	-5.18	-5.18	-5.18	-5.18	Erosion
9	20000	1072.2	5.4	-5.21	-5.21	-5.21	-5.21	Erosion
9	100000	1072.2	5.4	-5.02	-5.02	-5.02	-5.02	Erosion
9	1000000	1072.2	5.4	-5.10	-5.10	-5.10	-5.10	Erosion
10	100	1021.8	5.4	-4.83	-4.83	-4.83	-4.83	Erosion
10	500	1021.8	5.4	-5.23	-5.22	-5.23	-5.23	Erosion
10	5000	1021.8	5.4	-5.26	-5.27	-5.26	-5.27	Erosion
10	20000	1021.8	5.4	-5.25	-5.25	-5.25	-5.25	Erosion
10	100000	1021.8	5.4	-5.31	-5.31	-5.31	-5.31	Erosion
10	1000000	1021.8	5.4	-5.25	-5.25	-5.25	-5.25	Erosion

Table 13.—Starting bed elevations, starting sediment thickness, and erosion or deposition results at model conclusion, NM Reservoir WSE of 1,049 ft

MP	RI	Bed start (ft)	Sed thick (ft)	Tulloch 500 ft	Tulloch 505 ft	Tulloch 510 ft	Tulloch 515 ft	
				Bed Change (ft)	Bed Change (ft)	Bed change (ft)	Bed end (ft)	Erosion or Deposition >0.5 ft
1	20000	397.6	15	0.03	0.02	0.01	0.01	No
1	50000	397.6	15	0.03	0.02	0.01	0.01	No
1	100000	397.6	15	0.03	0.02	0.01	0.01	No
1	1000000	397.6	15	0.04	0.02	0.01	0.01	No
2	20000	514.5	1	4.63	4.70	5.36	7.63	Deposition
2	50000	514.5	1	2.81	2.83	2.86	8.13	Deposition
2	100000	514.5	1	1.17	1.54	1.85	4.20	Deposition
2	1000000	514.5	1	0.33	0.36	0.17	0.15	No
3	20000	982.3	5.4	-1.97	-1.97	-1.87	-2.02	Erosion
3	50000	982.3	5.4	-4.86	-4.86	-4.86	-5.00	Erosion
3	100000	982.3	5.4	-4.53	-4.53	-4.53	-4.53	Erosion
3	1000000	982.3	5.4	-5.40	-5.40	-5.40	-5.40	Erosion
4	20000	888.7	1	7.07	7.25	7.09	7.13	Deposition
4	50000	888.7	1	7.50	7.27	7.31	7.47	Deposition
4	100000	888.7	1	8.21	8.20	8.19	7.71	Deposition
4	1000000	888.7	1	9.46	12.00	11.37	11.35	Deposition
5	20000	932.3	4	-0.03	-0.10	-0.05	-0.06	No
5	50000	932.3	4	-1.07	-1.10	-1.02	-1.03	Erosion
5	100000	932.3	4	-1.36	-1.34	-1.35	-1.40	Erosion
5	1000000	932.3	4	-3.55	-3.53	-3.28	-3.54	Erosion
6	20000	489.8	8	11.72	13.51	15.50	14.58	Deposition
6	50000	489.8	8	14.85	16.51	18.50	20.09	Deposition
6	100000	489.8	8	14.52	15.91	18.21	20.91	Deposition
6	1000000	489.8	8	16.17	16.52	17.72	20.03	Deposition
7	20000	485.9	8	0.39	0.21	0.10	0.06	No
7	50000	485.9	8	0.77	0.48	0.25	0.13	No/Dep
7	100000	485.9	8	1.15	0.78	0.48	0.28	No/Dep
7	1000000	485.9	8	3.36	3.32	1.94	1.24	Deposition
8	20000	459.0	8	0.00	0.00	0.00	0.00	No
8	50000	459.0	8	0.00	0.00	0.00	0.00	No

Table 13.—Starting bed elevations, starting sediment thickness, and erosion or deposition results at model conclusion, NM Reservoir WSE of 1,049 ft

MP	RI	Bed start (ft)	Sed thick (ft)	Tulloch 500 ft	Tulloch 505 ft	Tulloch 510 ft	Tulloch 515 ft	
				Bed Change (ft)	Bed Change (ft)	Bed change (ft)	Bed end (ft)	Erosion or Deposition >0.5 ft
8	100000	459.0	8	0.00	0.00	0.00	0.00	No
8	1000000	459.0	8	0.08	0.05	0.03	0.02	No
9	20000	1072.2	5.4	-4.41	-4.41	-4.41	-4.41	Erosion
9	50000	1072.2	5.4	-4.71	-4.71	-4.71	-4.71	Erosion
9	100000	1072.2	5.4	-4.91	-4.91	-4.91	-4.91	Erosion
9	1000000	1072.2	5.4	-5.33	-5.33	-5.33	-5.33	Erosion
10	20000	1021.8	5.4	-4.49	-4.49	-4.49	-4.49	Erosion
10	50000	1021.8	5.4	-4.87	-4.87	-4.87	-4.87	Erosion
10	100000	1021.8	5.4	-5.03	-5.03	-5.03	-5.03	Erosion
10	1000000	1021.8	5.4	-5.39	-5.39	-5.39	-5.39	Erosion

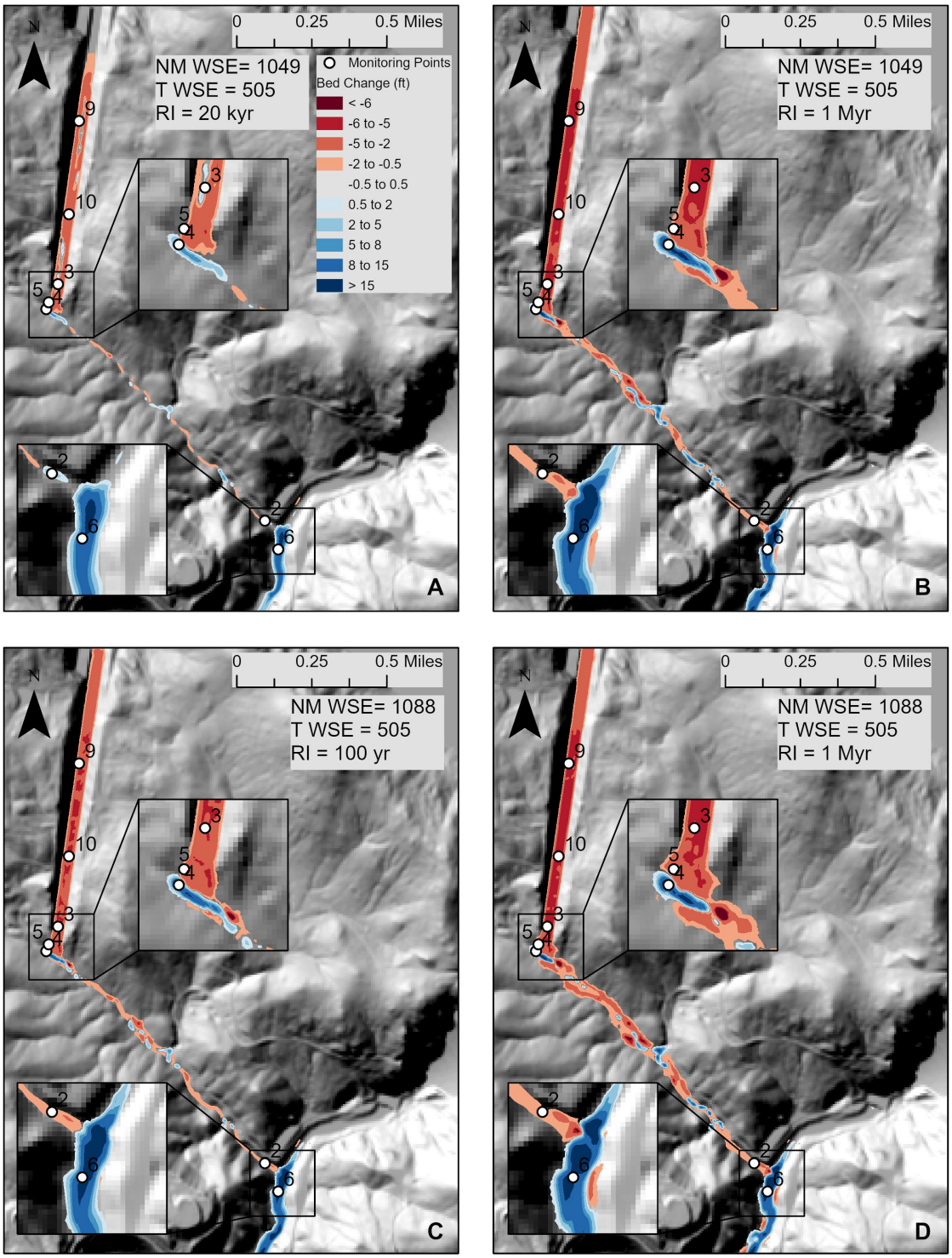

Figure 20.—Erosion and deposition results at model conclusion. Negative values are erosion, positive values are deposition. "NM WSE" is the New Melones Reservoir elevation, "T WSE" is the Tulloch Reservoir elevation, and "RI" is the recurrence interval for the modeled flow. The range of erosion to deposition for the four flows are: (A) -5.3 ft to 18.3 ft, (B) -11.3 to 28.3 ft, (C) -7.7 to 24.8 ft, and (D) -11.4 to 27.3 ft.

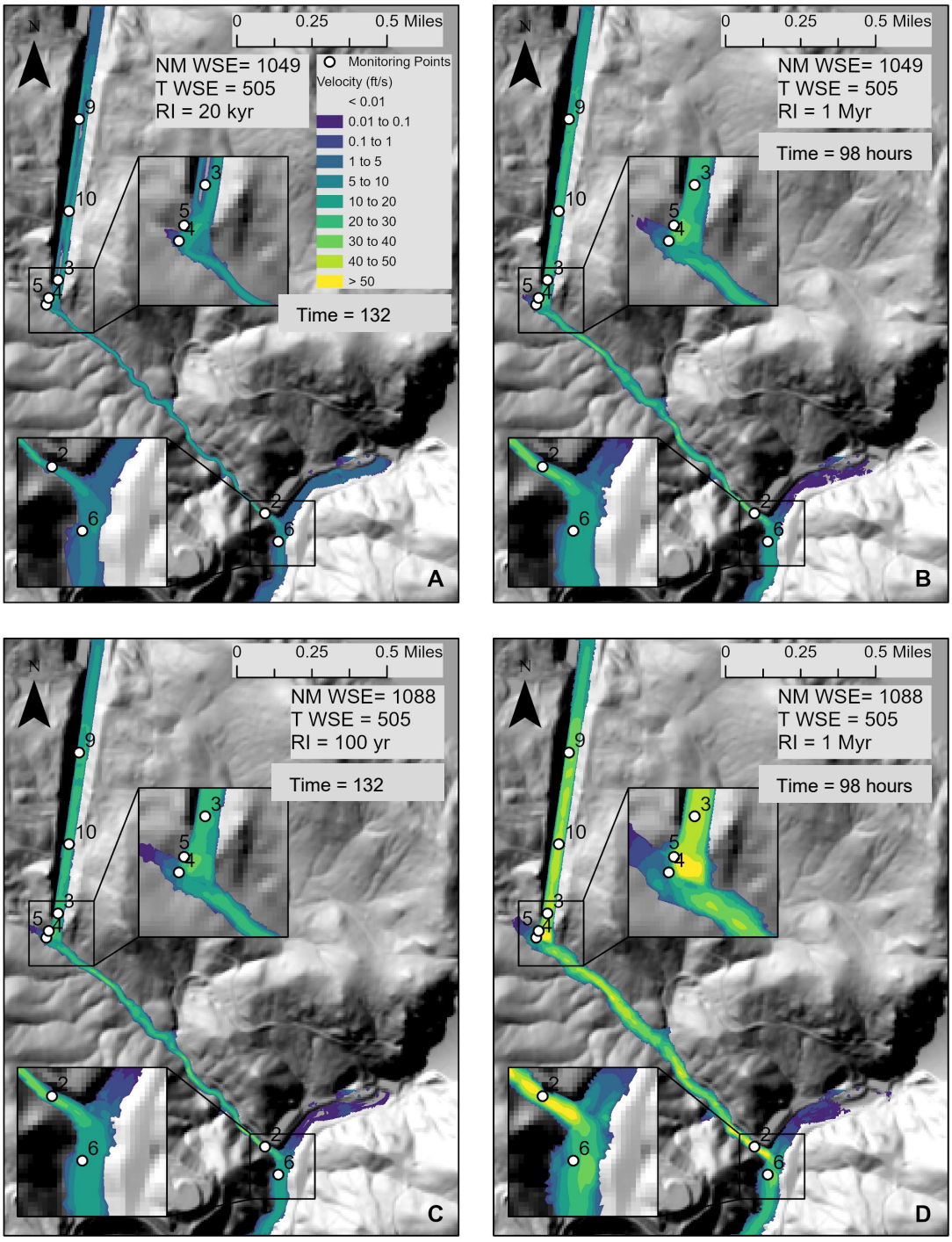

Figure 21.—Velocity results from intermediate output 80 hours after the model hydrograph start time. Plots A and C have discharge hydrographs that start at 52 hours and plots B and D have discharge hydrographs that start at 18 hours. "NM WSE" is the New Melones Reservoir elevation, "T WSE" is the Tulloch Reservoir elevation, and "RI" is the recurrence interval for the modeled flow.

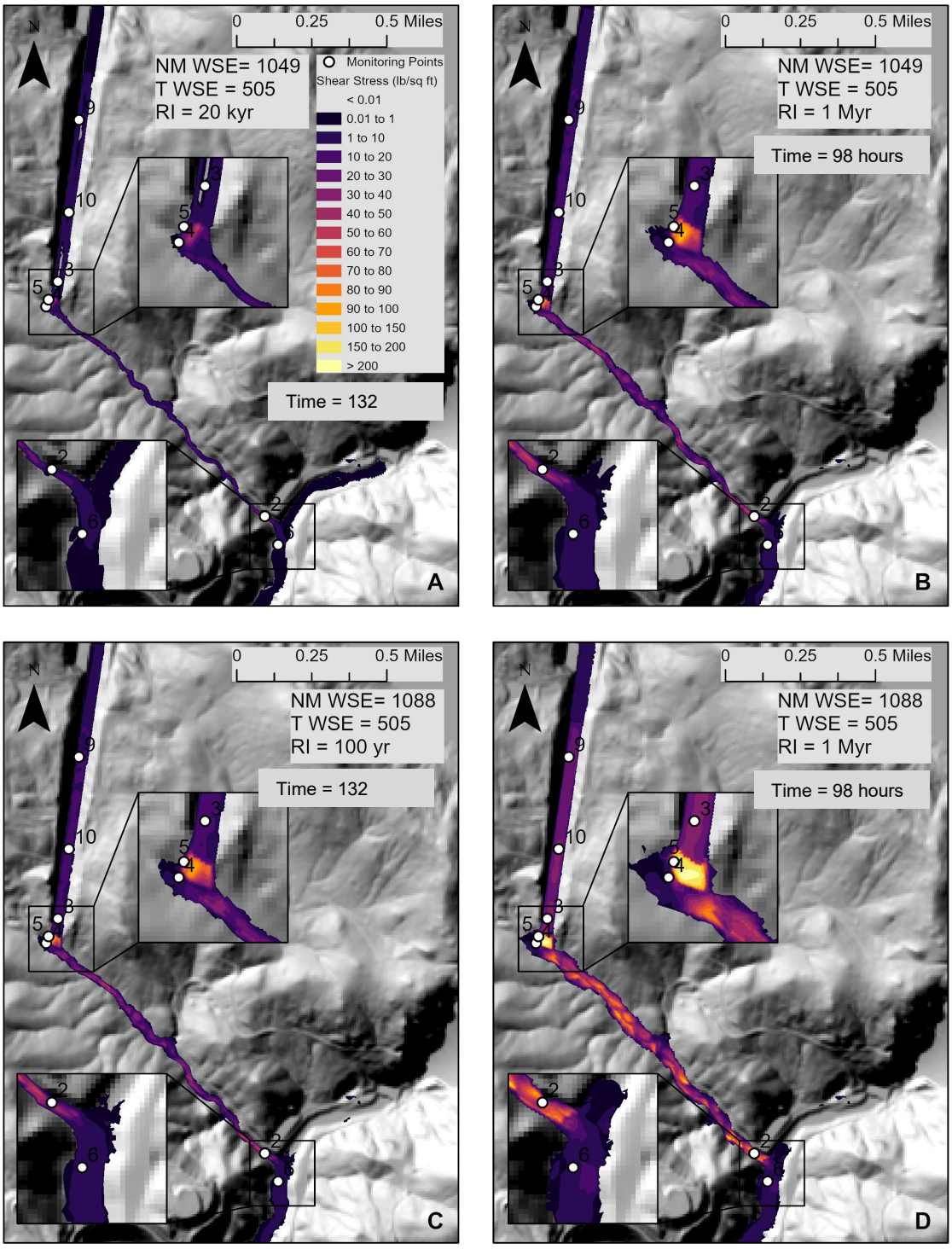

Figure 22.—Bed shear stress from intermediate output 80 hours after the model hydrograph start time. Plots A and C have discharge hydrographs that start at 52 hours and plots B and D have discharge hydrographs that start at 18 hours. "NM WSE" is the New Melones Reservoir elevation, "T WSE" is the Tulloch Reservoir elevation, and "RI" is the recurrence interval for the modeled flow.

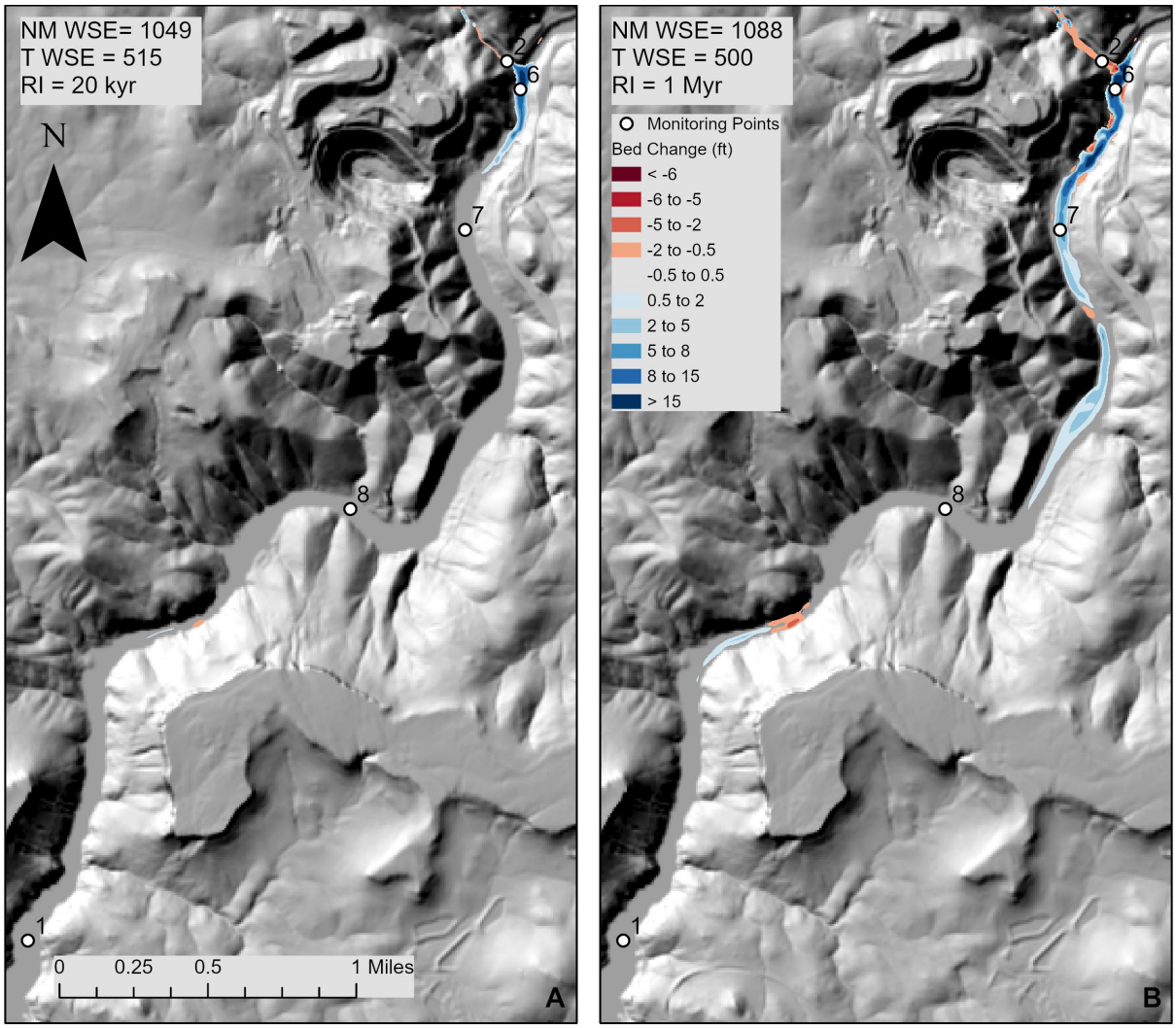

Figure 23.—Maximum extent of the deposition exceeding <0.5 ft of bed change in the Stanislaus River for (A) 20 kyr RI flood (NM1049, Tulloch WSE 515), extending 2,120 ft and (B) the 1 Myr flood (NM1088, Tulloch WSE 500), extending approximately 8,750 ft downstream to just above MP 8 (we did not include the separated deposit farther downstream, although this was included in the net volume change).

Key findings from time series data of model simulations

- Flow depths at MPs generally peak concurrent with the hydrograph peak, except for MP 6 in the Stanislaus River. This point decreases in depth concurrent with the outlet works ceasing operation when the spillway flow reaches an excess of 8,000 cfs. As flow from the spillway reaches the Stanislaus River, the flow depths again increase (Figure 24; Figure 25).

- The peak velocities and shear stresses closely matched the peak discharge for the hydrographs (Figure 24; Figure 25), except at MP 4, which is hydraulically complex. At MP 4, the velocities and shear stresses precipitously drop during a high rate of deposition. The shear stress and velocities then stabilize and slightly increase through the falling limb of the hydrograph. This increase is associated with a small amount of erosion (thinning the depositional package; there is still net deposition by the end of the model simulation).

- When looking at the end of the model simulation results, we were initially surprised that MP 5 did not exhibit erosion for all the modeled flows. We expected there to be massive erosion on the high gradient hillslope. However, the flow depths at MP 5 were exceptionally low for most of the model runs, because the flow was distributed across the hillslope. The flow depth only increases to an observable amount for the two largest modeled flows (RI 100 kyr and 1 Myr for NM1088); for these two flows, MP 5 exhibits the highest modeled shear stresses for all simulations, as expected (Figure 24).

- The highest rate of bed change for erosion and deposition occurs during the rising limb of the hydrograph Figure 24; Figure 25). This is consistent with research indicating that coarse sediment exhibits greater sediment transport on the rising limb of a hydrograph (e.g., Wang et al., 2021).

- MP 2 experienced net deposition, erosion, or no change at the end of the model simulation depending on the flow magnitude and base level (Table 12, Table 13). The time-series plots shows that MP 2 consistently experiences deposition during the early portion of the rising limb of the hydrograph for all the simulated flows (Figure 24, Figure 25), likely as it begins to receive sediment from upstream. The bed shear stresses and velocities observed at MP 2 are the highest or second highest observed from all the MPs. Following an initial peak of deposition that precedes the hydrograph peak, MP 2 erodes. The net erosion or net deposition is controlled by duration of the hydrograph, rate of transport, and the rate of sediment supply from upstream. The largest hydrographs have the longest duration and greatest rate of erosion following deposition at MP 2.

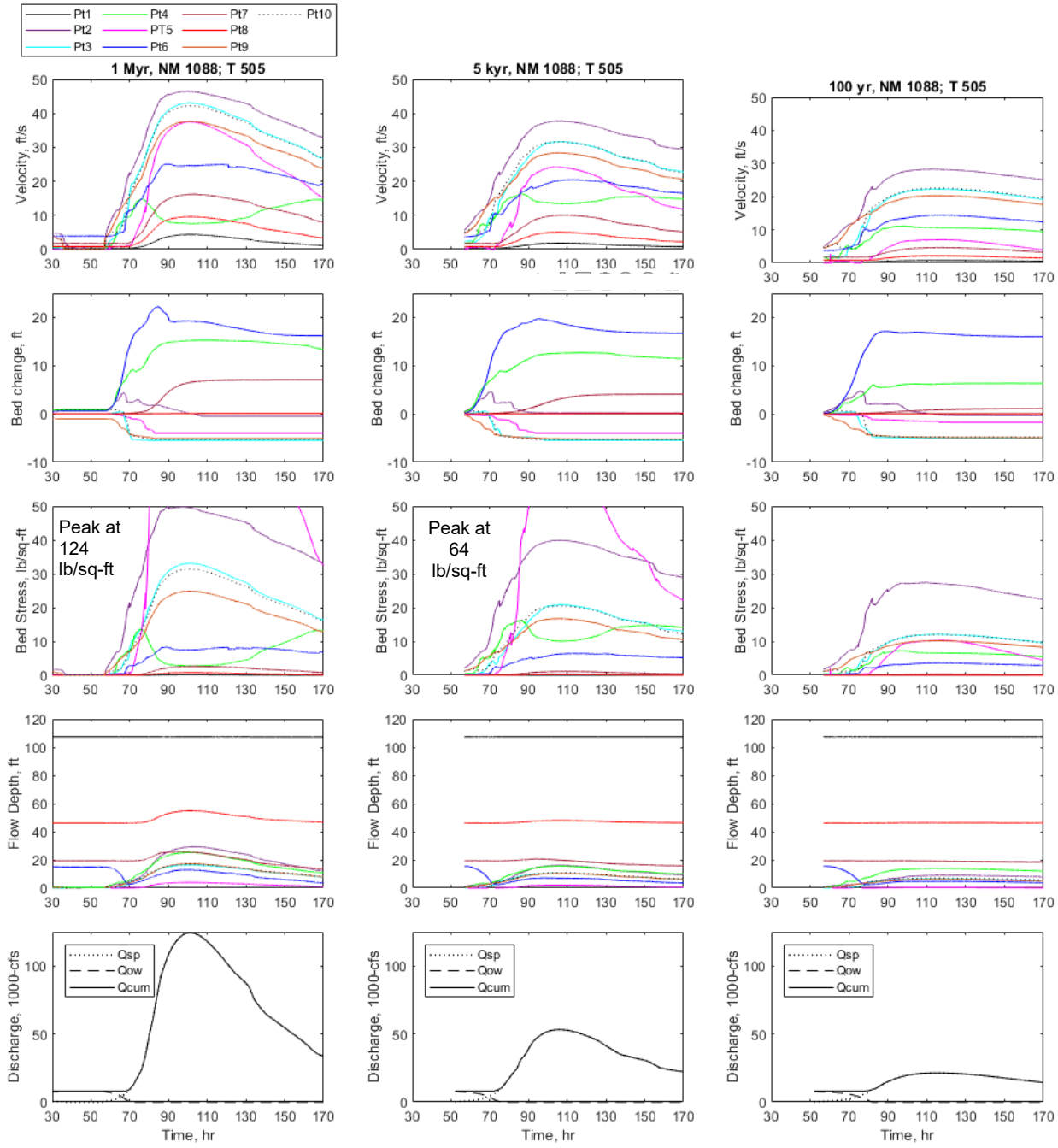

Figure 24.—Model results at monitoring points for the 1 Myr, 5 kyr, and 100 yr recurrence interval flows using a starting water surface elevation of 1088 ft at New Melones Reservoir and a downstream water surface elevation of 505 ft at Tulloch Reservoir. Qsp= spillway discharge; Qow= outlet works discharge, Qcum= cumulative discharge. For monitoring point locations, Figure 12.

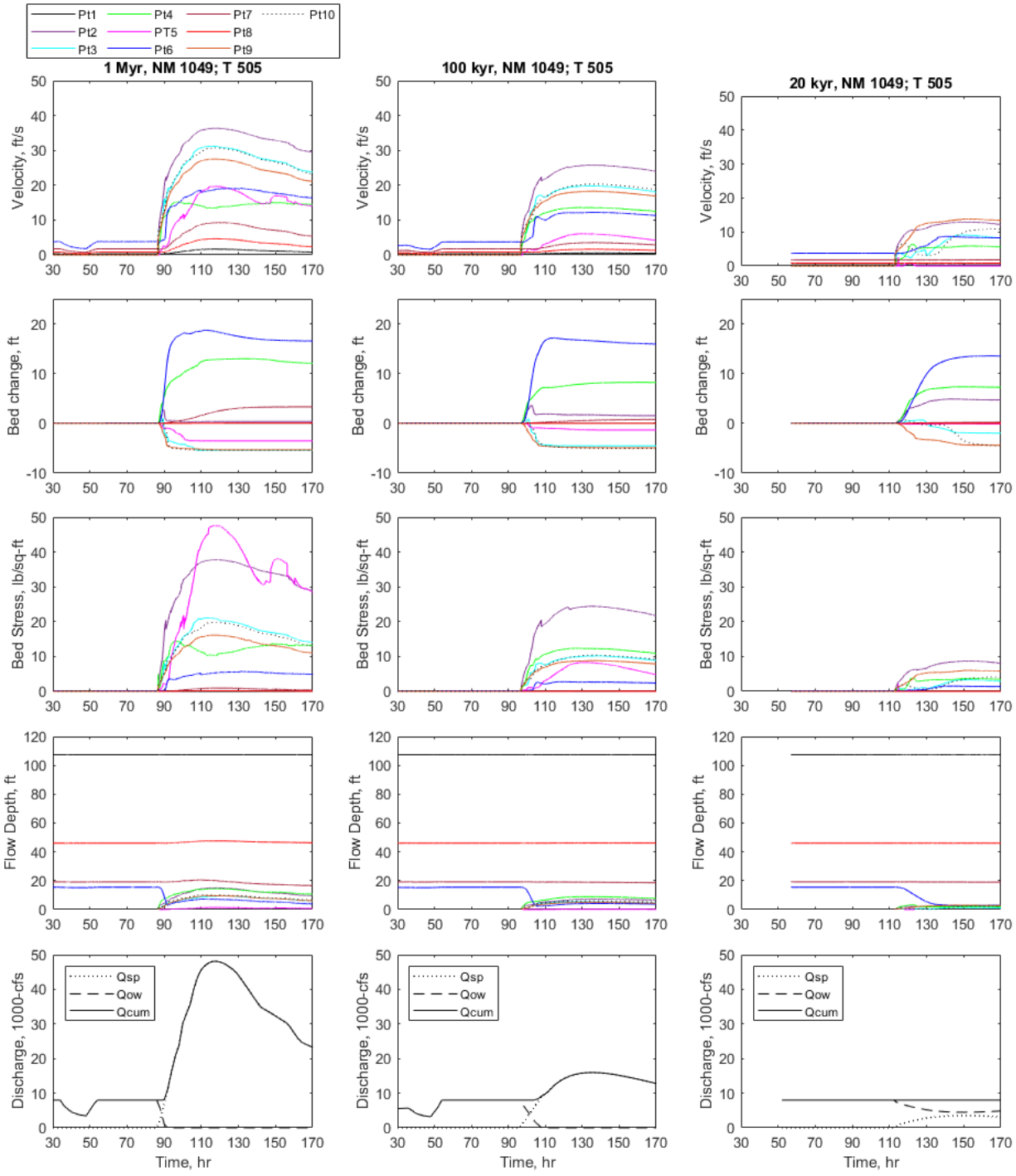

Figure 25.—Model results at monitoring points for the 1 Myr, 100 kyr, and 20 kyr recurrence interval flows using a starting water surface elevation of 1049 ft at New Melones Reservoir and a downstream water surface elevation of 505 ft at Tulloch Reservoir. Qsp= spillway discharge; Qow= outlet works discharge, Qcum= cumulative discharge. For monitoring point locations, Figure 12.

4.1.4 SRH-2D Sensitivity Testing

The SRH-2D mobile bed transport model was tested by the developers on a series of test cases with calibration data. Simulating sediment transport on the New Melones Dam Spillway pushes the application of SRH-2D to an extreme that wasn't previously tested. Therefore, we chose to explore the model sensitivity to the timestep and sediment transport capacity formulations. The goal of this sensitivity testing is not to generate identical results, as the overall erosion and deposition in any particular cell is dictated by the interplay between cell size, timestep, and the governing equations. Rather, we seek to confirm that the qualitative trends in erosion and deposition are consistent. We also test the model's sensitivity to sediment characteristics, such as overall thickness and grain size distribution since our understanding of these data are poorly constrained in this application. We selected a subset of model flows to conduct sensitivity testing, typically with a New Melones starting elevation of 1088 ft and Tulloch Reservoir elevation of 505 ft.

Increasing and Decreasing Spillway Thickness

One of the greatest sources of uncertainty in our model is thickness of sediment overlying the spillway invert. We do not have the precision or spatial extent of geophysical data to vary the thickness spatially in any meaningful way. Therefore, we simply tested the overall effect of increasing or decreasing the uniform thickness. We tested 0.2 ft of thickness to simulate sediment transport in the Stanislaus River without the deluge of sediment eroded from the spillway. We also tested decreasing and increasing the spillway thickness by 2 ft, resulting in thicknesses of 3.4 ft and 7.4 ft, respectively.

Key Findings at the End of the Model Simulations, from Varying Spillway Thickness

- It takes larger flows to fully remove the entire thickness of sediment cover when the sediment cover is thicker (see MP 3, MP 9, MP 10) (Table 14).
- MP 4 experiences more aggradation with increasing spillway sediment thickness. However, this pocket of deposition is localized immediately below the spillway (Table 14).
- The spatial maps of erosion and deposition do not differ greatly within Bean Gulch, based on the spillway sediment cover (Figure 26; Figure 27). Erosion in Bean Gulch, downstream from MP 4, dominates regardless of the incoming volume of sediment from the spillway. Small pockets of deposition exist in all scenarios, but erosion dominates.
- The upper Stanislaus River experiences less aggradation with less sediment cover (Table 14).
- MP 1, near the downstream boundary experiences no change in aggradation due to changing spillway thickness for flows under a RI of 5,000 cfs (NM1088). For higher flows, the maximum change in aggradation between 0.2 ft of spillway cover and 7.4 ft of spillway cover is 0.05 ft (Table 14). This small value likely exceeds the model's sediment transport precision. This further supports our conclusion that Tulloch is unlikely to be impacted by New Melones Spillway sediment.

Table 14.—Erosion and deposition results with varying spillway thickness, New Melones Reservoir starting elevation of 1088 ft and Tulloch Reservoir starting elevation of 505 ft

RI	MP	Sediment thickness start Ero/Dep (ft)	~No thickness (0.2 ft) Ero/Dep (ft)	-2ft thick (3.4 ft) Ero/Dep (ft)	Regular run (5.4 ft) Ero/Dep (ft)	+ 2 ft thick (7.4 ft)) Bed end (ft)
100	1	15	0.02	0.02	0.02	0.02
100	2	1	-1.36	0.54	-0.33	0.09
100	3	varies	-0.19	-3.36	-4.95	-5.47
100	4	1	2.30	4.39	6.31	6.95
100	5	4	-3.20	-2.96	-1.75	-1.60
100	6	8	9.01	14.58	16.04	17.41
100	7	8	0.09	0.65	1.10	1.72
100	8	8	0.00	0.00	0.00	0.00
100	9	varies	-0.19	-3.04	-4.88	-6.69
100	10	varies	-0.19	-3.11	-4.83	-6.81
500	1	15	0.02	0.02	0.02	0.02
500	2	1	-1.37	-0.37	-0.31	-0.08
500	3	varies	-0.19	-3.44	-5.37	-4.29
500	4	1	2.04	5.44	6.60	7.95
500	5	4	-3.83	-3.14	-3.27	-3.56
500	6	8	10.59	15.00	16.64	17.42
500	7	8	0.14	1.05	1.90	2.97
500	8	8	0.00	0.01	0.01	0.02
500	9	varies	-0.19	-3.14	-4.96	-6.81
500	10	varies	-0.20	-3.31	-5.22	-6.57
5000	1	15	0.02	0.03	0.03	0.03
5000	2	1	-1.36	-0.03	0.19	1.00
5000	3	varies	-0.19	-3.44	-5.45	-6.31
5000	4	1	4.72	9.32	11.42	12.26
5000	5	4	-4.03	-3.98	-3.97	-3.58
5000	6	8	12.94	16.41	16.73	17.67
5000	7	8	0.30	2.01	4.09	6.04
5000	8	8	0.02	0.04	0.06	0.08
5000	9	varies	-0.20	-3.27	-5.18	-7.16
5000	10	varies	-0.19	-3.34	-5.27	-6.93

Table 14.—Erosion and deposition results with varying spillway thickness, New Melones Reservoir starting elevation of 1088 ft and Tulloch Reservoir starting elevation of 505 ft

RI	MP	Sediment thickness start Ero/Dep (ft)	~No thickness (0.2 ft) Ero/Dep (ft)	-2ft thick (3.4 ft) Ero/Dep (ft)	Regular run (5.4 ft) Ero/Dep (ft)	+ 2 ft thick (7.4 ft)) Bed end (ft)
20000	1	15	0.03	0.05	0.06	0.07
20000	2	1	-1.37	0.66	2.02	2.82
20000	3	varies	-0.19	-3.44	-4.77	-5.98
20000	4	1	4.16	9.95	12.22	12.99
20000	5	4	-4.00	-3.98	-3.99	-3.98
20000	6	8	14.30	17.16	17.81	20.41
20000	7	8	0.44	2.50	4.81	6.71
20000	8	8	0.03	0.05	0.08	0.10
20000	9	varies	-0.20	-3.27	-5.21	-7.16
20000	10	varies	-0.20	-3.37	-5.25	-6.89
100000	1	15	0.05	0.07	0.08	0.10
100000	2	1	-1.35	0.00	0.86	1.28
100000	3	varies	-0.21	-3.44	-5.44	-5.20
100000	4	1	5.40	11.41	12.60	13.19
100000	5	4	-3.99	-3.98	-3.97	-3.96
100000	6	8	15.74	17.64	17.93	19.90
100000	7	8	0.71	3.30	5.72	7.90
100000	8	8	0.03	0.06	0.08	0.11
100000	9	varies	-0.20	-3.26	-5.02	-7.15
100000	10	varies	-0.19	-3.39	-5.31	-7.24
100000	1	15	0.07	0.09	0.10	0.12
100000	2	1	-1.35	-0.54	-0.43	-0.19
100000	3	varies	-0.19	-3.46	-5.47	-6.29
100000	4	1	5.55	11.17	13.28	15.05
100000	5	4	-4.01	-3.99	-3.96	-3.94
100000	6	8	16.79	17.73	16.21	18.38
100000	7	8	1.25	4.92	7.10	7.69
100000	8	8	0.04	0.07	0.10	0.12
100000	9	varies	-0.20	-3.28	-5.10	-7.02
100000	10	varies	-0.19	-3.27	-5.25	-7.22

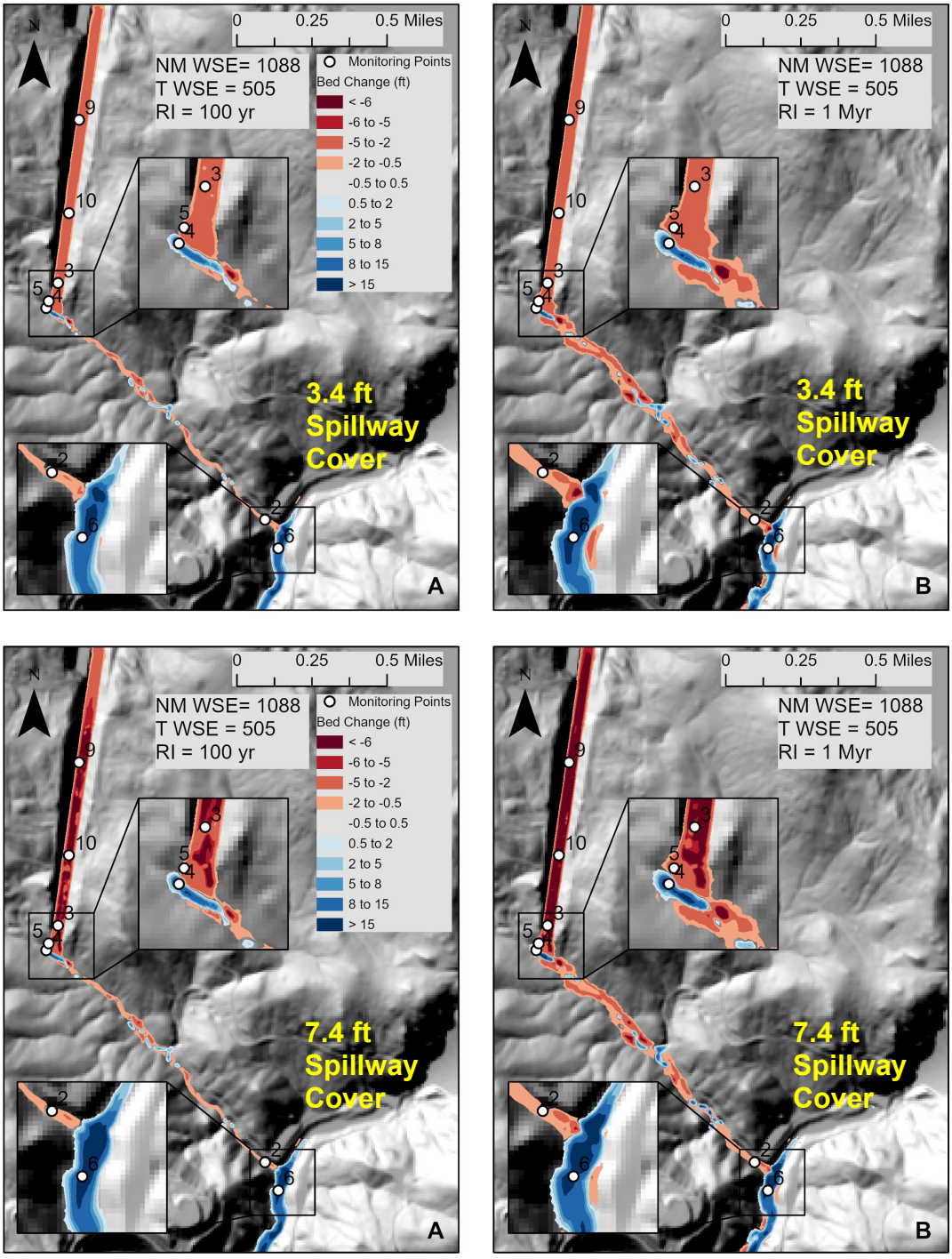

Figure 26.—Erosion and deposition results at model conclusion for thinner and thicker spillway cover assumptions. Negative values are erosion, positive values are deposition. "NM WSE" is the New Melones Reservoir elevation, "T WSE" is the Tulloch Reservoir elevation, and "RI" is the recurrence interval for the modeled flow. (A and B). Spillway thickness was decreased to 3.4 ft. (C and D). Spillway thickness was increased to 7.4 ft. Monitoring points are shown in white. The range of values for the four flows are: (A) -7.8 ft to 21.9 ft, (B) -11.9 to 26.3 ft, (C) -7.6 to 26.7 ft, and (D) -11.4 to 29.4 ft.

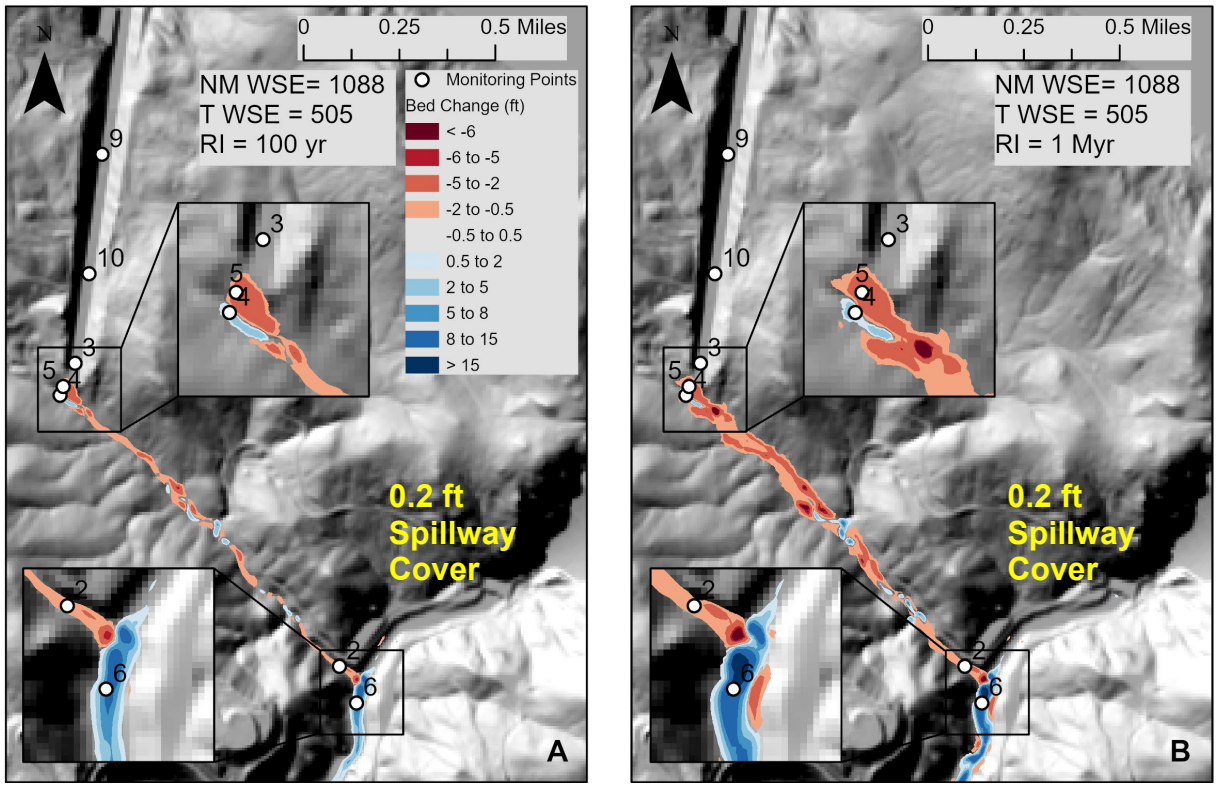

Figure 27.—Erosion and deposition results at model conclusion for approximately no spillway sediment cover (0.2 ft thickness). Negative values are erosion, positive values are deposition. "NM WSE" is the New Melones Reservoir elevation, "T WSE" is the Tulloch Reservoir elevation, and "RI" is the recurrence interval for the modeled flow. Monitoring points are shown in white. The range of values for the two flows are: (A) -5.7 ft to 13.5 ft and (B) -12.1 to 21.5 ft.

Timestep Sensitivity

We initially ran our models using a timestep of 1 second (s). We checked 2D spatial results at intermediate and final model output and the model results appeared stable. However, a deeper analysis of time series results, specifically at MP 4, revealed an instability in the modeled depth for the largest flow (NM1088 RI 1 Myr). Therefore, we dropped the timestep to 0.5 s for the larger flows (NM1088 RI ≤ 20 kyr and NM1049 RI 1 Myr). We conducted analysis at MP 4 for these flows, and everything appeared stable (overall smooth plots of time-series results).

Afterward, we decided to conduct timestep sensitivity testing as well by rerunning the models with the timestep reduced by half. Y. Lai, the model developer, advises caution in conducting this type of sensitivity test. He states that a model user should not expect identical results for any particular cell (Y. Lai, oral comm., 1/30/2023). Rather, he advises that the goal of this type of sensitivity testing should be to yield similar spatial patterns in results. Model results at any particular cell are the result of an interplay between the cell size (dx) and the timestep (dt) (e.g., Chow, 1959).

Key Findings at the End of the Model Simulations, from Testing Timestep Sensitivity

- Spatial patterns in the results are generally consistent among the regular model runs and the timestep sensitivity runs (Table 15; Figure 20 and Figure 28).

- MP 4 remains sensitive to the timestep change, as large changes are evident in the aggradation for the runs with the regular and halved timestep at the lower RI runs (NM1088 RI 100 yr; NM1049 RI 20 kyr) (Table 15). The difference is evident in the models that used an original timestep of 1 s. This indicates we likely should have cut the timestep to 0.5 s for all model runs. The need to decrease the timestep also explains the differing results with base level at MP 4 (e.g., NM1088, RI 500 yr, Table 12). Preliminary runs showed results with varying base level were more consistent with a lower timestep (Y. Lai, verbal communication during model testing, 1/30/2023). However, the general trends in the model results remain unchanged and this sensitivity does not affect any of the conclusions derived from the model results. This model is an extreme application of SRH-2D. Further sensitivity testing could be conducted to assess how the model is sensitive to various parameters and this testing could be used to make recommendations for modeling extreme scenarios. However, this is beyond the scope of this project.

Table 15.—Comparison of total erosion and deposition at monitoring points at the model conclusion to test the model's timestep sensitivity

NM1088 Runs				NM1049 Runs			
RI	**MP**	**Regular run Ero/Dep (ft)**	**Halved Timestep Ero/Dep (ft)**	**RI**	**MP**	**Regular run Ero/Dep (ft)**	**Halved Timestep Ero/Dep (ft)**
100	1	0.02	0.02	20000	1	0.02	0.02
100	2	-0.33	0.41	20000	2	4.70	4.81
100	3	-4.95	-4.91	20000	3	-1.97	-2.02
100	4	6.31	9.68	20000	4	7.25	6.36
100	5	-1.75	-1.78	20000	5	-0.10	-0.08
100	6	16.04	16.19	20000	6	13.51	13.38
100	7	1.10	1.08	20000	7	0.21	0.21
100	8	0.00	0.00	20000	8	0.00	0.00
100	9	-4.88	-4.88	20000	9	-4.41	-4.40
100	10	-4.83	-4.82	20000	10	-4.49	-4.50
1000000	1	0.10	0.10	1000000	1	0.02	0.02
1000000	2	-0.43	0.07	1000000	2	1.54	1.99
1000000	3	-5.47	-5.46	1000000	3	-4.53	-4.39
1000000	4	13.28	13.79	1000000	4	8.20	8.83
1000000	5	-3.96	-3.95	1000000	5	-1.34	-1.28

Table 15.—Comparison of total erosion and deposition at monitoring points at the model conclusion to test the model's timestep sensitivity

NM1088 Runs				NM1049 Runs			
RI	**MP**	**Regular run Ero/Dep (ft)**	**Halved Timestep Ero/Dep (ft)**	**RI**	**MP**	**Regular run Ero/Dep (ft)**	**Halved Timestep Ero/Dep (ft)**
1000000	6	16.21	17.72	1000000	6	15.91	16.03
1000000	7	7.10	7.00	1000000	7	0.78	0.78
1000000	8	0.10	0.10	1000000	8	0.00	0.00
1000000	9	-5.10	-5.10	1000000	9	-4.91	-4.92
1000000	10	-5.25	-5.23	1000000	10	-5.03	-5.05

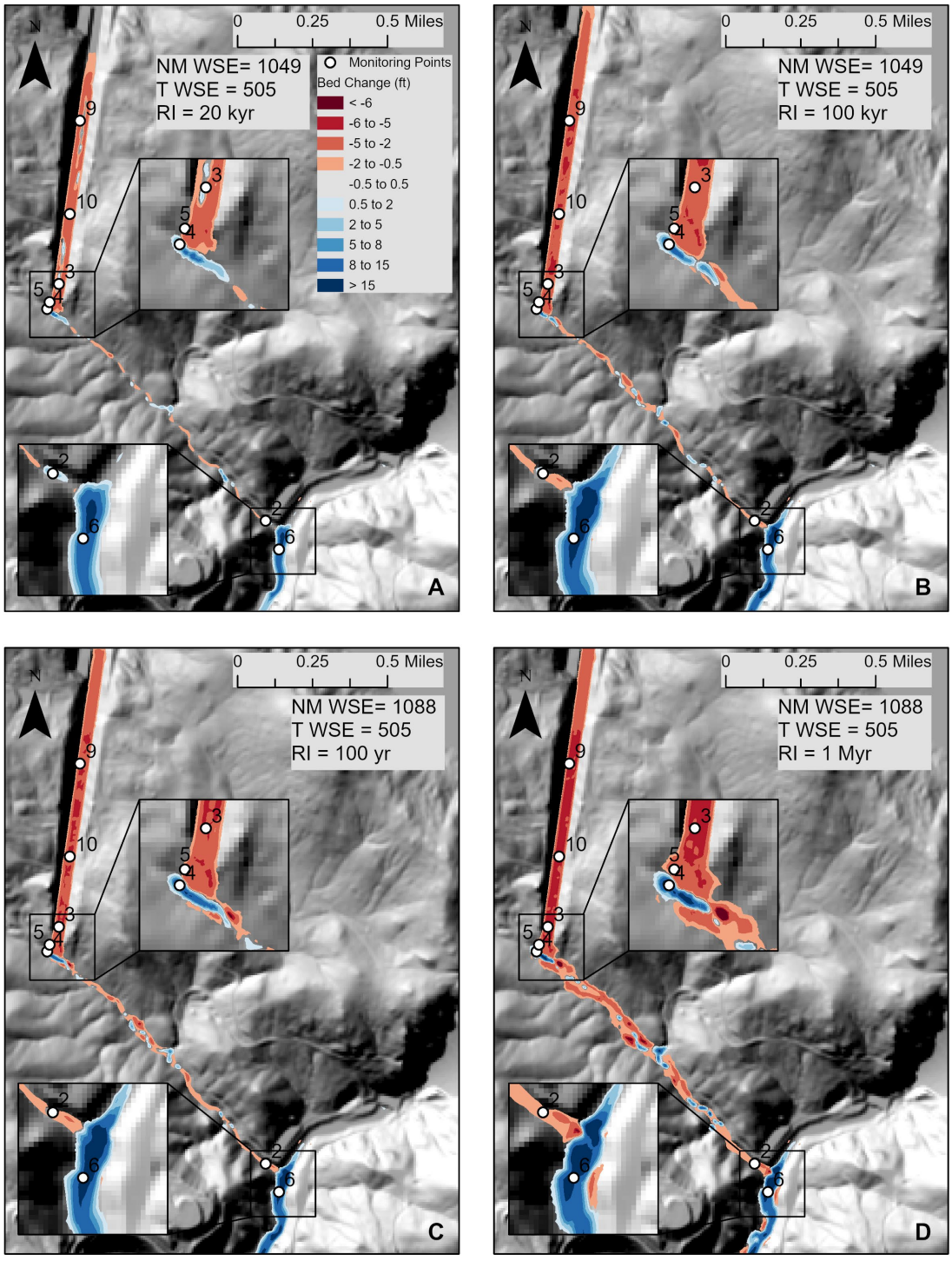

Figure 28.—Erosion and deposition results at model conclusion for the timestep sensitivity test (halved timestep). Negative values are erosion, positive values are deposition. "NM WSE" is the New Melones Reservoir elevation, "T WSE" is the Tulloch Reservoir elevation, and "RI" is the recurrence interval for the modeled flow. Monitoring points are shown in white. The range of values for the two flows are: (A) -5.3 ft to 18.3 ft, (B) -5.9 ft to 24.2 ft, (C) -11.5 to -27.9, and (D) -7.2 to 24.8.

Eliminating Coarse Fraction Assumption from the Spillway

We conducted pebble counts on the spillway, but we assumed that these data underrepresented coarse sediment below the surface. Therefore, we assumed that 15% of the sediment package was cobble-sized (250 mm) or larger (see section 2.2.5). We test the model's sensitivity to this coarse fraction assumption by rerunning the model with the original pebble count data.

Key Findings at the End of the Model Simulations, from Testing Coarse Fraction Assumption

- More erosion of spillway sediment occurs without the coarse fraction assumption (see MP 3, MP 9, MP 10 in Table 16). It also likely takes less time to evacuate the spillway sediment without the coarse fraction, as boulders persist longer as fines are removed by lower flows earlier in the hydrograph.

- Far less deposition occurs at MP 4 without the coarse assumption (Table 16). This indicates the majority of deposition at MP 4 was due to cobble-sized or coarser material. Although the model is very dynamic at MP 4 and this point is likely influenced by the timestep, the larger RI runs consistently show the same trend.

- The reduction in deposition in Bean Gulch at MP 4 does not continue into the Stanislaus River. MP 6, located just below the confluence with Bean Gulch, experiences more deposition (Table 16). This is because more material is transported out of Bean Gulch, but the backwatered Stanislaus is unable to efficiently transport the additional sediment, even if the overall D_{50} is lower.

- The overall spatial trend of removing the coarse sediment assumption results in a change of more erosion in Bean Gulch and more deposition in the Stanislaus River (Figure 29). More erosion also occurs in the spillway at lower RI flows (e.g., RI 100 yr in Figure 29). At higher RI flows, all sediment is eroded from the spillway with and without the coarse fraction included.

Table 16.—Erosion and deposition results for runs with a coarse fraction assumption on the spillway (regular run) and without the coarse fraction assumption (no coarse)

RI	MP	Regular run, with coarse	No coarse	RI	MP	Regular run, with coarse	No coarse
		Ero/Dep (ft)	Ero/Dep (ft)			Ero/Dep (ft)	Ero/Dep (ft)
100	1	0.02	0.02	20000	1	0.06	0.06
100	2	-0.33	0.59	20000	2	2.02	0.91
100	3	-4.95	-5.41	20000	3	-4.77	-5.42
100	4	6.31	1.97	20000	4	12.22	2.48
100	5	-1.75	-1.84	20000	5	-3.99	-3.95
100	6	16.04	16.50	20000	6	17.81	18.13
100	7	1.10	1.15	20000	7	4.81	5.85
100	8	0.00	0.00	20000	8	0.08	0.09
100	9	-4.88	-5.39	20000	9	-5.21	-5.38
100	10	-4.83	-5.36	20000	10	-5.25	-5.27
100000	1	0.08	0.09	1000000	1	0.10	0.12
100000	2	0.86	0.88	1000000	2	-0.43	0.87
100000	3	-5.44	-5.39	1000000	3	-5.47	-5.34
100000	4	12.60	2.44	1000000	4	13.28	2.74
100000	5	-3.97	-3.97	1000000	5	-3.96	-3.96
100000	6	17.93	19.00	1000000	6	16.21	22.03
100000	7	5.72	7.46	1000000	7	7.10	8.09
100000	8	0.08	0.10	1000000	8	0.10	0.12
100000	9	-5.02	-5.37	1000000	9	-5.10	-5.37
100000	10	-5.31	-5.36	1000000	10	-5.25	-5.37

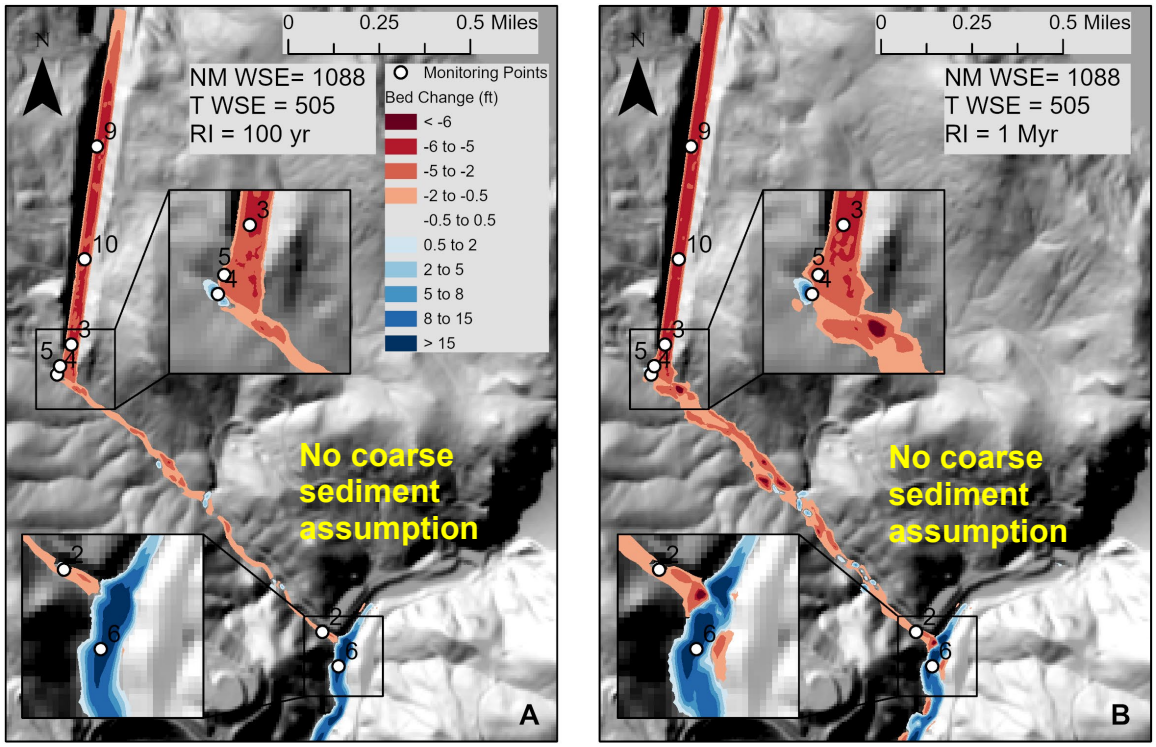

Figure 29.—Erosion and deposition results at model conclusion to test how the coarse sediment assumption on the spillway effects results. Negative values are erosion, positive values are deposition. "NM WSE" is the New Melones Reservoir elevation, "T WSE" is the Tulloch Reservoir elevation, and "RI" is the recurrence interval for the modeled flow. These models removed the coarse fraction assumption on the spillway. Monitoring points are shown in white. The range of values for the two flows are: (A) -6.07 ft to 25.9 ft and (B) -12.3 to 26.9 ft.

Testing Other Sediment Transport Capacity Formulations

We tested the Wilcock (Wilcock and Crowe, 2003) and Wu (Wu et al., 2000) sediment transport capacity formulations to compare the results with our regular runs using the Parker formulation (Parker, 1990). The purpose of this test was to ensure that other sediment transport capacity formulations produce the same general trend of erosion and deposition. Lai, the model developer, advises caution in conducting this type of sensitivity test. He states that a model user should not expect identical results for any particular cell (Y. Lai, oral comm., 1/30/2023). In addition, he notes that the Wilcock and Wu models more often exhibit numerical instabilities in the SRH-2D model solution. In fact, we found that when testing the 1 Myr RI flow, we had to drop the timestep to 0.25 s for the Wilcock and Wu models.

Key Findings at the End of the Model Simulations, from Testing Timestep Sensitivity

- The general trends for either erosion or deposition at monitoring points and spatially throughout the model domain are consistent (Figure 30 and Figure 31).
- The most notable difference between the three models is the amount of deposition that occurs at MP 4 and MP 6 (Figure 30).

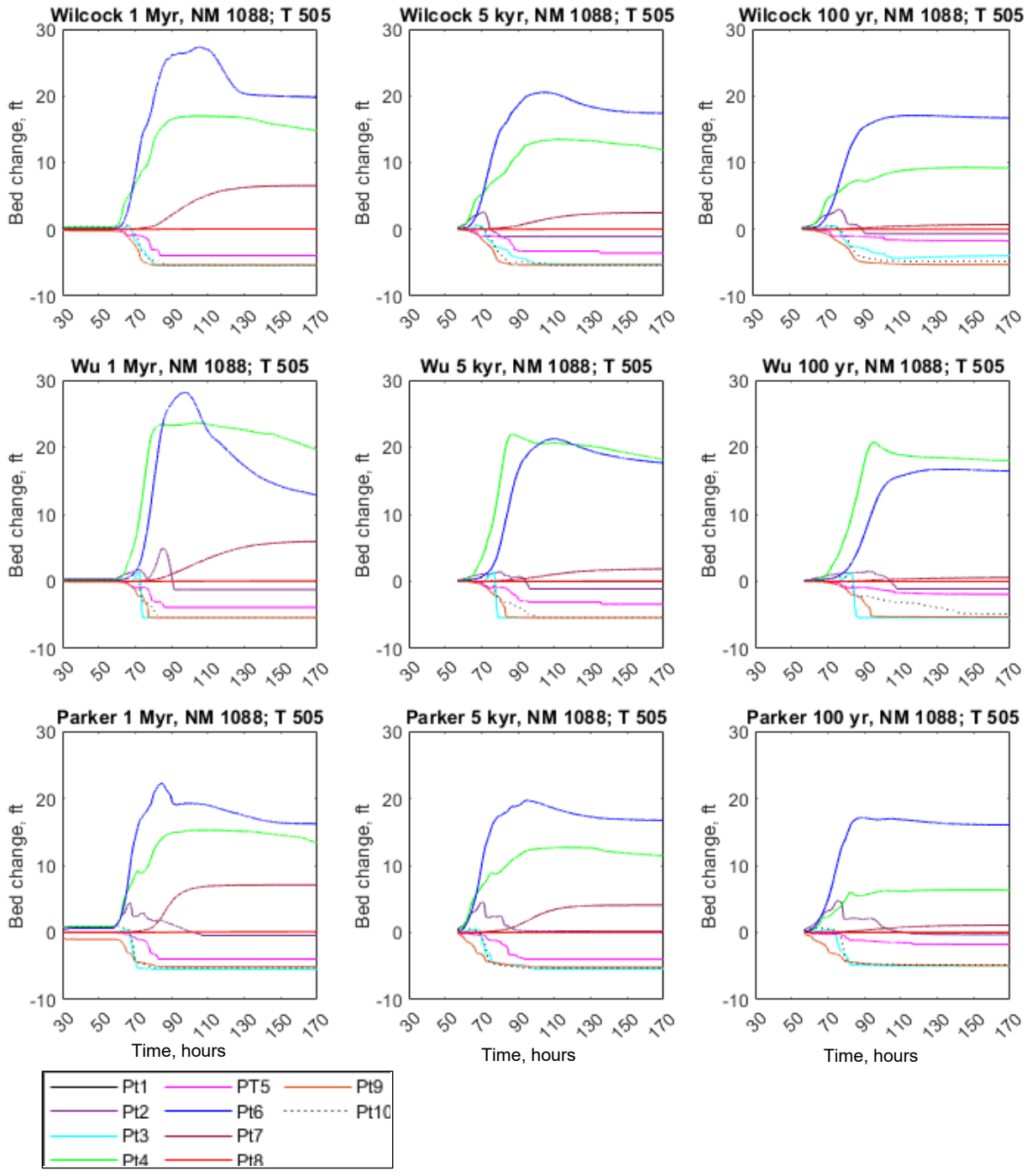

Figure 30.—Model results at monitoring points for the 1 Myr, 5 kyr, and 100 yr recurrence interval flows using a starting water surface elevation of 1088 ft at New Melones Reservoir and a downstream water surface elevation of 505 ft at Tulloch Reservoir. Results from three different sediment transport models are shown: (Top Row) the Wilcock model, (Middle Row) the Wu model, and (Bottom Row) the Parker model (the default model). For monitoring point locations, Figure 12.

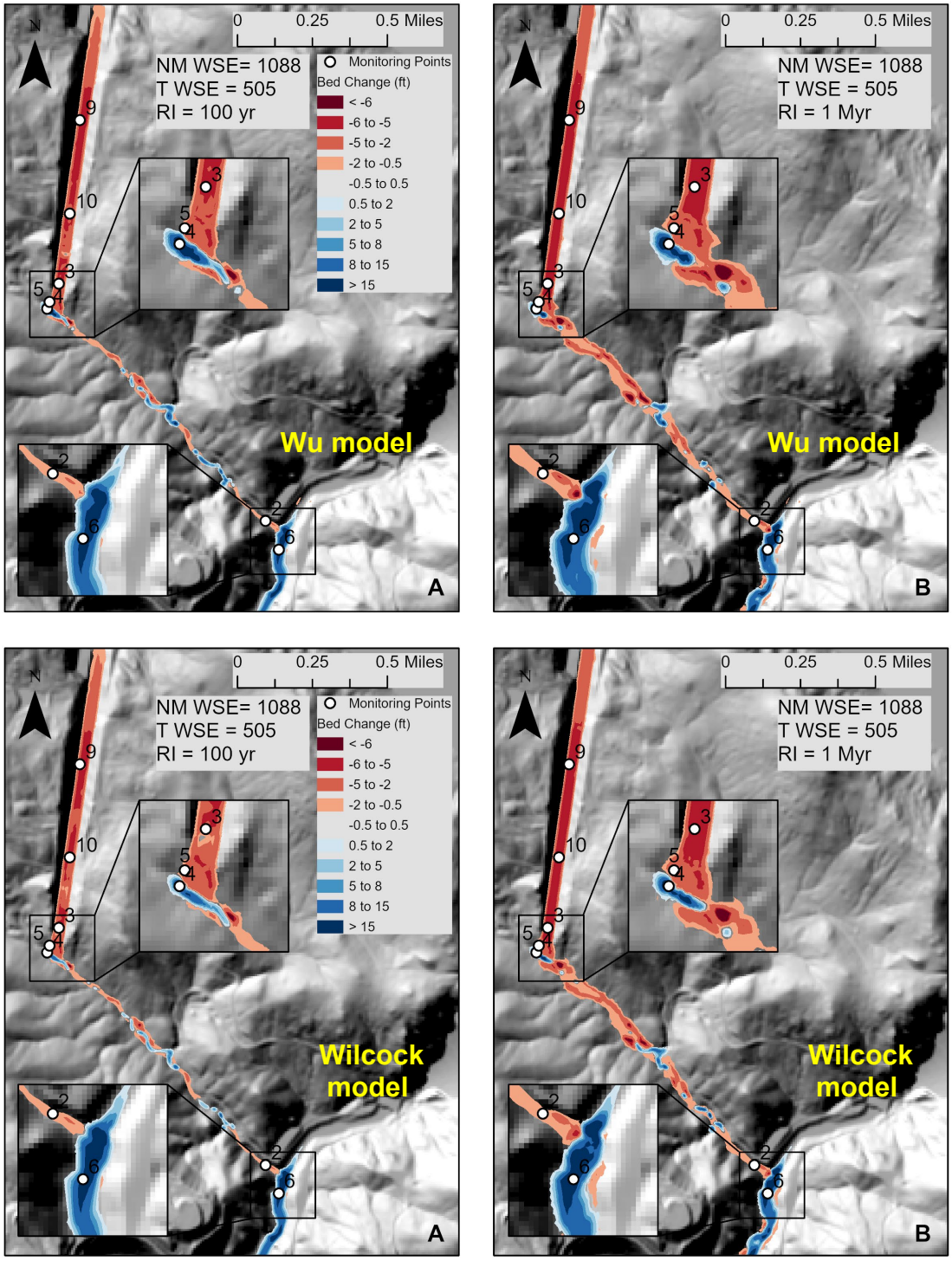

Figure 31.—Erosion and deposition results at model conclusion for the Wu and Wilcock Models. Negative values are erosion, positive values are deposition. Starting WSE at New Melones and Tulloch Reservoirs are 1088 and 505, respectively; flow recurrence interval (RI) is either 100 yr (A) or 1 Myr (B). These models removed the coarse fraction assumption on the spillway. Monitoring points are shown in white. The range of values for the two flows are: (A) -9.0 ft to 26.7 ft, (B) -13.5 to 28.1 ft, (C), -8.0 to 25.6, (D) -11.4 to 27.5 ft.

4.1.5 Model Uncertainty

Within the SRH-2D model, several parameters can be adjusted to yield slightly different results. One of the parameters that we did not test for sensitivity is Manning's *n*. We use a constant value for Manning's *n* within each mapped land use (Table 5). In reality, as flow depths increase, the resistance to flow will also decrease. In numerical models, the Manning's *n* represents this resistance to flow, but the *n* value also needs to be appropriate for the cell size. While this is an uncertainty in our model, other uncertainties likely have a far greater impact.

We followed Lai's recommendation to calculate the active layer as $T_{PARA} \cdot D_{90}$, where the active layer is defined as a multiple of D_{90} based on empirical data (Lai, 2019). These empirical data are likely based on floods with lower recurrence intervals than the hypothetical floods we modeled. For extreme flood events, it is feasible that erosion could occur deeper (higher T_{PARA} values) than empirical data suggest. We also had poor constraints on D_{90} throughout our project area. We assumed coarser sediment was present on the spillway and adjusted our grain size distribution to account for this; therefore, we chose not to increase the T_{PARA} above 2 because we had already increased the representative D_{90} values throughout the spillway. This is a source of uncertainty in the model that may affect the rate of erosion or deposition at any given cell. However, this uncertainty would not change the general trend of erosion and deposition throughout the model domain.

Grain size distribution on the spillway significantly affects the volumes of erosion and deposition within the spillway and Bean Gulch for lower flows (see Section 4.1.4, Eliminating the coarse fraction assumption from the spillway). However, we have little data to constrain the grain size distribution. If the erosion model on New Melones Spillway is investigated further, we suggest collecting additional data to constrain the thickness of sediment cover in both the spillway and Bean Gulch, including test pits. Additional data to constrain the sediment size distribution would likely improve the model accuracy.

The timestep is also a potential source of model error at the lower RI flows; in particular, results at MP 4 exhibit sensitivity. Model results also vary with the base level condition at Tulloch Reservoir. We tested values between 500 ft and 515 ft based on observed data. However, we do not know how forecasting for an exceptional flood event may alter operations at Tulloch Reservoir. If operators significantly draw down the reservoir below 500 ft to accommodate flood inflows, then sediment transport could extend farther downstream in the Stanislaus River and potentially into Tulloch Reservoir. Collaborative planning for large flood events between Tulloch Reservoir and New Melones Reservoir would provide better constrained input data for this model.

The routed hydrographs represent spillway and outlet works discharges based on two starting elevations at New Melones Reservoir, 1088 ft and 1049 ft, which cover a large range of potential flows on the spillway sufficient to explore potential erosion. However, the hydrographs we modeled need to be updated with new regional data (K. Neff, oral comm., project scoping in 2019). Updating flood hydrographs was originally scoped as part of this project. However, we

ultimately decided to move forward with existing estimates for flood hydrographs because they are sufficient to answer the key questions of whether sediment cover and the underlying bedrock are susceptible to erosion and where the eroded material will be deposited.

4.2 Annandale Erodibility Index Method

We calculated results for a downstream WSE at Tulloch Reservoir of 505 ft and two starting New Melones reservoir elevations: 1,049 ft and 1,088 ft. We then divided the streampower generated by the flow by the critical streampower needed to erode the bed. We took the absolute value of this to allow for backwater flow to erode the bed (i.e., erosion can occur regardless of the flow direction). Anywhere that ratio was greater than one, the bed is expected to erode for that flow event (red). Anywhere less than one is not likely to erode (green).

Bedrock erosion in all flow scenarios is limited to the serpentinite at the downstream end of the spillway into Bean Gulch (Figure 32). At the lowest analyzed flows, the majority of expected bedrock erosion is concentrated in the gully connecting the end of the spillway with Bean Gulch. Within Bean Gulch, bedrock erosion is probable along the contact between the serpentinite and the meta-volcanics within the channel.

No bedrock erosion is predicted within the spillway for any of the flow scenarios or downstream boundary conditions that we tested (Figure 32, Appendix D). These results are based on the stream flows applied to the current topography. Higher elevations for Tulloch of 510 ft or 515 ft may be more likely for a flood scenario, so we performed these simulations as well (Appendix D). The results for these three downstream boundary conditions are similar.

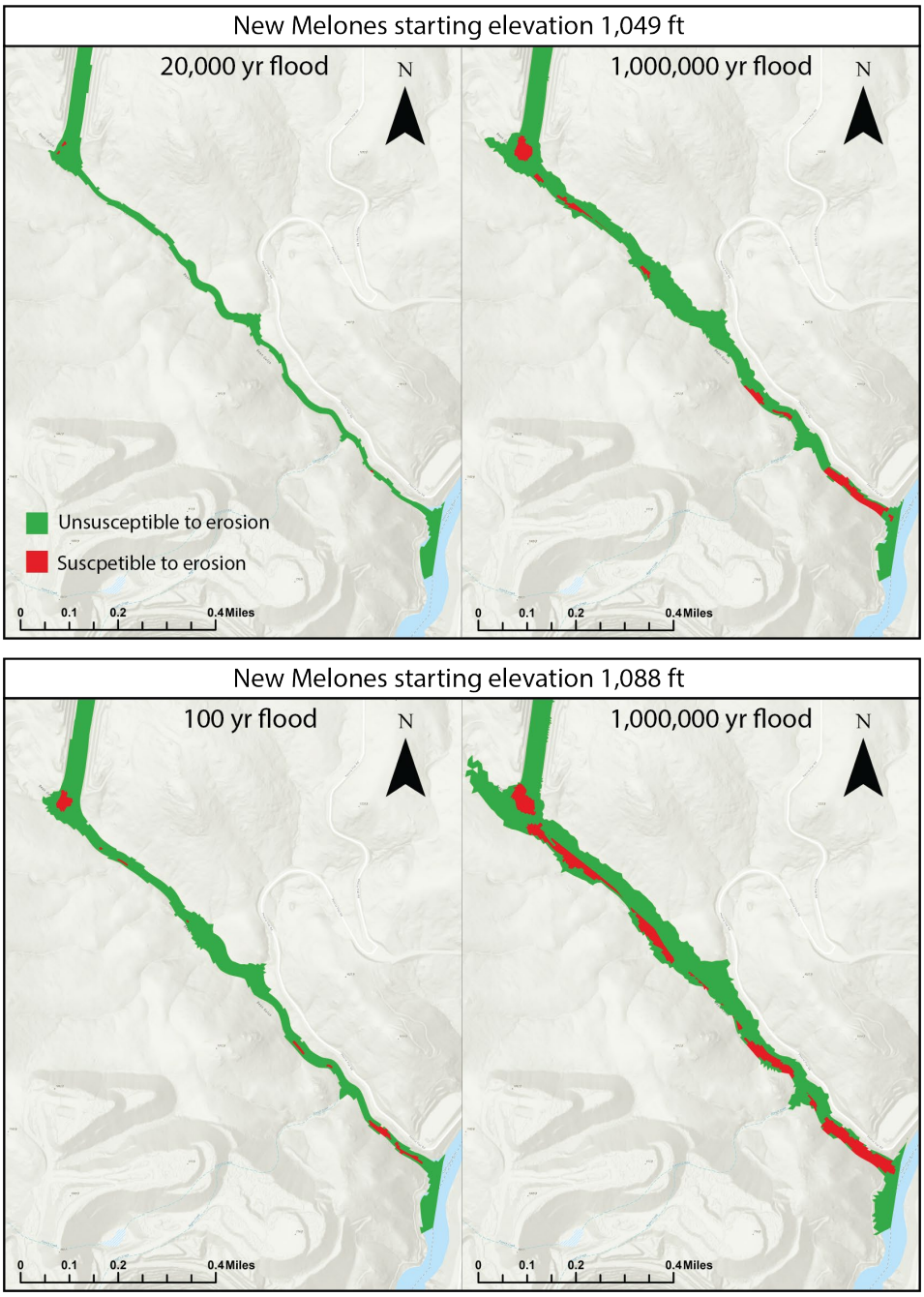

Figure 32.—Results from the Annandale erodibility assessment for a downstream Tulloch Reservoir elevation of 505 ft show that erosion is limited to the downstream end of the spillway into Bean Gulch for all flows that we tested. Here we plot the lowest and highest flow recurrence intervals for a starting reservoir elevation at New Melones of 1,049 ft (top) and 1,088 ft (bottom). The results are focused on the downstream end of the spillway and Bean Gulch. Results above the mapped portion are non-eroding. Red areas are susceptible to erosion for that flow event, and green areas are unlikely to erode.

4.3 1D Bedrock Erosion Model

We ran the H1DE model for two transects along the spillway: one along the right side of the spillway and one along the left side of the spillway. We assume that all sediment has already been removed and are only modeling bedrock erosion with this model. For both transects, we ran 10 different flow scenarios with 50 randomly generated beds for fracture spacing and block size. The same bed was used for all 10 flows before generating the next bed. The results represent the mean and standard deviation of these 50 iterations.

4.3.1 Left Spillway

Along the left spillway transect, the majority of bedrock erosion occurs within the first 10-20 hours of the hydrograph for the starting New Melones Reservoir WSE of 1,088 ft (NM1088) (Figure 33). The maximum average bedrock erosion for all of the runs is ~300,000 cubic feet (ft^3). For the NM1088 runs, this maximum is reached for the 5 kyr flood and bedrock erosion volume remains stable for the 20 kyr, 100 kyr, and 1 Myr flood runs. This is likely because the only material that erodes for these runs is within the gully. Without erosion at the downstream end of the model, the gully has a maximum erodible capacity. Lowering at the downstream boundary due to erosion within Bean Gulch could allow for higher eroded volumes within the gully if that erosion propagated upstream. The 5 kyr flood exceeds this threshold for erosion and any flow in excess of that has no more available material that is susceptible to erosion. This range can vary from 200,000 to 400,000 ft^3. For the New Melones WSE of 1,049 ft (NM1049), only the 1 Myr flood erodes all of the available gully rock material (Figure 34). Figure 35 and Figure 36 show the timeseries of bedrock erosion at different points along the spillway and gully. This is taken as the average incision depth at each point for the 50 iterations. MP 5 is within the gully and is where all of the incision occurs except for the NM1088 100 kyr and NM1088 1 Myr floods. The gully incises up to 3.28 ft into bedrock. Considering that this gully already shows evidence of erosion from precipitation-driven overland flow, these results are reasonable. For the NM1088 100 kyr and 1 Myr flows, 0.12 and 0.18 ft, respectively, incise at the downstream end of the gully (MP 3) (Figure 35). Incision does not progress upstream of this point.

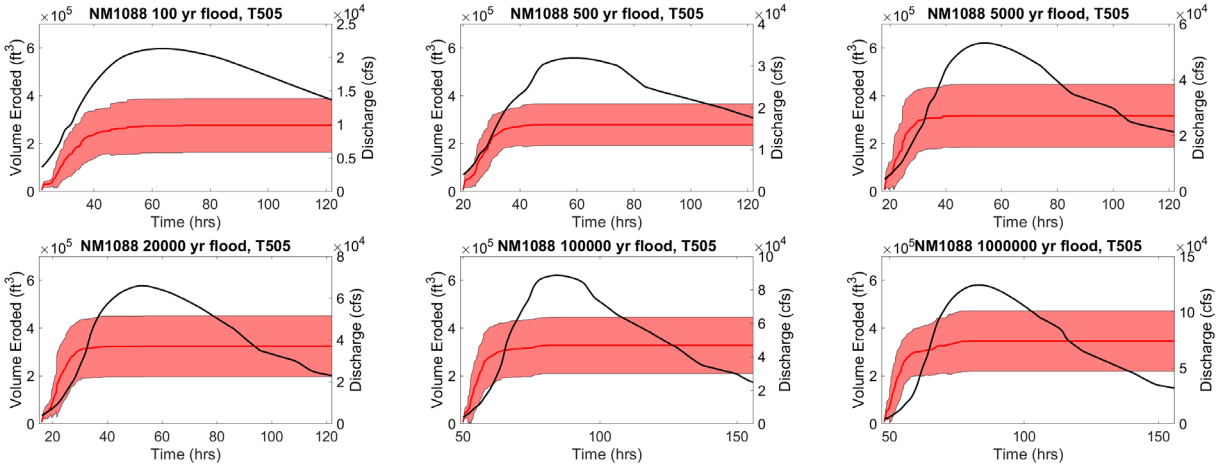

Figure 33.—Magnitude of bedrock erosion for the left spillway transect and New Melones Reservoir WSE of 1,088 ft. The eroded volume is calculated assuming bedrock erosion occurs across the entire width of the spillway. The black line is the discharge hydrograph. The solid red line is the mean volume eroded for 50 model iterations and the shaded red area encompasses the standard deviation of those runs.

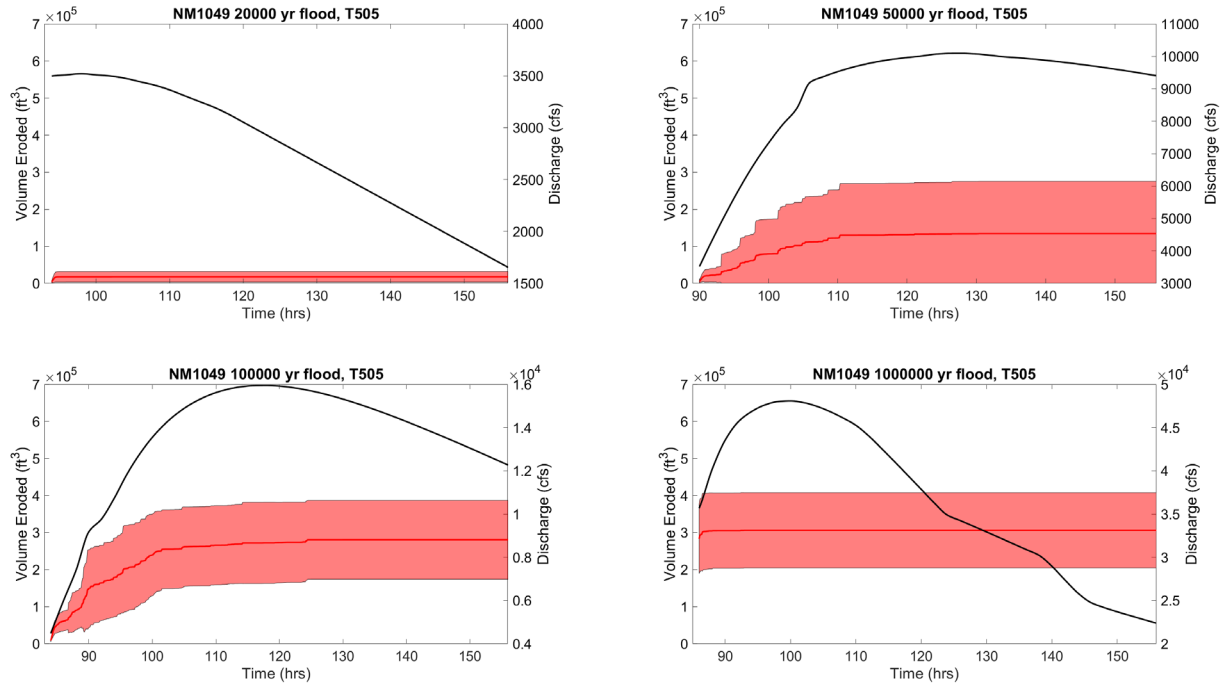

Figure 34.—Magnitude of bedrock erosion for the left spillway transect and New Melones Reservoir WSE of 1,049 ft. The eroded volume is calculated assuming that bedrock erosion occurs across the entire width of the spillway. The black line is the discharge hydrograph. The solid red line is the mean volume eroded for 50 model iterations and the shaded red area encompasses the standard deviation of those runs.

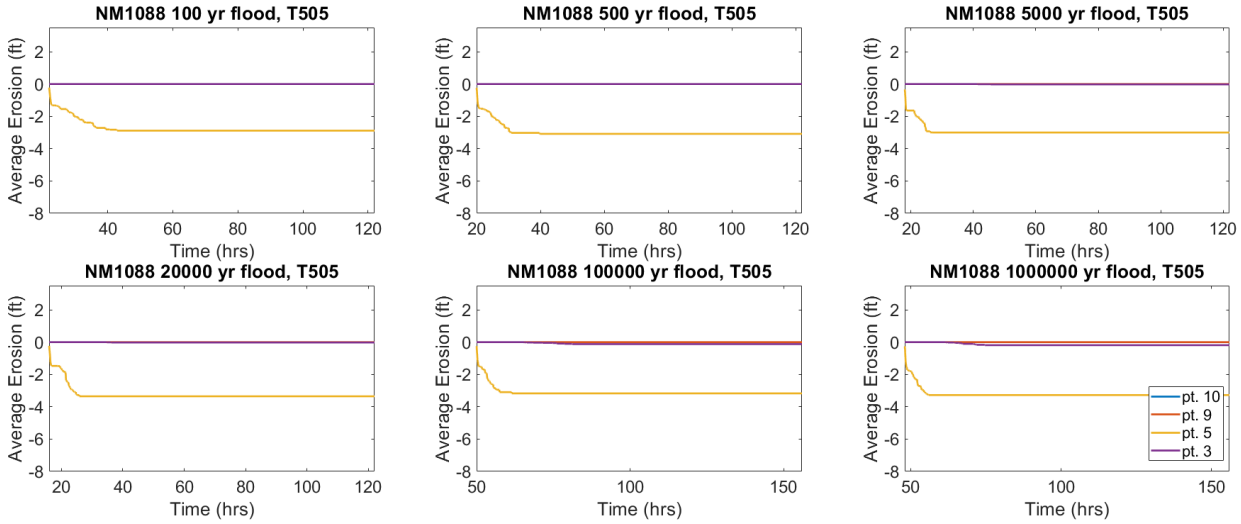

Figure 35.—Bedrock erosion at four points along the left spillway transect. Bedrock erosion at MP 5 is in the gully downstream of the spillway and maxes out for all six floods at 3.8 ft of bedrock erosion. Minor bedrock erosion occurs at the downstream end of the spillway (MP 3) for the 100 kyr flood and greater.

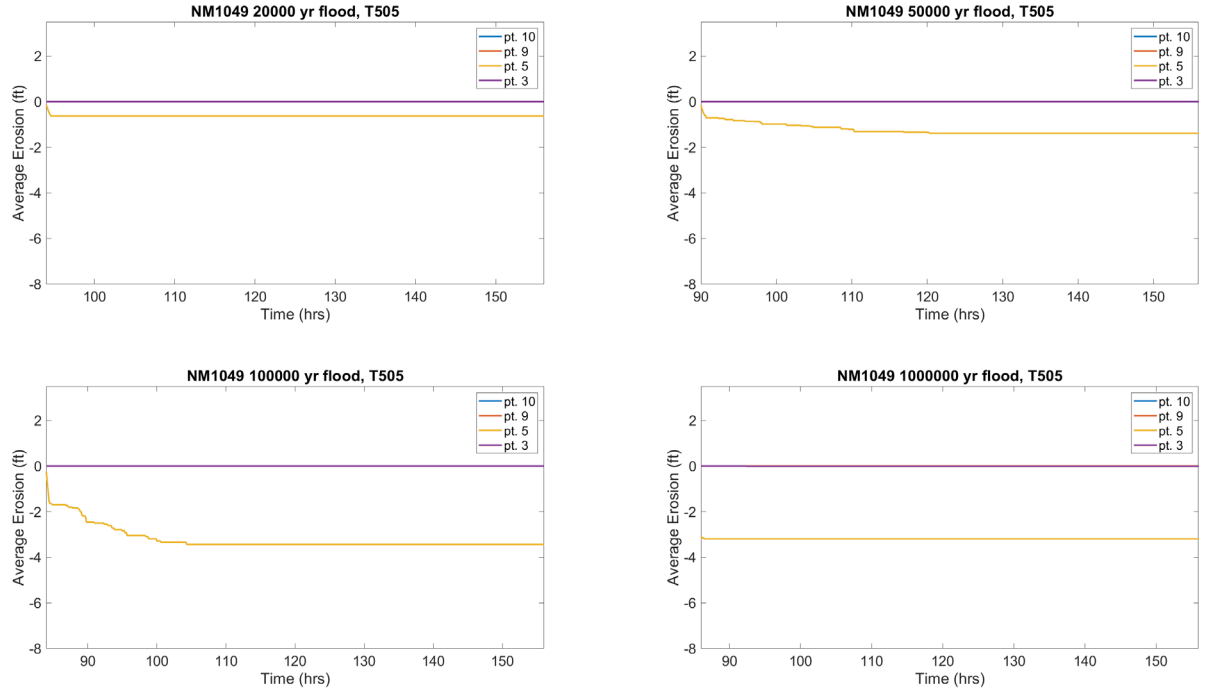

Figure 36.—Bedrock erosion at four points along the left spillway transect. Bedrock erosion at MP 5 is in the gully downstream of the spillway and maxes out for all four floods at ~3 ft of bedrock erosion. Very minimal bedrock erosion occurs at the points within the spillway.

4.3.2 Right Spillway

The rock along the right spillway transect was generally more highly fractured than the left spillway. This resulted in smaller, more erodible blocks. However, the metabasalt at the downstream end of the spillway is cohesive (unfractured) along the right side of the spillway (1,063.39–1,130.88 ft from the start of the right spillway transect shown in Figure 16) and is fractured along the left spillway (1,046.5-1,162.56 ft from the start of the left spillway transect shown in Figure 16). The result is that the metabasalt along the right spillway stalls bedrock erosion until flows are high enough to remove it (Figure 37). For the NM1049 runs, the flows are not high enough to achieve this and the maximum average eroded volume is ~150,000 ft^3 (Figure 38). For the NM1088 runs, bedrock erosion steadily increases from the 5 kyr flood to the 1 Myr flood and the maximum average eroded volume is 645,000 ft^3. For the NM1088 runs, incision can progress up to the middle of the spillway for the 1 Myr flow, where MP 10 incises 0.15 ft (Figure 39). At MP 3, the downstream end of the spillway incises 0.2 ft. For the right spillway scenario, significant incision (>0.1 ft) within the spillway only occurs for the NM1088 1 Myr flood (Figure 39, Figure 40).

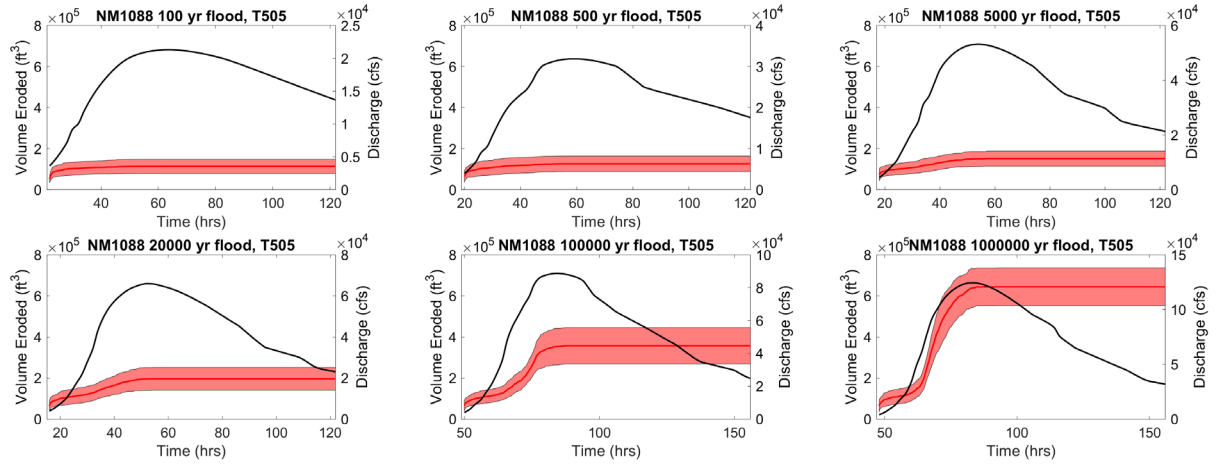

Figure 37.—Magnitude of bedrock erosion for the right spillway transect and New Melones Reservoir WSE of 1,088 ft. The eroded volume is calculated assuming that bedrock erosion occurs across the entire width of the spillway. The black line is the discharge hydrograph. The solid red line is the mean volume eroded for 50 model iterations and the shaded red area encompasses the standard deviation of those runs.

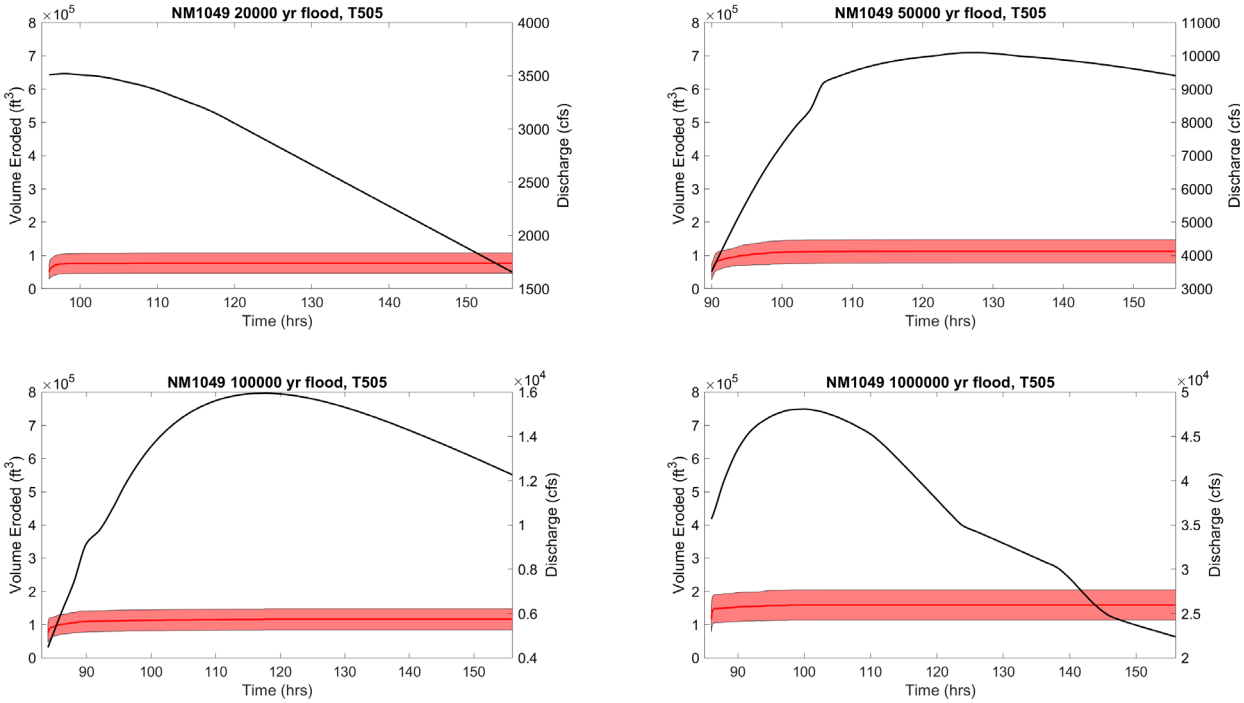

Figure 38.—Magnitude of bedrock erosion for the right spillway transect and New Melones Reservoir WSE of 1,049 ft. The eroded volume is calculated assuming that bedrock erosion occurs across the entire width of the spillway. The black line is the discharge hydrograph. The solid red line is the mean volume eroded for 50 model iterations and the shaded red area encompasses the standard deviation of those runs.

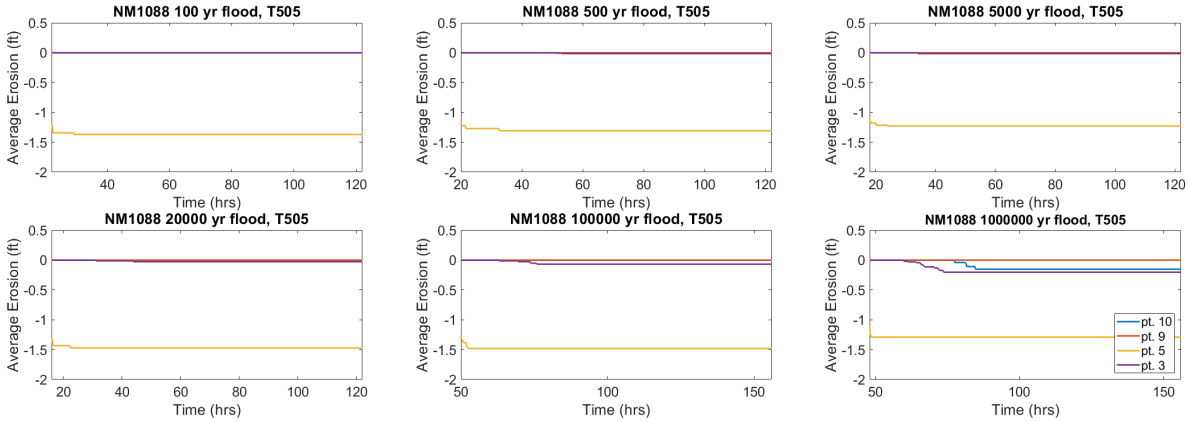

Figure 39.—Bedrock erosion at four points along the right spillway transect and NM starting WSE of 1088 ft. Bedrock erosion at MP 5 is in the gully downstream of the spillway and maxes out for all six floods at ~1.5 ft of incision. Minor incision occurs at the downstream end of the spillway (MP 3) for the 5 kyr flood and greater, and incision occurs at MP 10 for the 1 Myr flood.

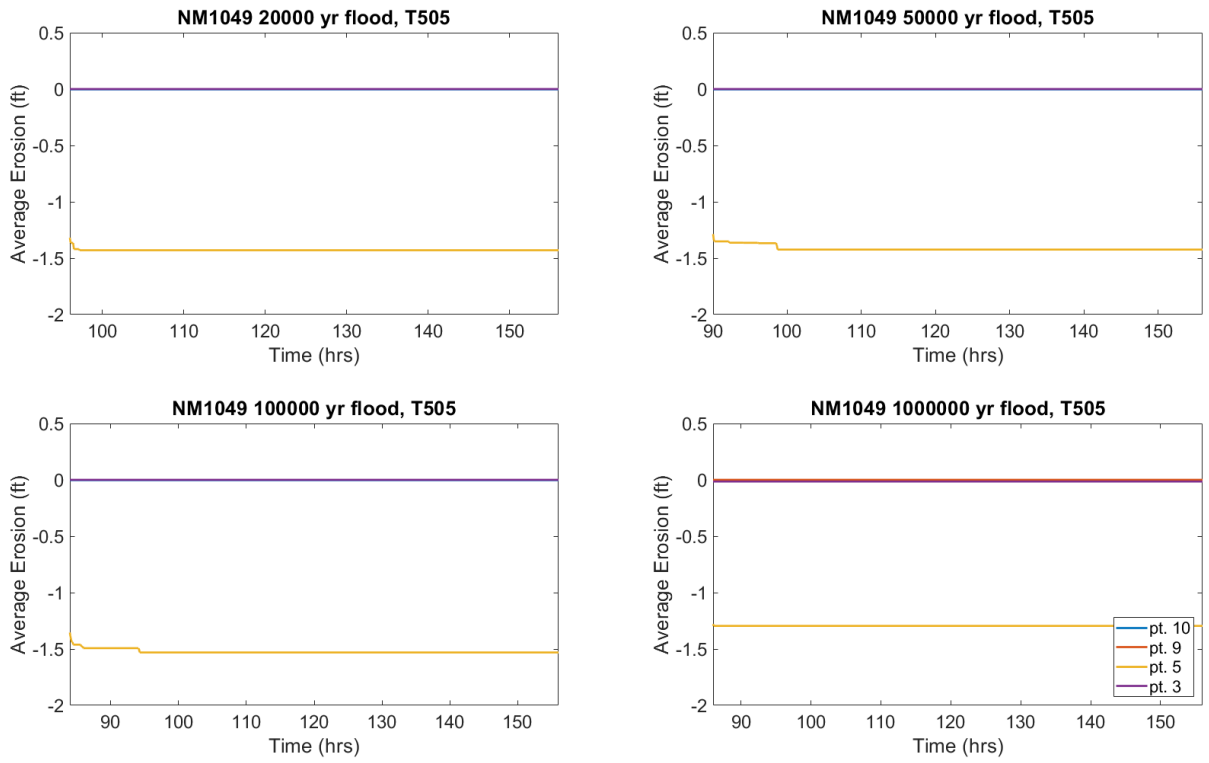

Figure 40.—Bedrock erosion at four points along the right spillway transect and NM starting WSE of 1049 ft. Bedrock erosion at MP 5 is in the gully downstream of the spillway and maxes out for all four floods at ~1.5 ft of incision.

4.3.3 Discussion

In the models of the left spillway transects, the spillway and gully eroded more for both the NM1049 and NM1088 runs than the right spillway transects at lower flows. However, the NM1088 1 Myr flood eroded almost double the volume for the right spillway than the left spillway due to the closer fracture spacing along the right side of the spillway. The left spillway transect also showed more incision within the gully, but less of the incision progressed upstream into the spillway than for the right spillway transect. This implies that if the average fracture network is more consistent with the left spillway transect, then more incision can be expected within the gully downstream of the spillway, but the spillway itself will be minimally impacted. If the fracture network is more consistent with the right spillway transect, there will be less incision within the gully, but the incision can progress up to the midpoint of the spillway. However, 0.15 ft of incision within the spillway should not be concerning. We ran a sensitivity analysis to the different DSBC flows and found no significant differences in the results (Appendix E).

We made several assumptions in building this model that could affect the results. We assumed that the beds were flat lying. In reality, the rock was highly metamorphosed and displayed a complex distribution of intersecting fractures with a wide range of dips. Dips that were generally in the downstream direction could result in more bedrock erosion within our model domain, while dips in the upstream direction would result in less bedrock erosion. We also assumed that bedrock erosion was evenly distributed across the width of the spillway. This is likely an overestimate because shear stress and block size are variable across the width of the spillway and erosion would not likely occur as a large swath across the entire width of the spillway. We had to assume that the fractures that we could observe on the surface of the spillway and gully extended at depth. This assumption likely did not affect our model results within the spillway, as there was limited incision. For our initial and boundary conditions, we assumed that all of the sediment within the spillway was instantaneously removed at the first timestep. This exposed the rock in the spillway to flow for the entire hydrograph. All of the sediment is not eroded until approximately 70 hours, so we again are over-predicting bedrock erosion in the spillway for a sediment thickness of 5.4 ft (Figure 24). We finally assumed no change in our model downstream boundary at MP 4. In reality, the model results typically show deposition at MP 4 (Figure 24 and Figure 25). Adding in this history of baselevel rise at MP 4 to the H1DE model could reduce the amount of incision within the gully.

5.0 Conclusions

We used a three-tiered approach to model potential erosion on the New Melones Spillway using a series of hypothetical hydrographs based on two potential starting elevations for New Melones Reservoir: 1,088 ft and 1,049 ft. First, we used SRH-2D to simulate flow and sediment transport from the spillway, through the Stanislaus River, and down to Tulloch Reservoir. Flows as low as 50 cfs are capable of mobilizing silt and sands on the spillway. By 3,000 cfs, sands, fine pea gravel, and pebbles are also mobilized on the spillway (Table 11). For the hypothetical hydrographs we simulated, we found that erosion is dominant in both the spillway and in Bean Gulch. The minimum volume of spillway erosion is 77,490 yd^3 for the 20 kyr RI flow (NM1049) using a starting spillway sediment volume of 210,000 yd^3. The maximum amount of erosion on the spillway is 207,703 yd^3 for the 1 Myr RI flow (NM1088).

Tulloch Reservoir was not impacted by significant deposition associated with the modeled flow events. In contrast, the upstream portions of the Stanislaus River were heavily impacted. The minimum amount of deposition in the Stanislaus River was 84,769 yd^3 for the 20 kyr RI flow (TM1049 with a Tulloch Reservoir elevation of 515 ft); this deposit extended approximately 2,120 ft downstream from the junction of Bean Gulch and the Stanislaus River. The maximum amount of deposition in the Stanislaus River was 296,583 yd^3 for the 1 Myr RI flow (TM1088 with a Tulloch Reservoir elevation of 500 ft); this deposit extended approximately 8,750 ft downstream from the junction of Bean Gulch and the Stanislaus River. If the deposit remains in the upper Stanislaus River, it could be subsequently transported farther downstream. Additional

runs using flows from the outlet works at 8,000 cfs or less should likely be conducted to better understand how this deposit will be transported with time. Given enough time, finer grains within the deposit will likely reach Tulloch Reservoir. If deposition within Tulloch needs to be avoided, in-river dredging would likely be the only candidate to remove the large sediment deposits in the upper Stanislaus River.

Due to the uncertainty in the sediment cover thickness and distribution and the fact that the majority of the spillway sediment was removed for many of the modeled hydrographs, we chose to model the potential of bedrock erosion assuming no protective sediment cover for both the 2D Annandale model and the H1DE model. We performed a 2D probabilistic model (Annandale Erodibility Index Method) to identify spatial zones of potential bedrock erosion. Minor bedrock erosion can be expected in the gully that connects the spillway to Bean Gulch for flows as low as 50 cfs (NM1049, 20 kyr RI). Localized bedrock erosion is currently evident in this gully in the absence of spillway flow, so this is not surprising. The serpentinite is more fractured, and thus more erodible. For higher flows, more bedrock erosion is expected within the gully and within Bean Gulch along the contact between the serpentinite and the meta-volcanics (Figure 32). The spillway is not expected to be impacted based on the outcome of the 2D probabilistic model.

We finally performed the H1DE model to quantify potential bedrock incision and volume of eroded material due to block plucking. We ran the model for separate transects along the left and right spillway, which had different block fracture properties. The result is that for lower RI floods and Tulloch Reservoir elevation of 505 ft, the left spillway erodes a similar volume of material as the right spillway. However, for NM1088 100 kyr RI and greater, the right spillway has the potential for more erosion. The worst-case scenario is for the NM1088 1 Myr RI flood on the right spillway. Projecting erosion from this transect across the width of the spillway, the average eroded volume could be 645,000 ft^3 (Figure 37). This bedrock erosion can progress all the way upstream to MP 10 within the spillway. However, the majority of the bedrock erosion in this scenario is concentrated within the gully at MP 5 and only 0.15 ft of incision occurs at MP 10, which is not a dam safety threat (Figure 39).

Bedrock erosion on the New Melones Spillway does not pose a dam safety risk. For the 1Myr RI flow (NM1088) bedrock erosion of sediment within the spillway and Bean Gulch could contribute up to 296,583 yd^3 of sediment, assuming an initial spillway sediment cover of 210,000 yd^3. Bedrock erosion within the spillway and gully could contribute an additional 23,889 yd^3 (645,000 ft^3), an order of magnitude less sediment. The SRH-2D model results show that this sediment is largely deposited at the junction between the Stanislaus River and Bean Gulch. The deposition of sediment into the river will be dominated by the sediment cover in the spillway. The portion of asbestos-laden serpentinite deposited into the Stanislaus River is very small compared to the overall deposit volume. Nonetheless, the influx of sediment to the Stanislaus River likely qualifies as an incident, as described in the Public Protection Guidelines (DSO, 2022).

Tulloch Reservoir is not likely to be impacted by sediment transport during the initial floods, but later flows could redistribute sediment and transport it to Tulloch Reservoir. Additional data collection and flow hydrographs could be necessary to test any other scenarios, as outlined in this report. The models for all three components are built, and we can easily modify the models with updated data if Dam Safety wishes to further investigate the potential for erosion to the spillway. Easy updates to the models include: (1) downstream boundary conditions based on Tulloch operations with knowledge of an incoming flood event, (2) decreased timestep or adjusted model parameters following a further investigation of applying SRH-2D to extreme modeling scenarios, as part of SRH-2D model development and testing, (3) new sediment gradation data and sediment zone thicknesses, and (4) adjusted and updated hydrographs.

6.0 References

Annandale, G.W. 1995. Erodibility. Journal of Hydraulic Research 33(4), 471–494.

Andrews, E.D. 2000. Bed material transport in the Virgin River, Utah. Water Resources Research 36, 102–128.

Barton, N. 1978. Suggested methods for the quantitative description of discontinuities in rock masses: International Journal of Rock Mechanics and Mining Sciences and Geomechanics, International Society for Rock Mechanics. In Abstracts, 15(6), 319–368.

Bollaert, E. 2004. A comprehensive model to evaluate scour formation in plunge pools: International Journal on Hydropower & Dams 11(1), 94–101.

Chow, V.T. 1959. Open-channel hydraulics. New York, McGraw-Hill Book Co., 680 pp.

Deere, D. and Deere, D. 1988. The Rock Quality Designation (ROD) Index. L. Kirkaldie, Rock Classification Systems for Engineering Purposes, 91–101.

Department of the Army, 1979. New Melones Lake Foundation Report Part III: Dam, Appurtenances, Powerhouse and Relocations. Sacramento District Corps of Engineers.

Dam Safety Office (DSO). December 2022. Public Protection Guidelines: a Risk Informed Framework to Support Dam Safety Decision-Making. Dam Safety Office, Dam Safety and Infrastructure Directorate, U.S. Department of Interior. 36 pp.

Feinberg, B. 2009. New Melones Dam -Dam Failure Flood Inundation Study. Bureau of Reclamation, Technical Service Center. 15 pp.

Greimann, B.P., Lai, Y.G., & Huang, J.C. 2008. Two-dimensional total sediment load model equations. Journal of Hydraulic Engineering 134, 1142–1146.

Hurst, A.A., Anderson, R.S., and Crimaldi, J.P. 2021. Toward entrainment thresholds in fluvial plucking. Journal of Geophysical Research: Earth Surface 126(5), doi.e2020JF005944.

Hurst, A.A. 2021. Bedrock River Erosion by Plucking (Doctoral dissertation, University of Colorado at Boulder), 90 pp.

Holmes, B. 2021. Field Geologic Mapping -New Melones Dam Spillway. Bureau of Reclamation– Interior Region 10, California-Great Basin – Division of Design and Construction – Geology Branch CGB-230, 544 pp.

Kirsten, H.A.D. 1982. A classification system for excavating in natural materials. Civil Engineering = Siviele Ingenieurswese 1982(7), 293–308.

Koskinas, A., Tegos, A., Tsira, P., Dimitriadis, P., Iliopoulou, T., Papanicolaou, P., Koutsoyiannis, D. and Williamson, T. 2019. Insights into the Oroville Dam 2017 Spillway incident. Geosciences 9(1), 37.

Lai, Y.G. 2010. Two-Dimensional Depth-Averaged Flow Modeling with an Unstructured Hybrid Mesh. Journal of Hydraulic Engineering 136 (1), 12–23.

Lai, Y.G. 2019. User's Manual: Sediment Transport and Mobile-Bed Modeling with SRH-2D. Bureau of Reclamation, Denver, Colorado. 179 pp.

Lai, Y.G. 2020. A Two-Dimensional Depth-Averaged Sediment Transport Mobile-Bed Model with Polygonal Meshes. Water 12(1032), 21 pp., doi:10.3390/w12041032.

Parker, G. 1990. Surface-based bedload transport relation for gravel rivers. Journal of Hydraulic Research 28, 417–428.

Phillips, J.V. and Tadayon, S. 2006. Selection of Manning's roughness coefficient for natural and constructed vegetated and non-vegetated channels, and vegetation maintenance plan guidelines for vegetated channels in Central Arizona. U.S. Geological Survey. 41 pp.

Rittgers, J.B. 2020. Geophysical Surveys: 2D Electromagnetic Mapping, 2D Seismic Refraction Tomography, and 1D MASW: New Melones Dam, California. Bureau of Reclamation Technical Memorandum 86-68320-2020-12, 35 pp.

Schneider, J. 2020. Written communication via email, 3/20/2020.

U.S. Department of the Interior, Bureau of Reclamation. 1998. Engineering Geology Field Manual (Second Edition Vol. 1), 57–127.

U.S. Geological Survey. 2011. USGS Lidar Point Cloud CA_CalaverasTuolumne_2011_000516 2014-08-27 LAS. https://www.sciencebase.gov/catalog/item/58276a78e4b01fad86ff4e50.

Wahl, T.L. 2016. Erosion Analysis for the Emergency Spillway at Willow Creek Dam. Bureau of Reclamation Technical Memorandum PAP, 80 pp.

Wang, L., Cuthbertson, A.J., Zhang, S.H., Pender, G., Shu, A.P., and Wang, Y.Q. 2021. Graded bed load transport in sediment supply limited channels under unsteady flow hydrographs. Journal of Hydrology 595 (126015), doi: 10.1016/j.jhydrol.2021.126015.

Wilcock, P.R. and Crowe, J.C. 2003. Surface-Based Transport Model for Mixed-Size Sediment. Journal of Hydraulic Engineering 129, 120–128.

Wolman, M.G. 1954. A method of sampling coarse river-bed material. Transactions. American Geophysical Union 35(6), 951–956.

Wu, W., Wang, S.S.Y., and Jia, Y. 2000. Nonuniform sediment transport in alluvial rivers. Journal of Hydraulic Research 38(6), 427–434.

Appendix A

Hydrographic Surveying Equipment and Methods

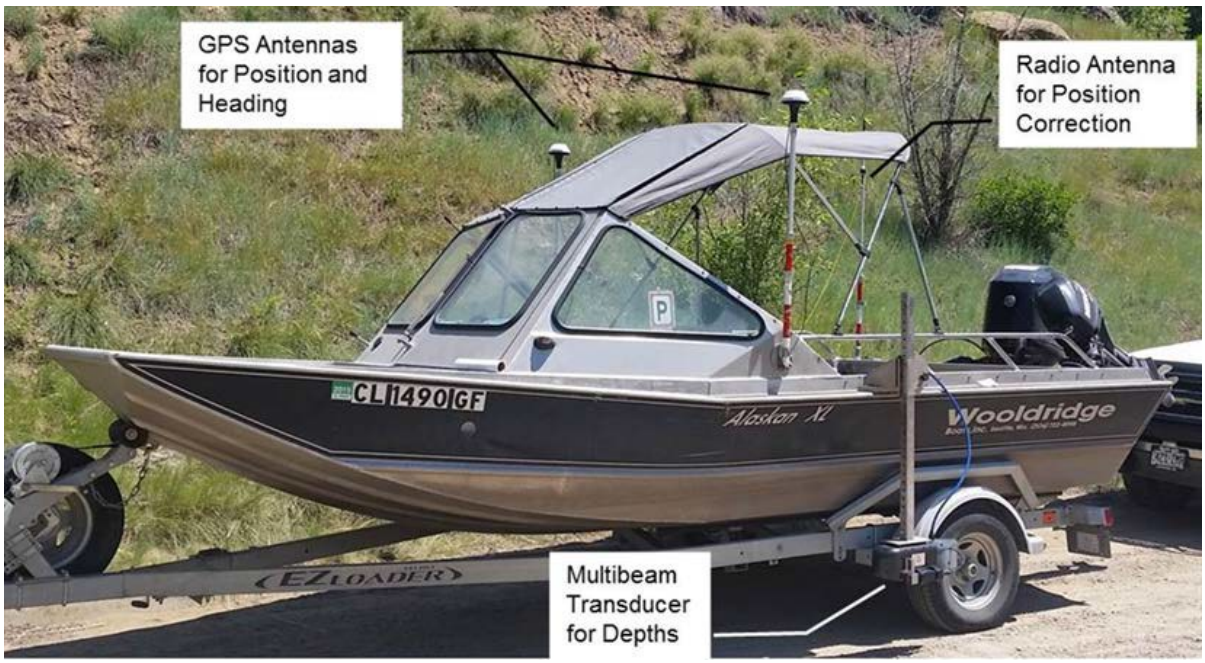

Figure A-1.—Wooldridge boat with RTK-GPS and multibeam depth sounder system.

The bathymetric survey was conducted in April of 2021. The survey was conducted along a series of cross section, longitudinal, and shoreline survey lines. The survey lines were spaced close enough for adequate interpolation between multi-beam depth data.

The survey employed an 18-foot, flat-bottom aluminum Wooldridge boat powered by outboard jet and kicker motors (Fig. A-1). Reservoir depths were measured using a multibeam echo sounders which consisted of the following equipment:

- variable-frequency transducer with integrated motion reference unit,
- near-surface sound velocity probe,
- two GPS receivers to measure the boat position and heading,
- an external GPS radio, and
- processor box for synchronization of all depth, sound velocity, position, heading, and motion sensor data.

The multibeam transducer emits up to 512 beams (user selectable) capable of projecting a swath width up to 120 degrees in 100 feet (30 meters) of water. Sound velocity profiles were collected over the full water depth at various locations throughout the reservoir. These sound velocity profiles measure the speed of sound through the water column, which can be affected by multiple characteristics such as water temperature and salinity. These sound velocity profiles were used to correct the depth measurements.

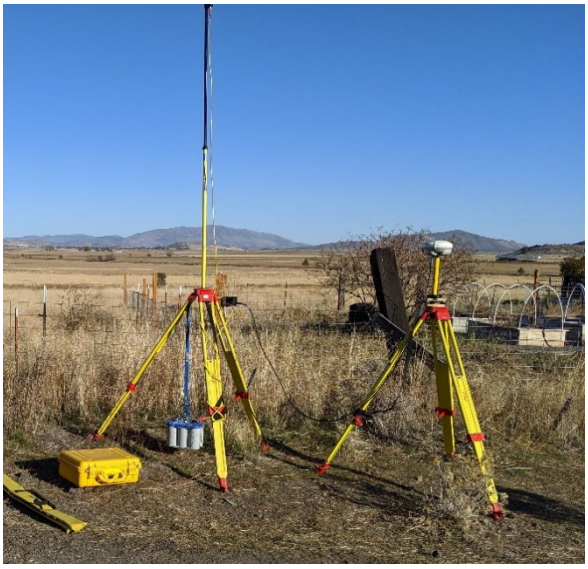

Figure A-2.—The RTK-GPS base station set-up used during the Klamath River Survey in Oregon is typical of the set up used for other bathymetric surveys.

RTK GPS survey instruments were used to continuously monitor the survey boat position and measure other ground control points. The GPS base station and receiver was set up on a tripod over a point overlooking the reservoir. The coordinates of this point were computed using the Online Positioning User Service (OPUS) developed by the National Geodetic Survey (NGS) (www.ngs.noaa.gov/OPUS/). During the survey, position corrections were transmitted to the GPS rover receivers using an external GPS radio and UHF antenna (Figure A-2). The base station was powered by a 12-volt battery.

The GPS rover receivers include an internal radio and external antenna mounted on a range pole (ground survey) or survey vessel (bathymetric survey). The rover GPS units receive the same satellite positioning data as the base station receiver, and at the same time. The rover units also receive real-time position correction information from the base station via radio transmission. This allows rover GPS units to measure accurate positions with precisions of ±2 cm horizontally and ±3 cm vertically for stationary points and within ±20 cm for the moving survey boat.

During the bathymetric survey, a laptop computer was connected to the GPS rover receivers and echo sounder system. Corrected positions from one GPS rover receiver and measured depths from the multibeam transducer were transmitted to the laptop computer through cable connections to the processor box. Using real-time GPS coordinates, the HYPACK software provided navigational guidance to the boat operator to steer along the predetermined survey lines.

The HYPACK hydrographic survey software was used to combine horizontal positions and depths to map the reservoir bathymetry in the user selected coordinate system. Water surface elevations from dam gage records and RTK GPS measurements were used to convert the sonar depth measurements to reservoir-bottom elevations in the NAVD88. The multibeam depth sounder generates millions of data points. Sometimes fish, underwater vegetation, or anomalies mean that a small portion of depth measurements do not represent the reservoir bottom and these data are deleted during the post processing. Final processing of the bathymetric data resulted in 2.5 million data points used in the development of the reservoir surface. Filtering of this large data file is necessary, so a raster is created in GIS (e.g., 1-foot square cells). For each raster cell, the reservoir bottom elevation is assigned equal to the median elevation of all available data points within that raster cell. The use of the median value reduces the influence of the highest and lowest elevations within the reservoir.

Appendix B

Pebble Count Data

The below data show measurements of sediment grain size along the B-axis (long axis) at seven measurement locations (Figure 7) following the Wolman pebble count method (Wolman, 1950).

Table A-1.—Wolman pebble count data from the New Melones Spillway and gully connecting the spillway and Bean Gulch

PC1	PC2	PC3	PC4	PC5	PC6	PC7
B-axis	B-axis	B-axis	B-axis	B-axis	B-axis	B-axis
23	359	156	51	80	17	25
10	60	256	245	52	7	4
42	6	407	98	235	4	30
30	110	960	77	155	9	13
7	24	14	333	196	9	7
17	12	380	30	16	5	silt
sand	27	34	180	162	15	13
25	coarse sand	195	128	47	13	3
39	188	340	228	221	12	2
20	49	255	8	51	3	5
39	12	85	102	656	9	6
4	188	153	104	39	20	16
4	10	614	7	38	19	silt
55	21	230	39	68	43	3
40	48	44	79	sand	18	11
20	69	70	63	16	5	14
sand	25	89	79	125	14	2
1	25	2	99	66	6	25
56	27	37	34	154	17	9
sand	45	132	9	103	16	13
5	6	93	63	35	15	2
35	10	5	50	225	7	30
30	30	116	65	218	4	4
sand	20	282	99	47	30	10
80	9	104	10	11	6	4
43	10	39	93	26	35	sand
sand	4	8	58	42	8	9
10	34	55	4	100	5	9
33	77	40	49	149	7	15
sand	31	70	96	20	6	3
		253		117	11	
		22				
		133				
		2050				

Appendix C

Script Input file for SRH-2D modeling

The script input file (SIF) is read in by the SRH-2D preprocessor to apply user-selected input parameters and read in the user mesh and data. Here, we include the SIF input file from the 100 kyr recurrence interval flow using starting water surface elevations of 1088 ft and 505 ft in New Melones Reservoir and Tulloch Reservoir, respectively (Table A-2). Blank line entries in the SIF imply the SRH-2D default choice.

Table A-2.—Example SIF file for SRH-2D mobile bed run with unsteady flow

```
// Simulation Description (not used by SRH):
NM1088 T505 mobile bed w/coarse 100ky unsteady, mobile bed with new version of SRH
// Solver Selection (FLOW MOBILE WQ TCUR TEM DIFF_EX DIFF_IM SED_DIFF_IM DYNAMIC ...)
mobile
// Monitor-Point-Info: NPOINT
10
// Monitor Point Coordinates: x1 y1 x2 y2 ...
6542348.00004 2150348.50014 6550869.45019 2165993.04005 6547227.23012 2170159.02023
6547027.32992 2169722.84
6547068.79014 2169844.32992 6551103.17529 2165493.01822 6550121.60978 2162990.02618
6548079.36065 2158026.59569
6547602.6724 2173032.3133 6547424.4040 2171391.5499
// Tstart Time_Step and Total_Simulation_Time: TSTART DT T_SIMU [FLAG]
18 0.5 174
// Turbulence-Model
para
// A_TURB for the PARA Model (0.05 to 1.0)
0.7
// Mesh-Unit (FOOT METER INCH MM MILE KM GSCALE)
foot
// Mesh FILE_NAME and FORMAT(SMS...)
NM_13_n.2dm SMS
// General Sediment Parameters: spec_grav sed_nclass
2.65 7
// Size-Class Diameter & Dry_Bulk_Density: D_Lower(mm) D_Upper(mm) [Den_Bulk UNIT]
0.04 2
2 5
5 20
20 76
76 250
250 600
600 2100
// Sediment Capacity Eqn
parker
// Capacity Equation Coefficients for Parker and Seminara (Theta_Critial Hiding Factor)

// Water Temperature (Celsius):

// Start Time in hours for the Sediment Solver

// Adaptation Coefs for Suspended Load: A_DEP A_ERO (0.25 1.0 are defaults)

// Bedload Adaptation Length: MOD_ADAP_LNG LENGTH(meter) (0=const;1=Sutherland; 2/3=van
Rijn; 4=Seminara)
0 155
```

```
// Active Layer Thickness: MOD_ALayer NALT (1=const;2=Nalt*d90)
2 2
// MOD_COHESIVE (0=non-cohesive >0 --> number of cohesive classes)
0
// Initial Flow Condition Setup Option (DRY RST AUTO ZONAL Vary_WSE/Vary_WD)
rst
// Restart File Name for initial condition setup
RST_OW8000_T505_RST4.dat
// Soil-Type Spatial Distribution Method (UNI ZON POINT)
zonal
// Number of Soil-Types in the File
8
// Number of Subsurface Sediment Layers in ZONE=   1
2
// Thickness Unit(SI/EN) Cohesive_TYPE for Zone&Layer =  1 1
2.7 en
// CUMULATIVE data (di Pi) for each bed layer and bed zone 1A
cumulative 2 9 5 22 20 63 76 84 250 85 600 95 2100 100
// Thickness Unit(SI/EN) Den_Clay(Cohesive) for each layer and zone 1b
2.7 EN
// CUMULATIVE data (di Pi) for each bed layer and bed zone
cumulative 2 9 5 22 20 63 76 84 250 85 600 95 2100 100
// Number of Bed Layers 2
0
// Number of Bed Layers 3
2
2 EN
cumulative 2 2 5 4 20 18 76 54 250 89 600 97 2100 100
2 EN
cumulative 2 2 5 4 20 18 76 54 250 89 600 97 2100 100
// Number of Bed Layers 4
2
0.5 EN
cumulative 2 2 5 4 20 18 76 54 250 89 600 97 2100 100
0.5 EN
cumulative 2 2 5 4 20 18 76 54 250 89 600 97 2100 100
// Number of Bed Layers 5
2
4 EN
cumulative 2 5 5 8 20 20 76 60 250 89 600 97 2100 100
4 EN
cumulative 2 5 5 8 20 20 76 60 250 89 600 97 2100 100
// Number of Bed Layers 6
2
7.5 EN
cumulative 2 8 5 11 20 27 76 70 250 97 600 100 2100 100
7.5 EN
cumulative 2 8 5 11 20 27 76 70 250 97 600 100 2100 100
// Number of Bed Layers 7
2
5.5 EN
cumulative 2 7 5 10 20 25 76 65 250 95 600 99 2100 100
5.5 EN
```

```
cumulative 2 7 5 10 20 25 76 65 250 95 600 99 2100 100
// Number of Bed Layers 8
2
10 EN
cumulative 2 8 5 11 20 27 76 70 250 97 600 100 2100 100
10 EN
cumulative 2 8 5 11 20 27 76 70 250 97 600 100 2100 100
// Soil-Type Zonal ID File: FileName FORMAT
NM_13_sed.2dm 2DM
// Manning Coefficient n Input Options: SPATIAL or SPATIAL VEG GRAIN for 2D Model; SPATIAL
for 3D model
VARY NONE D90
// Number of Material Types in 2D Mesh File
6
// Manning Coefficient in each mesh zone: a real value or a WD~n file name or Landuse
0.030 2.5
0.032 2.5
0.040 2.5
0.050 2.5
0.060 2.5
0.070 2.5
// Any-Special-Treatments? (0 or empty = NO; 1=YES)

// Boundary Type (INLET-Q EXIT-H etc)
Inlet-Q
// Boundary Values (Q W QS TEM H_rough etc)
NM1088_100000yr_SP_hydrographCFS.txt 0 0 0 0 0 0 0 en
// Boundary Type (INLET-Q EXIT-H etc)
Inlet-Q
// Boundary Values (Q W QS TEM H_rough etc)
NM1088_100000yr_OW_hydrographCFS.txt 0 0 0 0 0 0 0 en
// Boundary Type (INLET-Q EXIT-H etc)
exit-h
// Boundary Values (Q W QS TEM H_rough etc)
505 EN
// Boundary Type (INLET-Q EXIT-H etc)
monitor
// Boundary Type (INLET-Q EXIT-H etc)
monitor
// Boundary Type (INLET-Q EXIT-H etc)
monitor
// Boundary Type (INLET-Q EXIT-H etc)
monitor
// Boundary Type (INLET-Q EXIT-H etc)
monitor
// Boundary Type (INLET-Q EXIT-H etc)
monitor
// Boundary Type (INLET-Q EXIT-H etc)
monitor
// Boundary Type (INLET-Q EXIT-H etc)
monitor
// Wall-Roughess-Height-Specification (empty-line=DONE)
```

```
// Pressurized Zone exists? (empty-line or 0 == NO)

// Any In-Stream Flow Obstructions? (empty-line or 0 = NO)

// Results-Output-Format-and-Unit(SRHC/TEC/SRHN/XMDF/XMDFC/PARA;SI/EN) + Optional STL FACE
srhc en
// Output File _MAX.dat is requested? (empty means NO)

// Intermediate Result Output Control: INTERVAL(hour) OR List of T1 T2 ... EMPTY means the end
80
```

Appendix D

Annandale Erodibility Index Method Supplemental Results

The following show supplemental results for the Annandale Erodibility Index Method model for downstream boundary water surface elevations at Tulloch Reservoir of 510 ft and 515 ft. The model output was generated for low and high flows at NM1049 and NM1088.

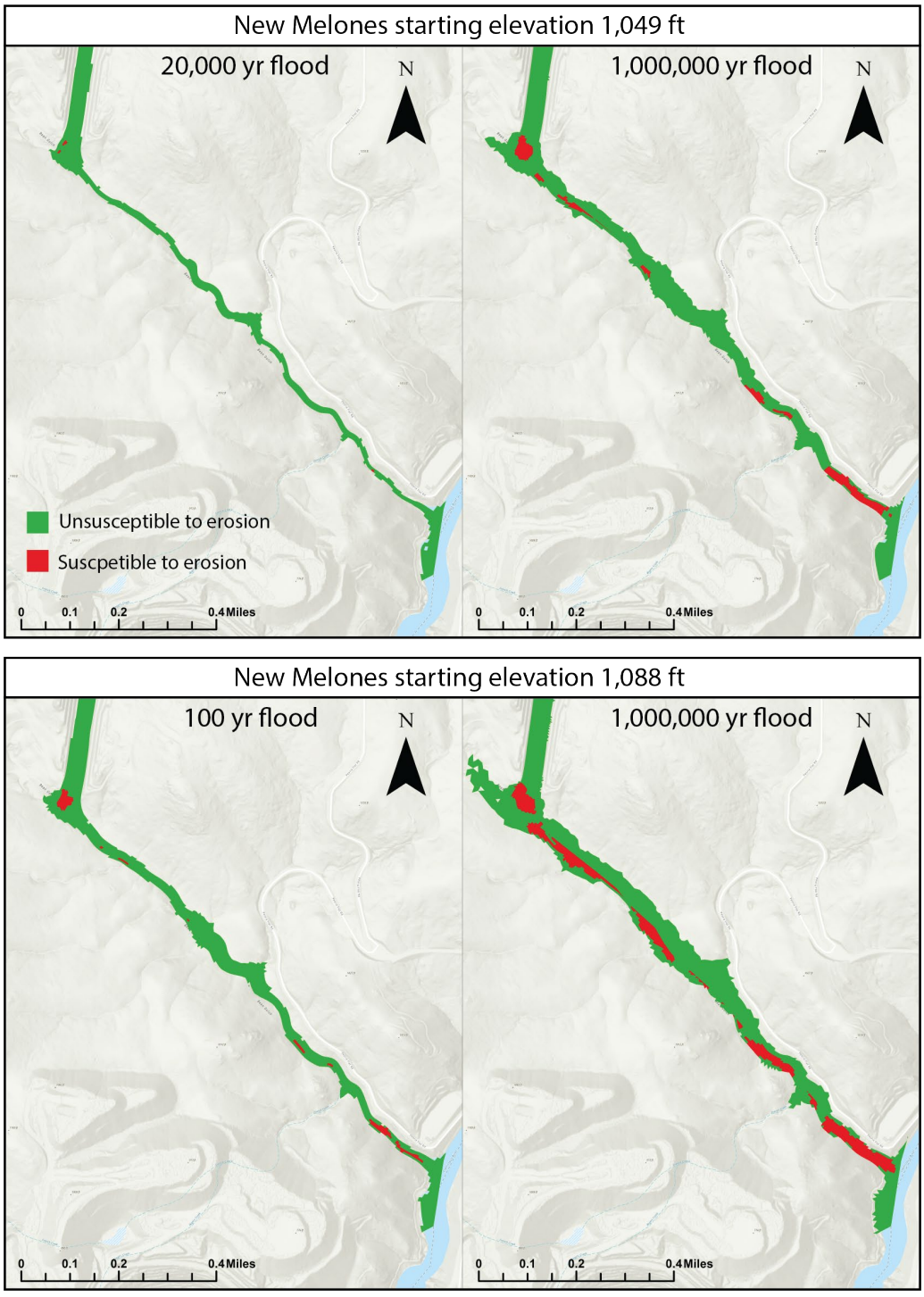

Figure A-3.—Annandale erodibility index method output for downstream boundary at Tulloch Reservoir of 510 ft.

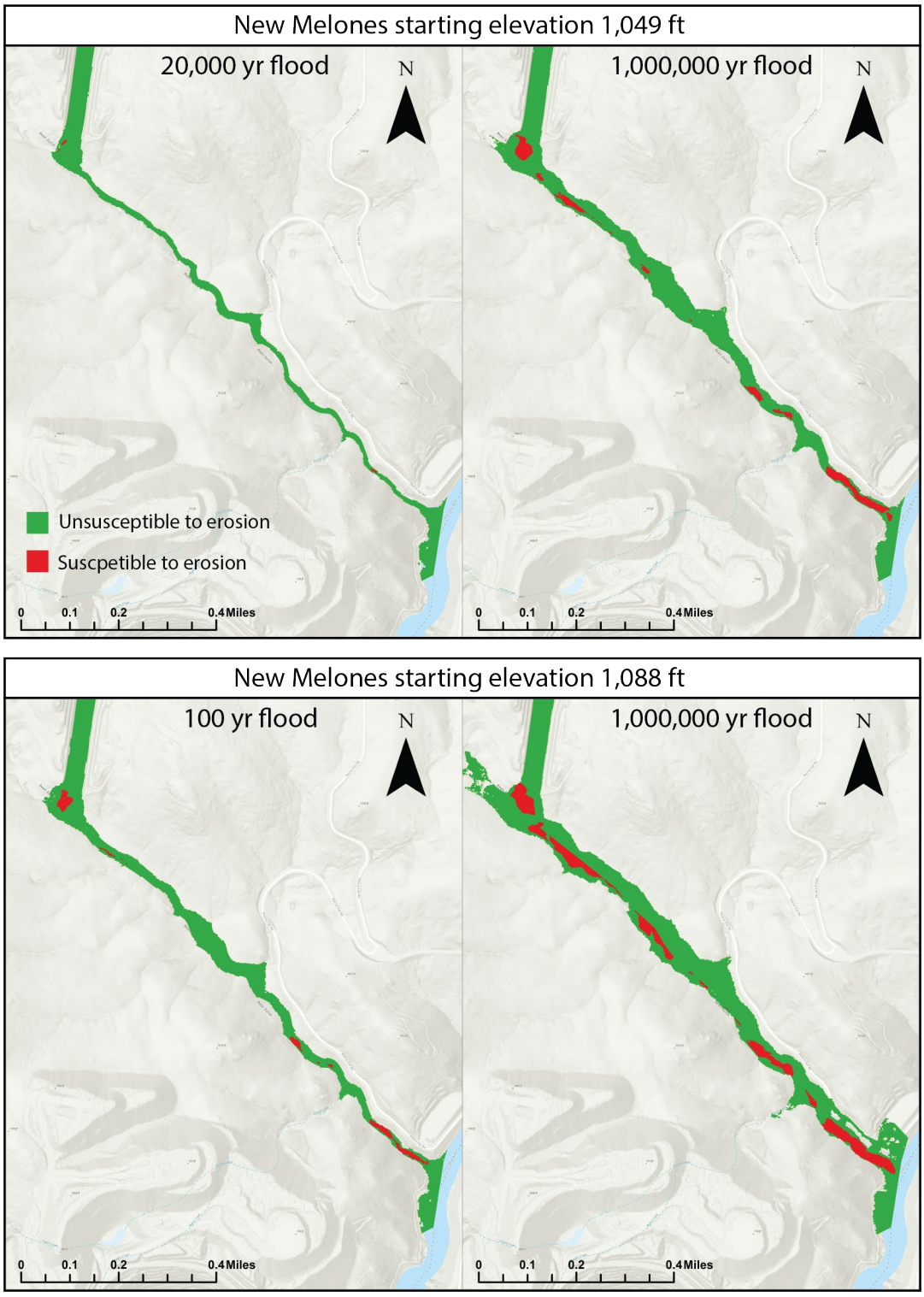

Figure A-4.—Annandale erodibility index method output for downstream boundary at Tulloch Reservoir of 515 ft.

Appendix E

H1DE Supplemental Results

The following show supplemental results for the H1DE model for downstream boundary water surface elevations at Tulloch Reservoir of 510 ft and 515 ft. The model was run for low and high flows at NM1049 and NM1088. The figures show volume eroded for the entire channel and vertical incision at monitoring points.

Left Spillway
T510

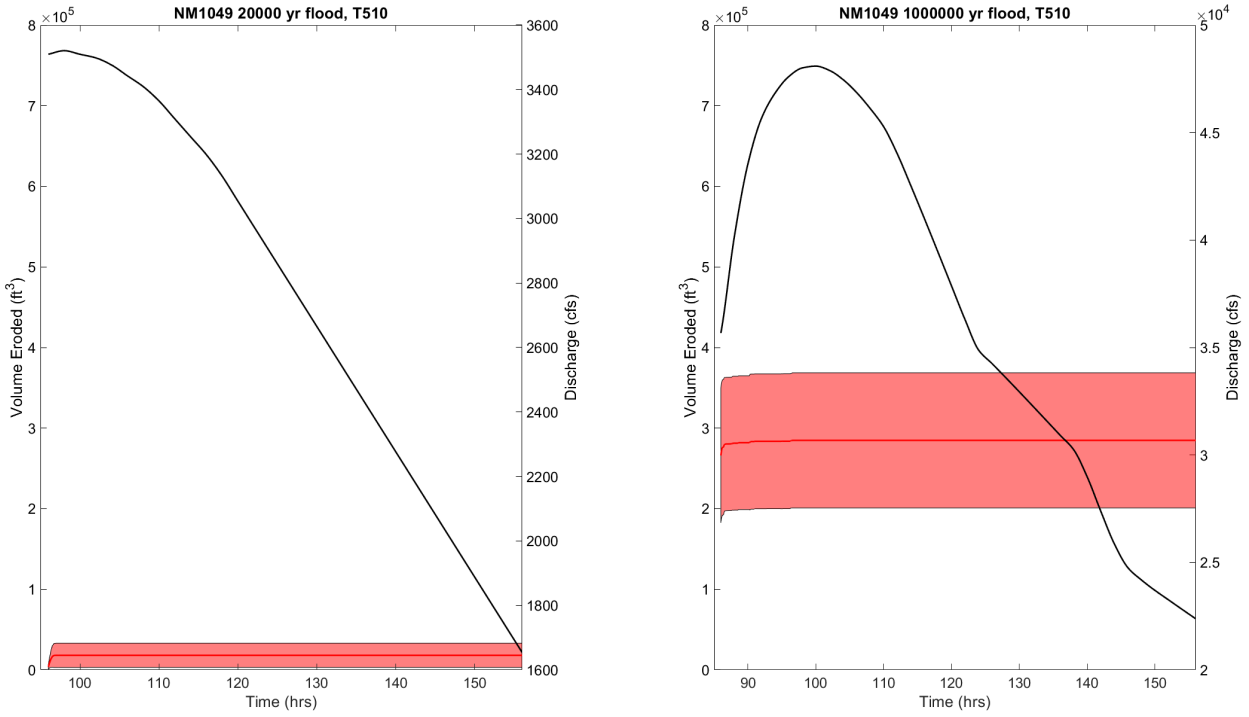

Figure A-5.—The red line shows average volume eroded with the shaded red area encompassing the standard deviation for New Melones starting reservoir elevation of 1,049 ft, Tulloch downstream boundary elevation of 510 ft, and low and high recurrence interval floods (left y-axis) along the left spillway. The black line plots the flow hydrograph (right y-axis).

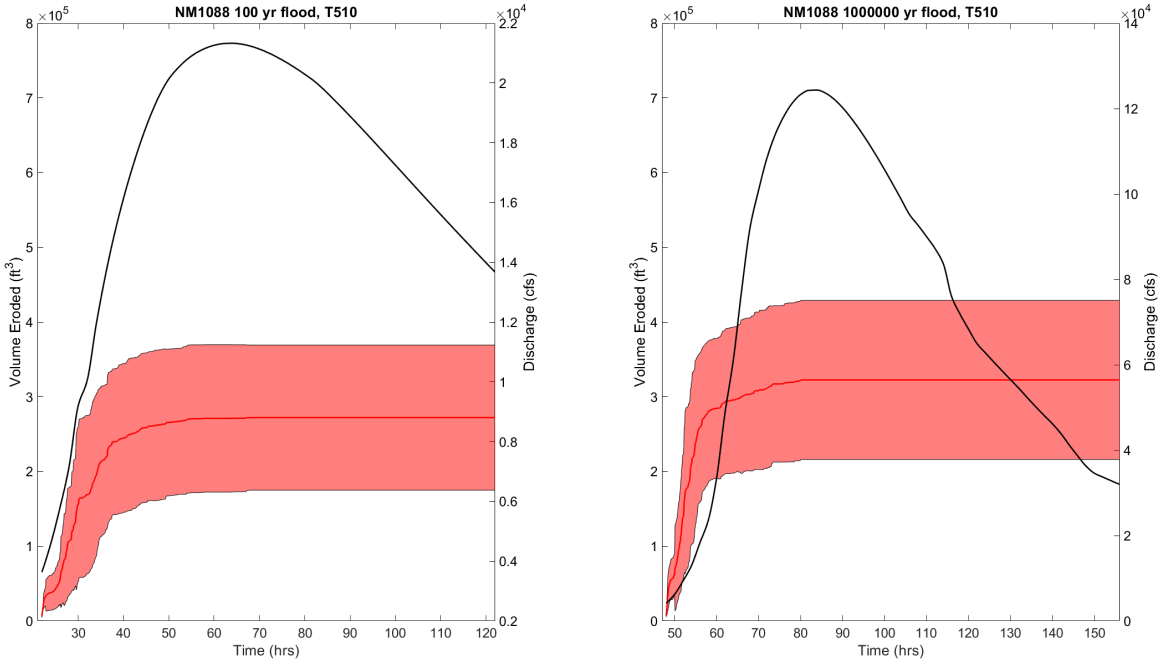

Figure A-6.—The red line shows average volume eroded with the shaded red area encompassing the standard deviation for New Melones starting reservoir elevation of 1,088 ft, Tulloch downstream boundary elevation of 510 ft, and low and high recurrence interval floods (left y-axis) along the left spillway. The black line plots the flow hydrograph (right y-axis).

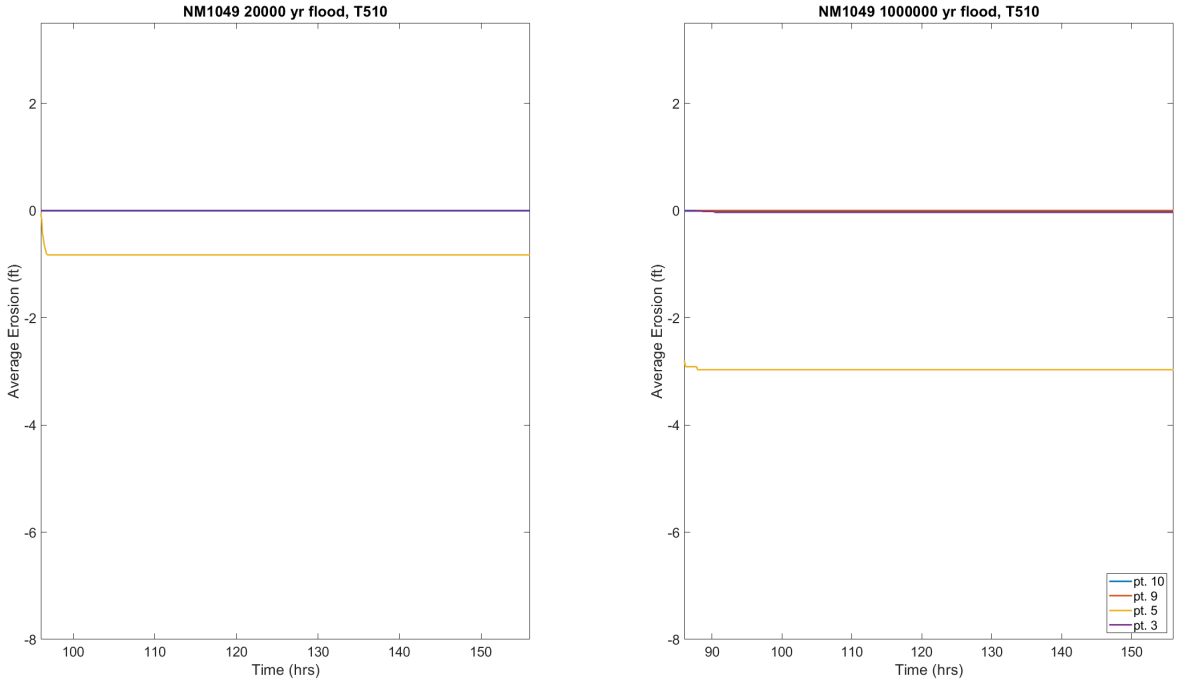

Figure A-7.—The figure shows monitoring point incision for New Melones starting reservoir elevation of 1,049 ft, Tulloch downstream boundary elevation of 510 ft, and low and high recurrence interval floods along the left spillway.

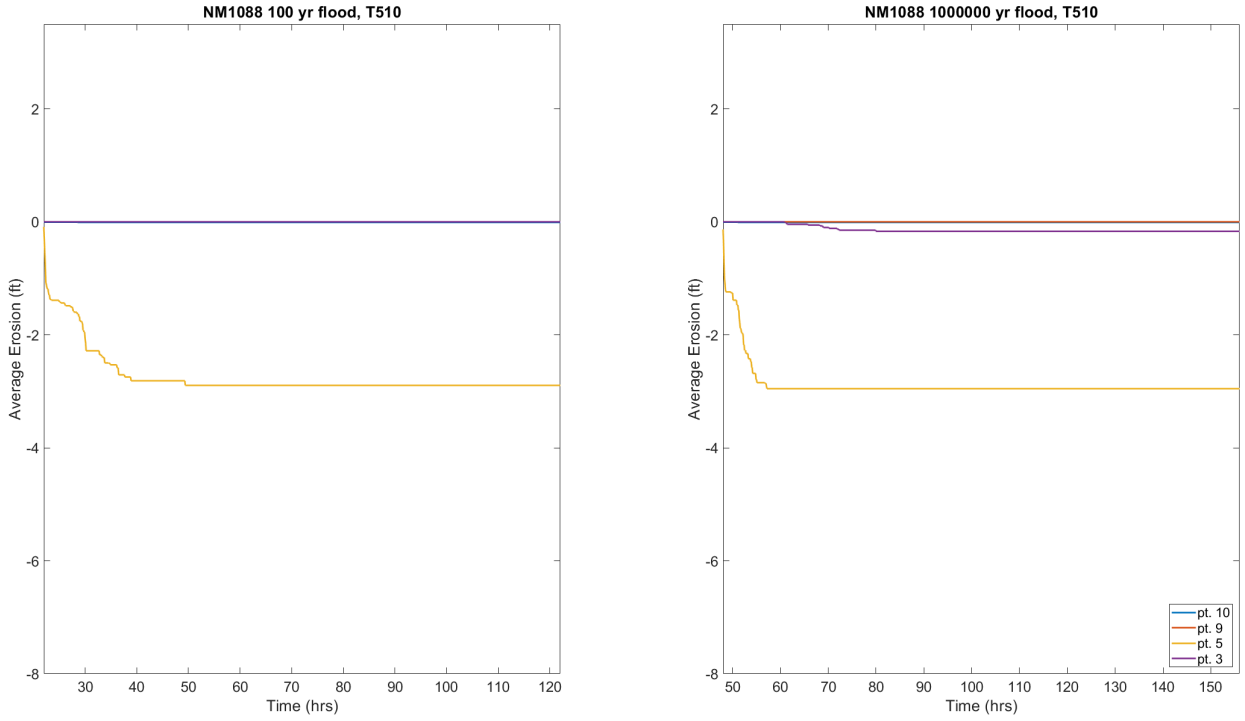

Figure A-8.—The figure shows monitoring point incision for New Melones starting reservoir elevation of 1,088 ft, Tulloch downstream boundary elevation of 510 ft, and low and high recurrence interval floods along the left spillway.

T515

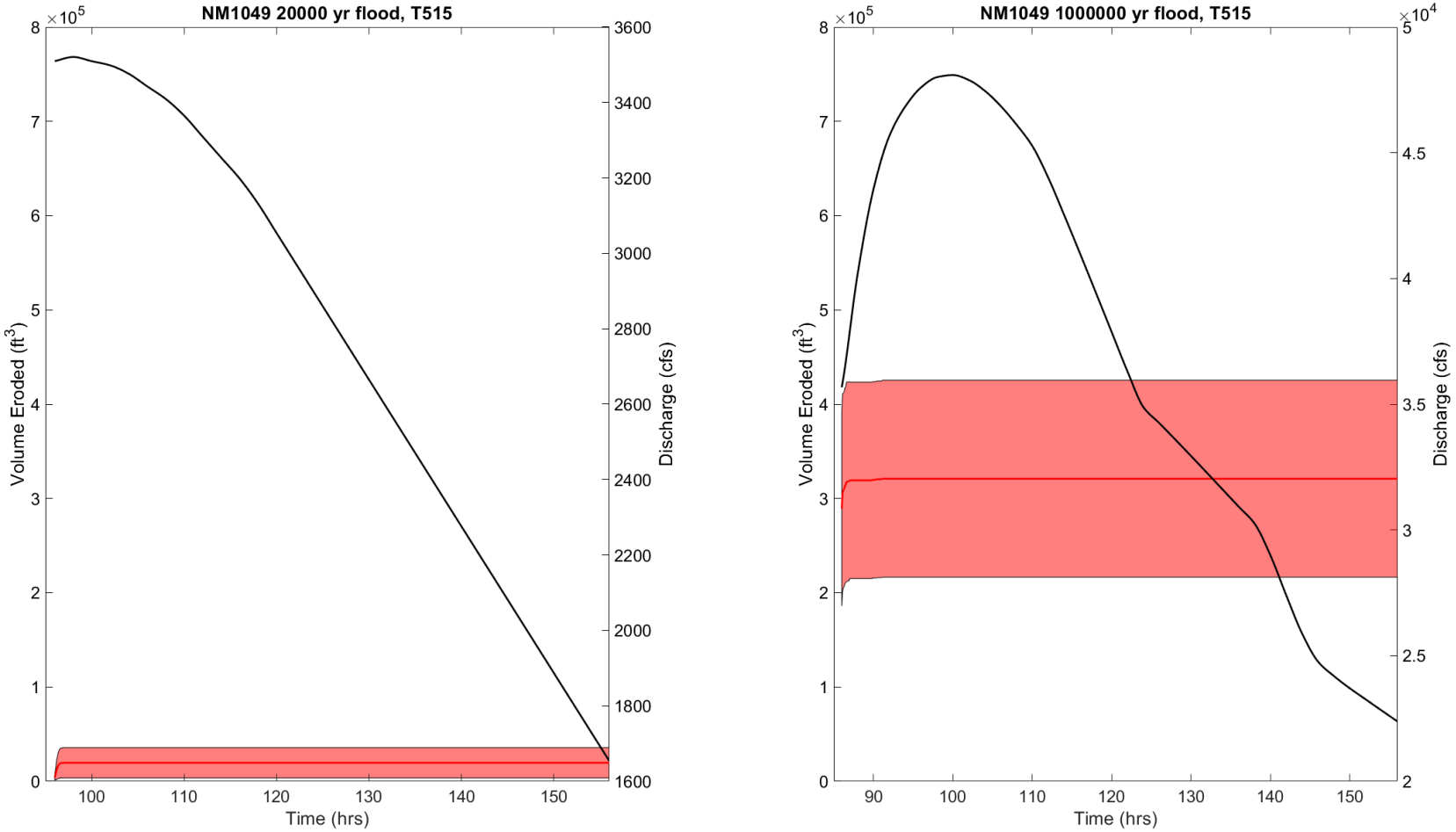

Figure A-9.—The red line shows average volume eroded with the shaded red area encompassing the standard deviation for New Melones starting reservoir elevation of 1,049 ft, Tulloch downstream boundary elevation of 515 ft, and low and high recurrence interval floods (left y-axis) along the left spillway. The black line plots the flow hydrograph (right y-axis).

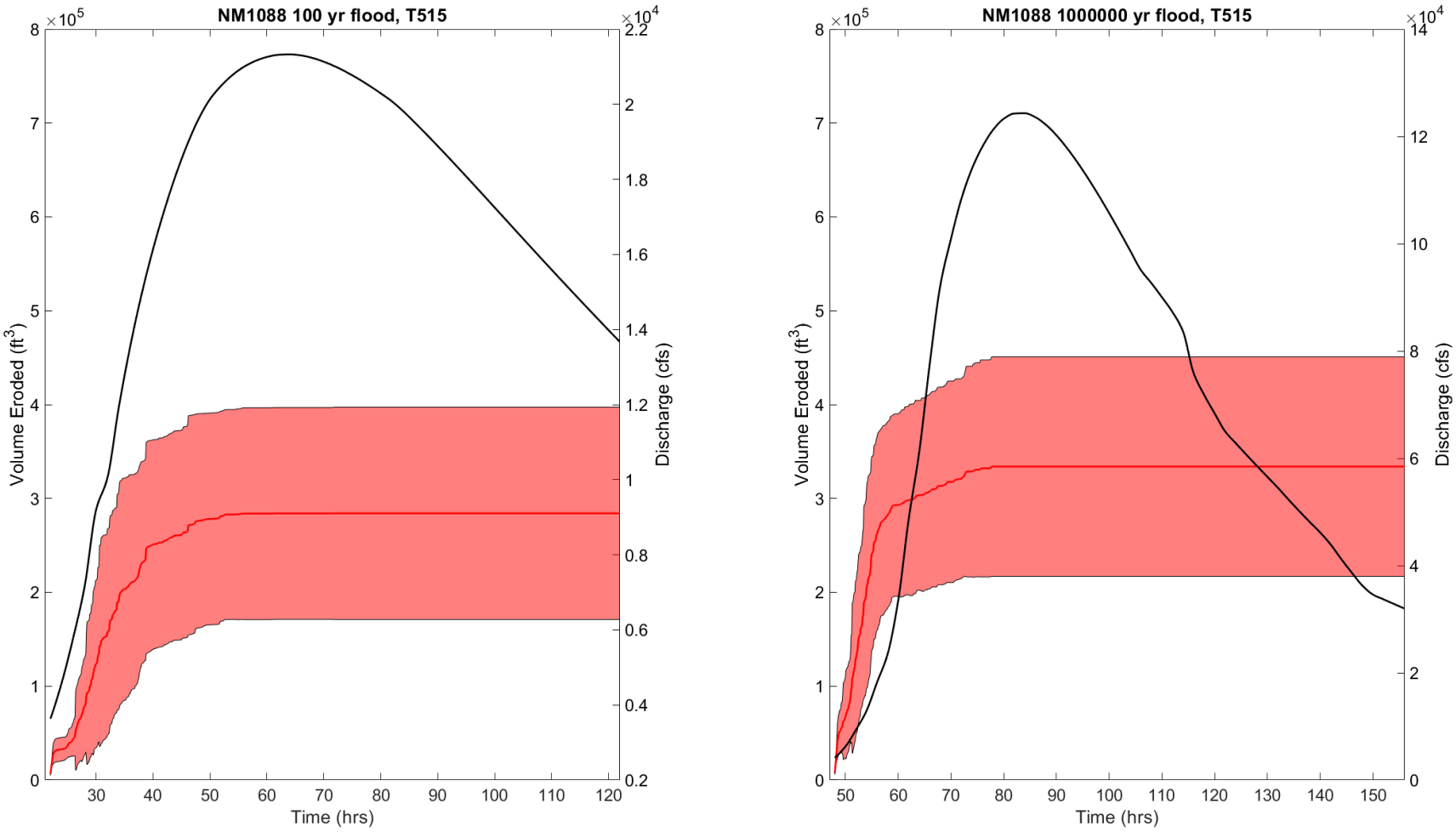

Figure A-10.—The red line shows average volume eroded with the shaded red area encompassing the standard deviation for New Melones starting reservoir elevation of 1,088 ft, Tulloch downstream boundary elevation of 515 ft, and low and high recurrence interval floods (left y-axis) along the left spillway. The black line plots the flow hydrograph (right y-axis).

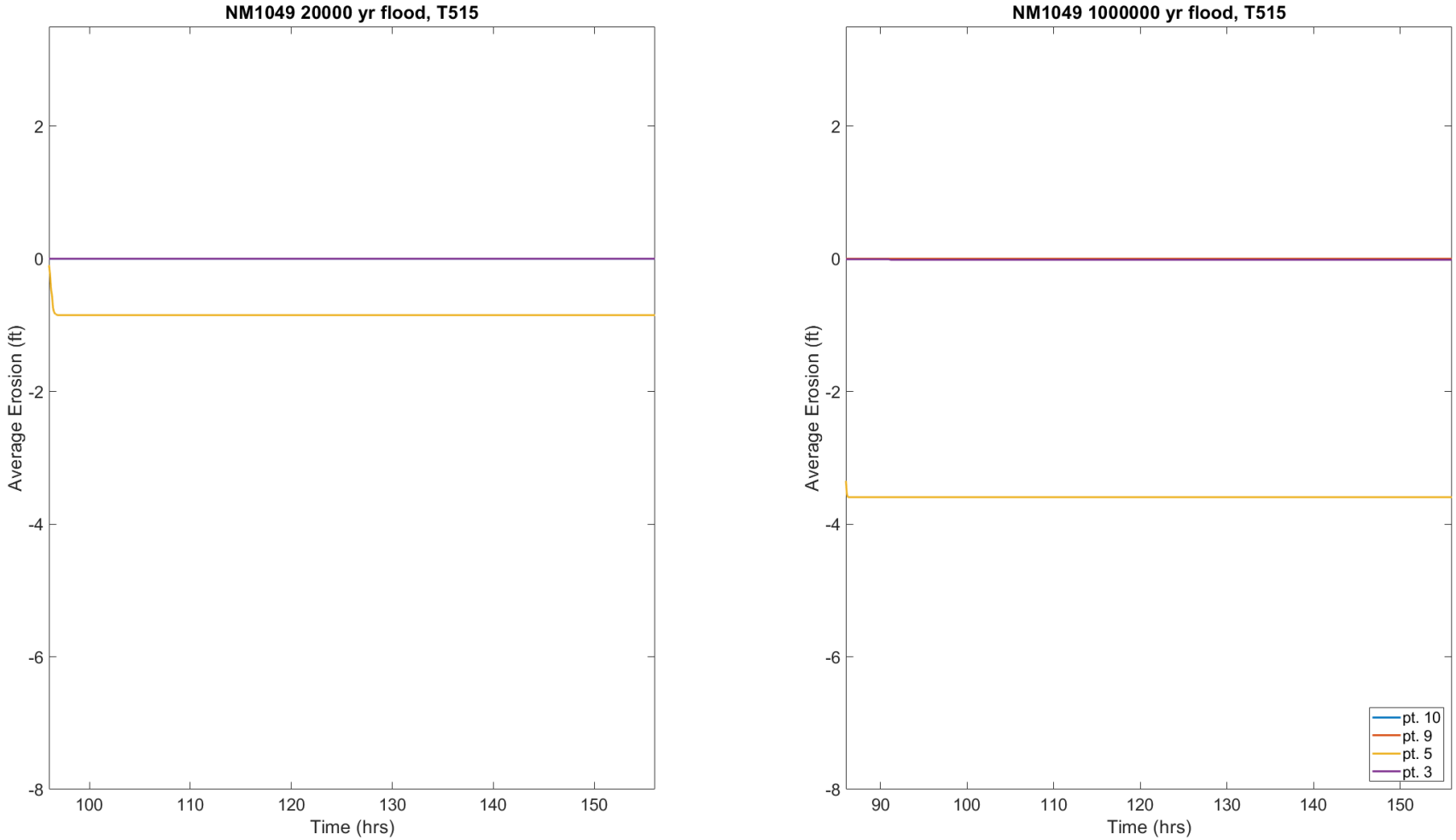

Figure A-11.—The figure shows monitoring point incision for New Melones starting reservoir elevation of 1,049 ft, Tulloch downstream boundary elevation of 515 ft, and low and high recurrence interval floods along the left spillway.

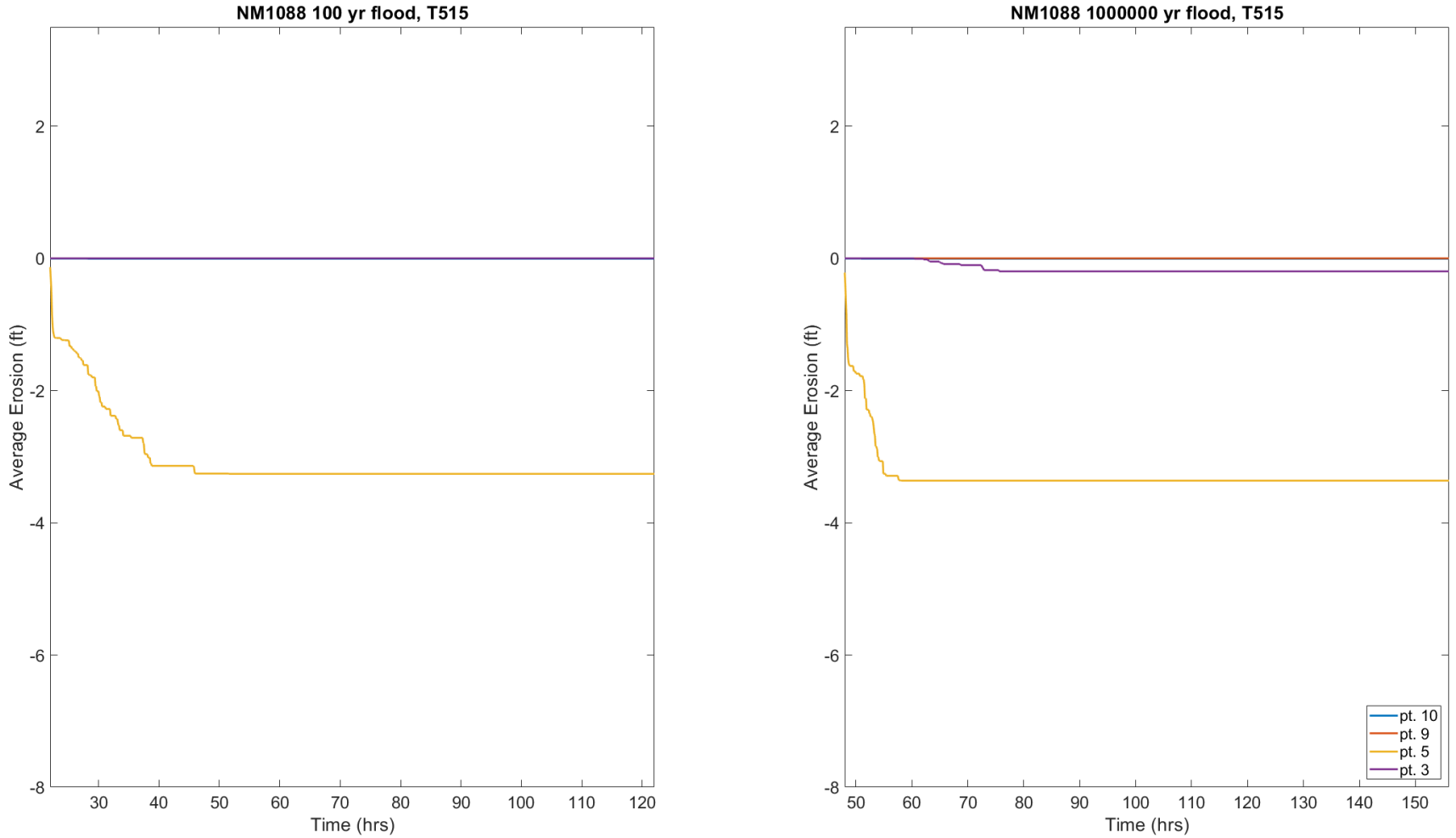

Figure A-12.—The figure shows monitoring point incision for New Melones starting reservoir elevation of 1,088 ft, Tulloch downstream boundary elevation of 515 ft, and low and high recurrence interval floods along the left spillway.

Right Spillway
T510

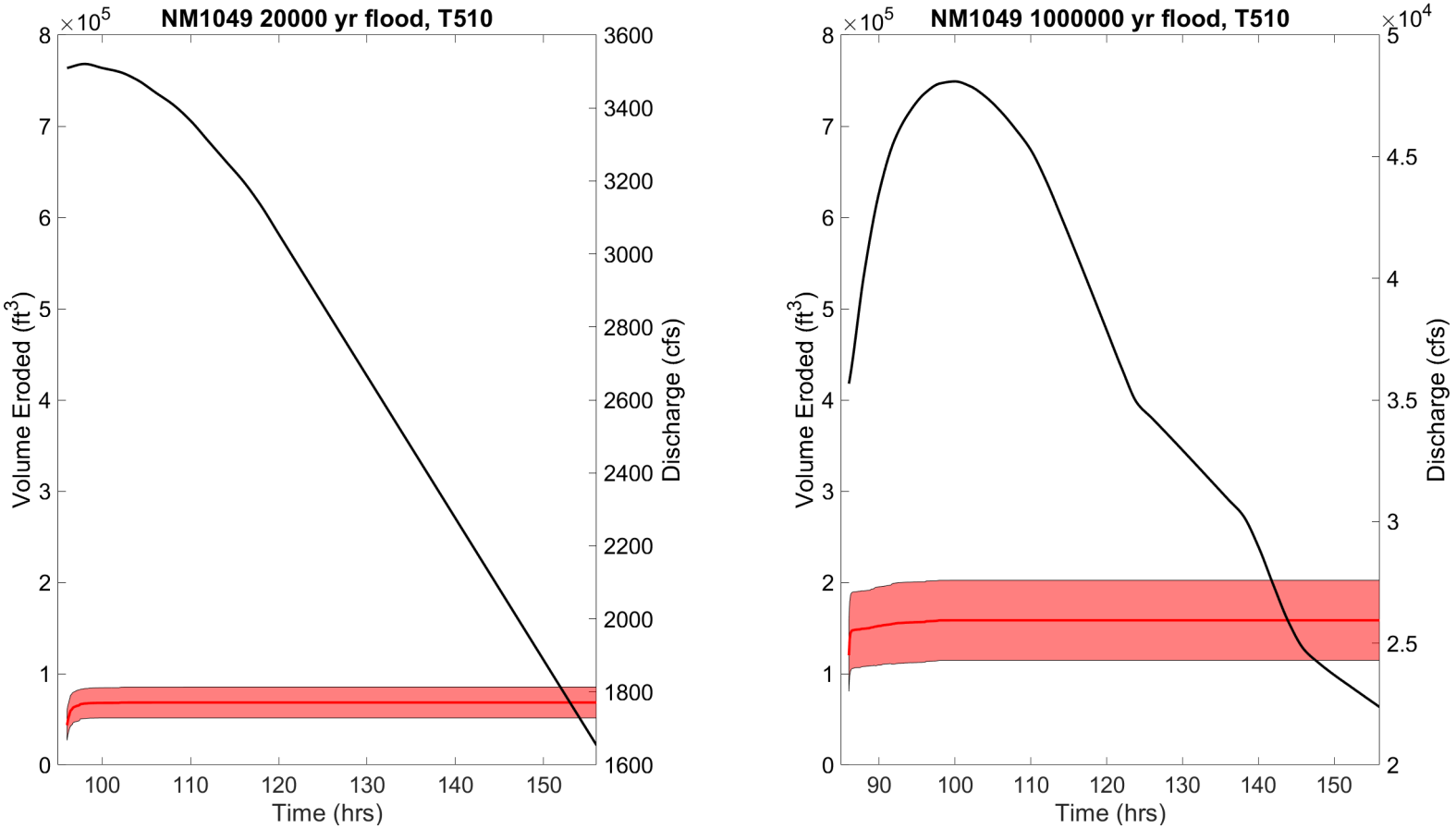

Figure A-13.—The red line shows average volume eroded with the shaded red area encompassing the standard deviation for New Melones starting reservoir elevation of 1,049 ft, Tulloch downstream boundary elevation of 510 ft, and low and high recurrence interval floods (left y-axis) along the right spillway. The black line plots the flow hydrograph (right y-axis).

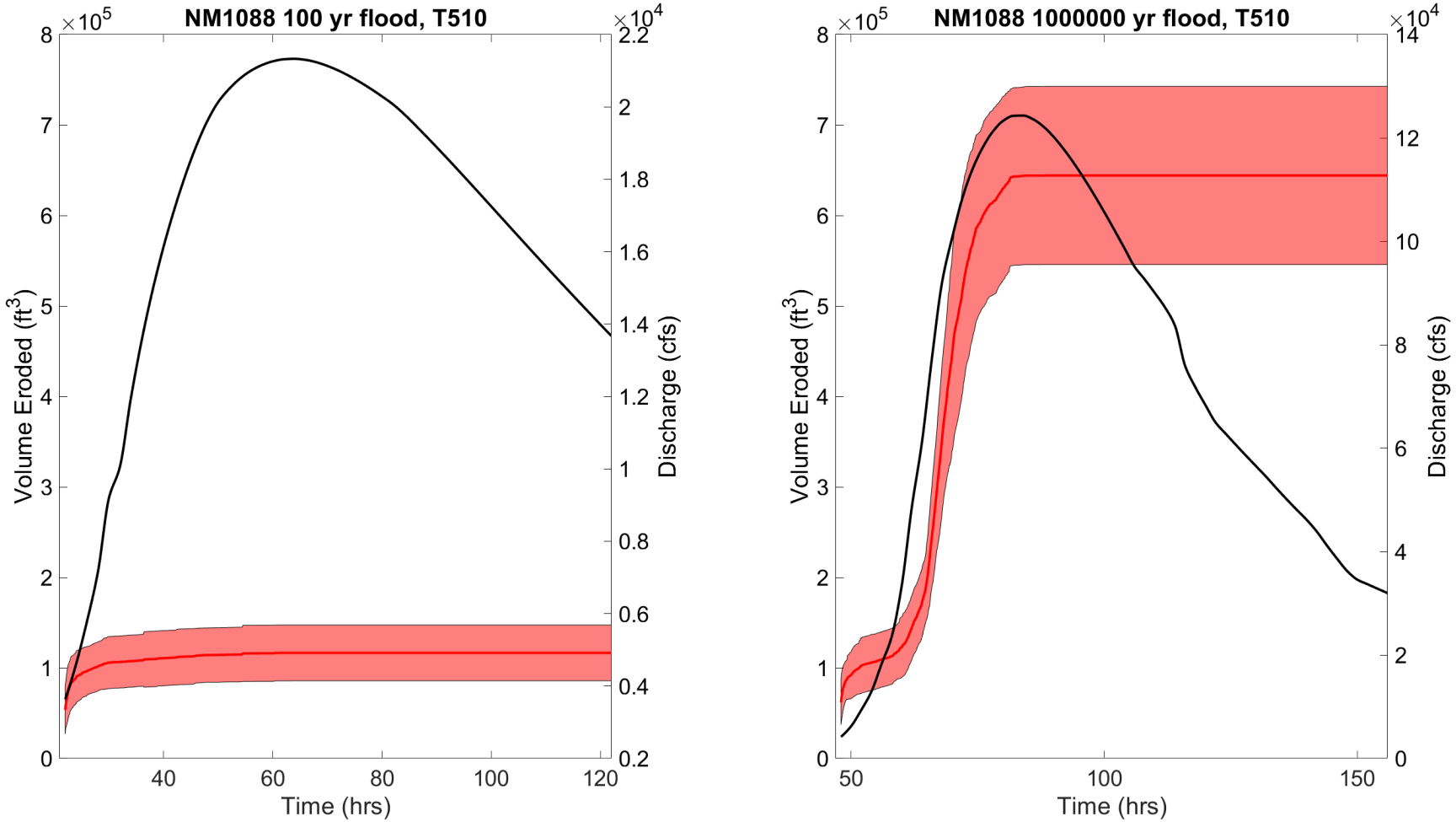

Figure A-14.—The red line shows average volume eroded with the shaded red area encompassing the standard deviation for New Melones starting reservoir elevation of 1,088 ft, Tulloch downstream boundary elevation of 510 ft, and low and high recurrence interval floods (left y-axis) along the right spillway. The black line plots the flow hydrograph (right y-axis).

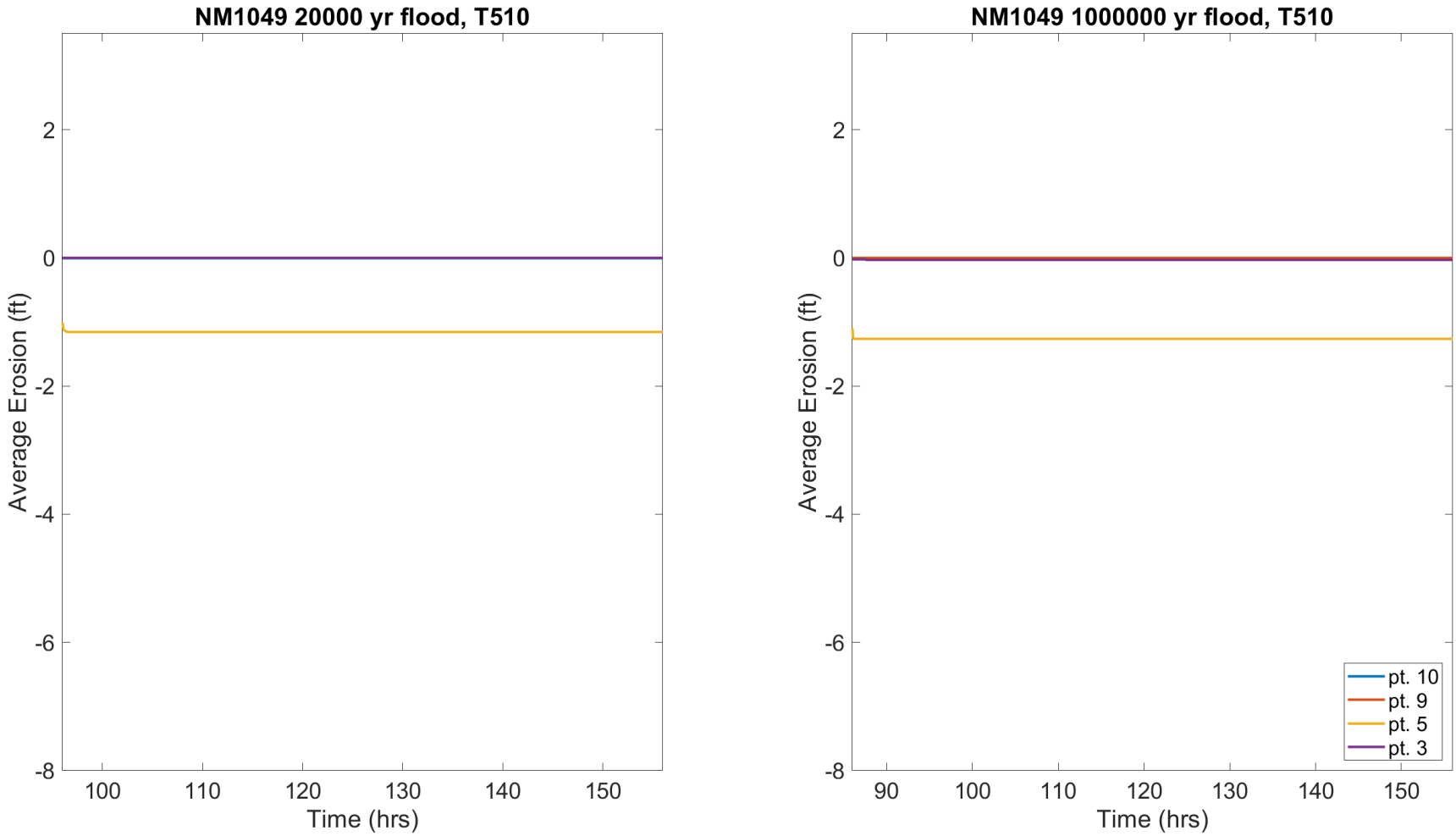

Figure A-15.—The figure shows monitoring point incision for New Melones starting reservoir elevation of 1,049 ft, Tulloch downstream boundary elevation of 510 ft, and low and high recurrence interval floods along the right spillway.

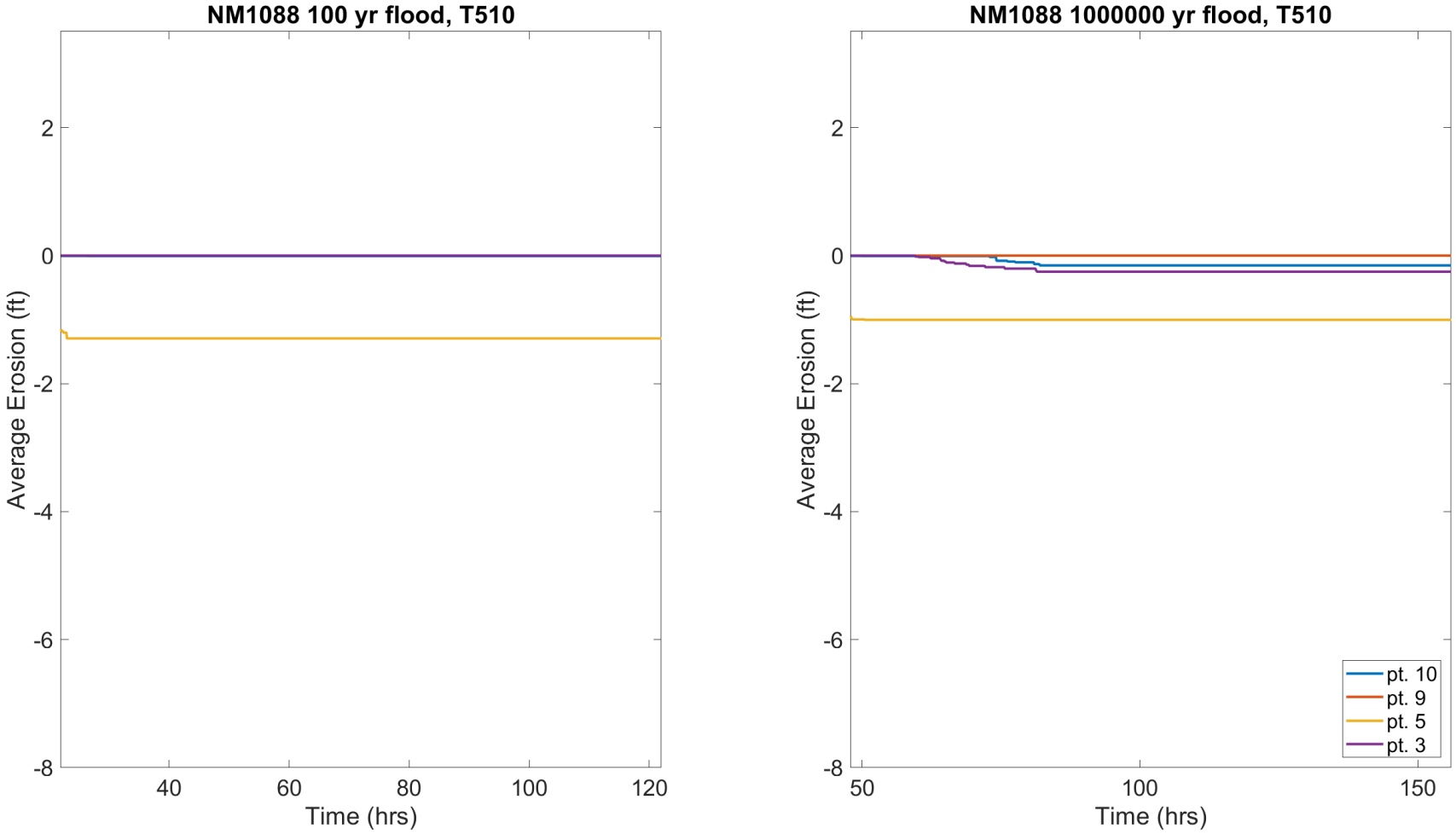

Figure A-16.—The figure shows monitoring point incision for New Melones starting reservoir elevation of 1,088 ft, Tulloch downstream boundary elevation of 510 ft, and low and high recurrence interval floods along the right spillway.

T515

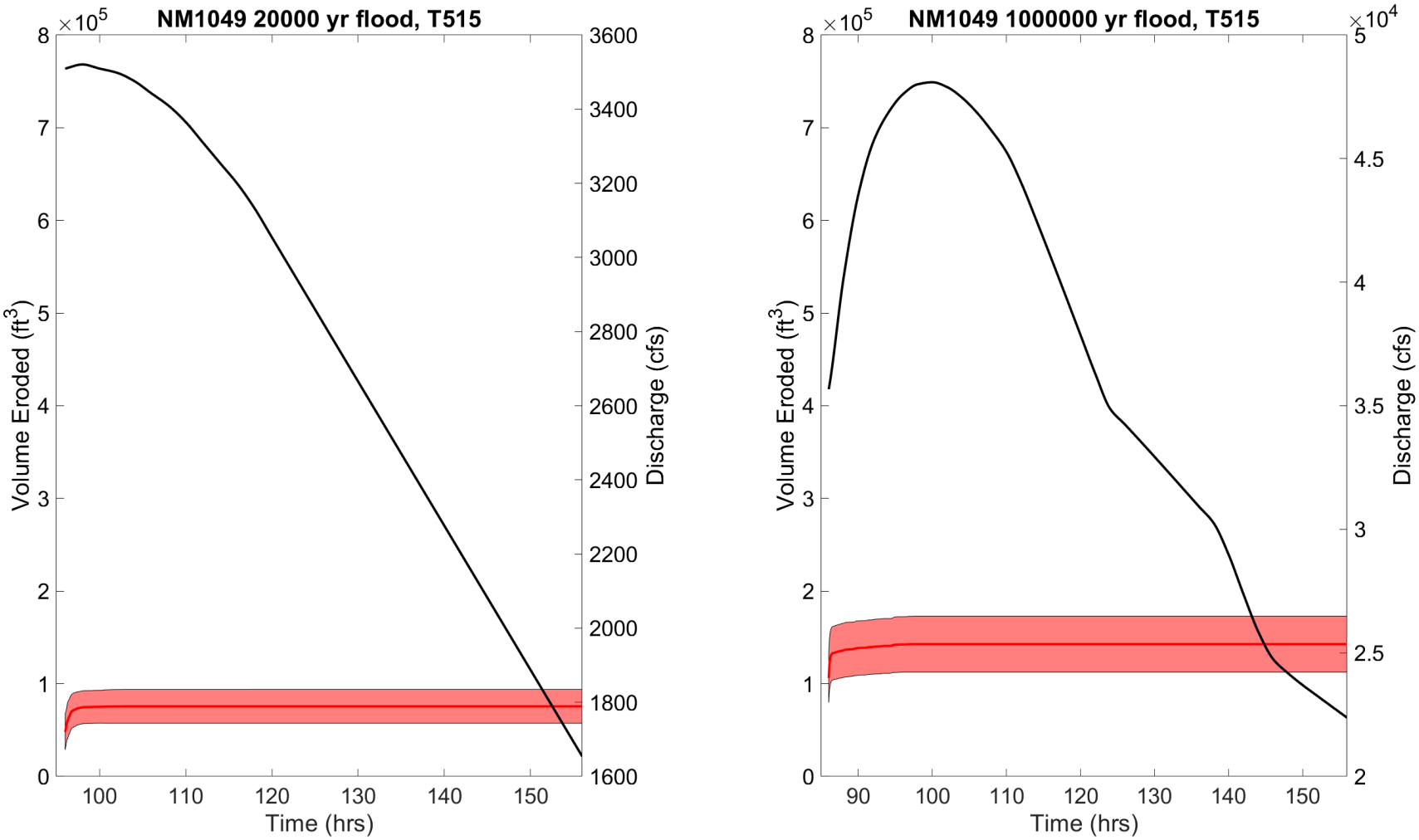

Figure A-17.—The red line shows average volume eroded with the shaded red area encompassing the standard deviation for New Melones starting reservoir elevation of 1,049 ft, Tulloch downstream boundary elevation of 515 ft, and low and high recurrence interval floods (left y-axis) along the right spillway. The black line plots the flow hydrograph (right y-axis).

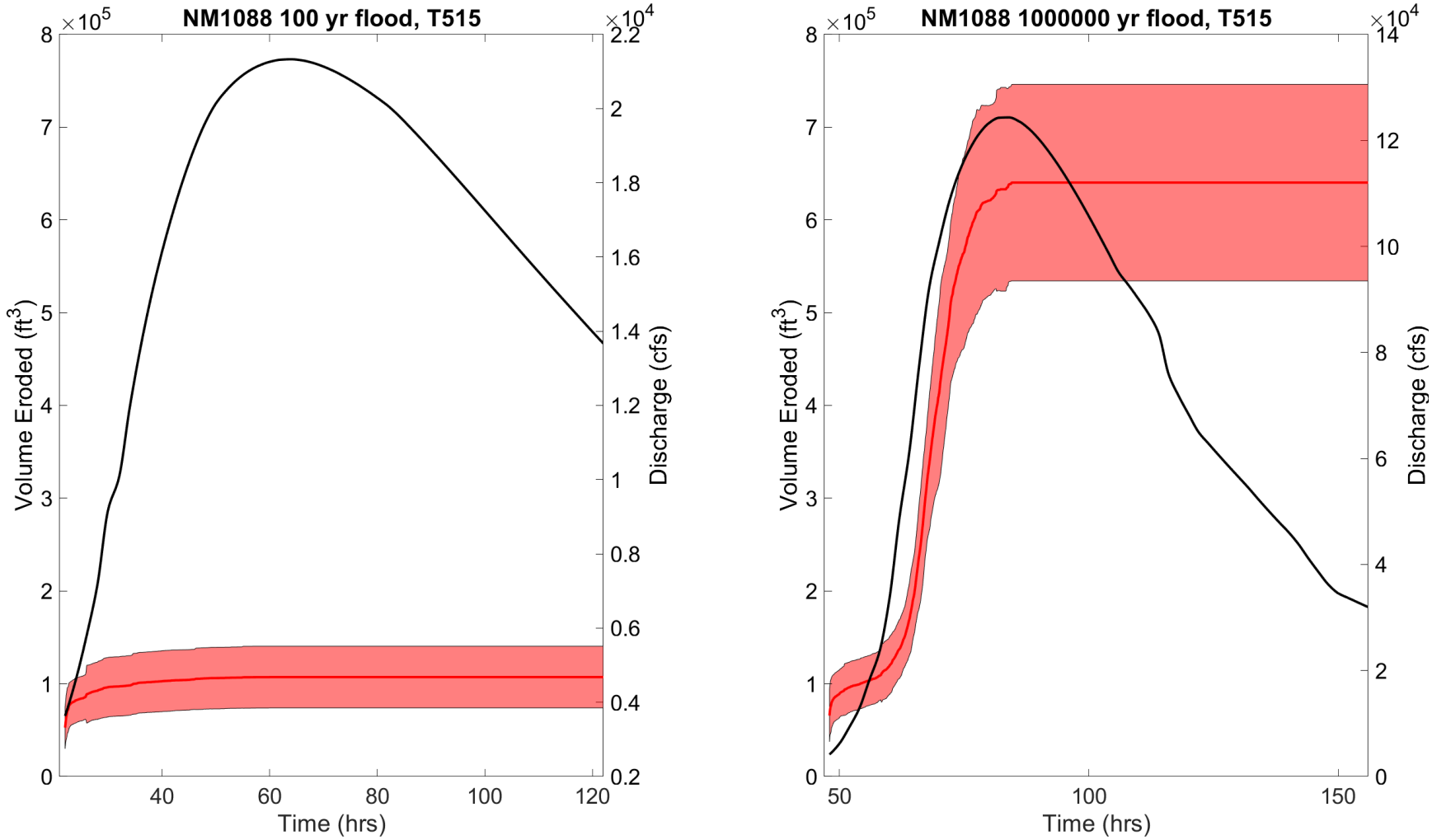

Figure A-18.—The red line shows average volume eroded with the shaded red area encompassing the standard deviation for New Melones starting reservoir elevation of 1,088 ft, Tulloch downstream boundary elevation of 515 ft, and low and high recurrence interval floods (left y-axis) along the right spillway. The black line plots the flow hydrograph (right y-axis).

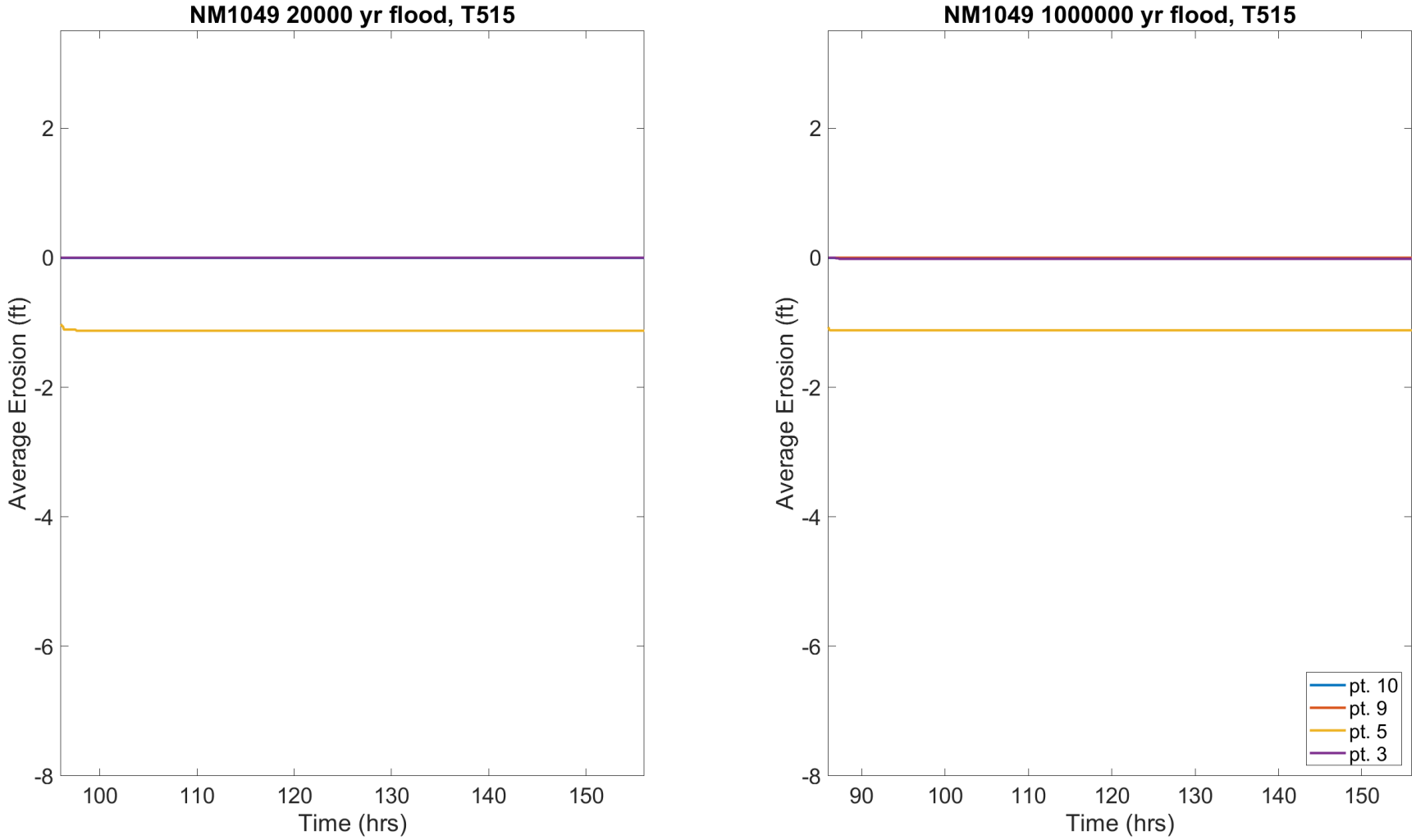

Figure A-19.—The figure shows monitoring point incision for New Melones starting reservoir elevation of 1,049 ft, Tulloch downstream boundary elevation of 515 ft, and low and high recurrence interval floods along the right spillway.

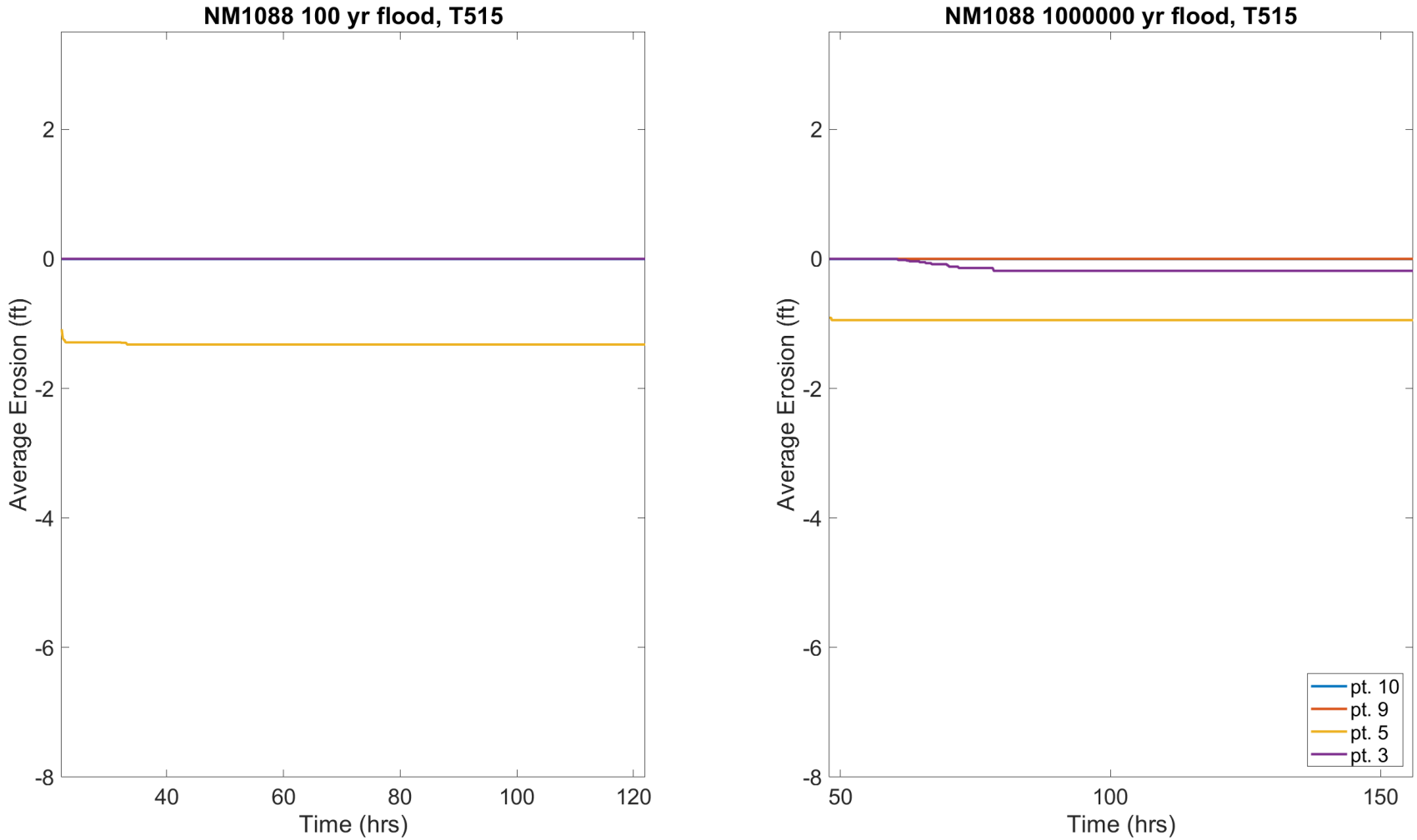

Figure A-20.—The figure shows monitoring point incision for New Melones starting reservoir elevation of 1,088 ft, Tulloch downstream boundary elevation of 515 ft, and low and high recurrence interval floods along the right spillway.